

UNCLASSIFIED

AD NUMBER

AD866821

LIMITATION CHANGES

TO:

Approved for public release; distribution is unlimited.

FROM:

Distribution authorized to U.S. Gov't. agencies and their contractors; Critical Technology; FEB 1970. Other requests shall be referred to Air Force Technical Application Center, VELA Seismological Center, Washington, DC 20333. This document contains export-controlled technical data.

AUTHORITY

usaf ltr, 25 jan 1972 xxx

THIS PAGE IS UNCLASSIFIED

TR 69-53

AD 866821

TECHNICAL REPORT NO. 69-53

EVALUATION OF THE DETECTION CAPABILITIES OF  
THE UBSO LONG-PERIOD ARRAY

NOTICE

THIS DOCUMENT IS SUBJECT TO SPECIAL  
EXPORT CONTROLS AND EACH TRANS-  
MITTAL TO FOREIGN GOVERNMENTS  
OR FOREIGN NATIONALS MAY BE MADE  
ONLY WITH PRIOR APPROVAL OF CHIEF,  
AFTAC.

*Alexandria, VA*

*22313*

Approved by the  
CLEARINGHOUSE  
for Foreign Security & Technical  
Information, Springfield, VA 22151

DDC  
RECEIVED  
APR 1 1970  
REGISTERED  
C

 **TELEDYNE  
GEOTECH**

TECHNICAL REPORT NO. 69-53  
EVALUATION OF THE DETECTION CAPABILITIES  
OF THE UBSO LONG-PERIOD ARRAY

by  
Don R. Phillips  
and  
John M. Ward

Sponsored by

Advanced Research Projects Agency  
Nuclear Test Detection Office  
ARPA Order No. 624

NOTICE

THIS DOCUMENT IS SUBJECT TO SPECIAL EXPORT CONTROLS AND EACH  
TRANSMITTAL TO FOREIGN GOVERNMENTS OR FOREIGN NATIONALS  
MAY BE MADE ONLY WITH PRIOR APPROVAL OF CHIEF, AFTAC.

GEOTECH  
A TELEDYNE COMPANY  
3401 Shiloh Road  
Garland, Texas

10 February 1970

### IDENTIFICATION

AFTAC Project No:	VELA T/9703
Project Title:	Operation of UBSO
ARPA Order No:	624
ARPA Program Code No:	8F10
Name of Contractor:	Teledyne Industries, Geotech Division Garland, Texas
Contract Number:	F33657-69-C-0759
Effective Date of Contract:	1 January 1969
Amount of Contract:	\$294,528
Contract Expiration Date:	31 December 1969
Program Manager:	B. B. Leichter, BR1-2561, ext. 222

## CONTENTS

	<u>Page</u>
ABSTRACT	
1. INTRODUCTION	1
1.1 General	1
1.2 Authority	1
1.3 Method of study	1
2. P-WAVE SIGNAL	4
2.1 P-wave signal loss	6
2.2 Noise loss	17
2.3 Signal-to-noise improvement for P waves	17
3. RAYLEIGH WAVES	25
3.1 Attenuation of Rayleigh wave signals	25
3.2 Noise attenuation	26
3.3 Signal-to-noise improvement for Rayleigh waves	36
APPENDIX 1 - Power density spectra of signal segments for each data sample	
APPENDIX 2 - Power density spectra of noise segments for each data sample	
APPENDIX 3 - Signal-to-noise ratios for each data sample	

## ILLUSTRATIONS

<u>Figure</u>		<u>Page</u>
1	Uinta Basin Seismological Observatory LP array	2
2	System responses of the long-period seismographs used in the UBSO long-period array	3
3	Flow diagram of method of study	5
4	UBSO digital long-period seismogram illustrating the P-wave signal arrival from the northern coast of Chile on 13 November 1969.	7/8
5	UBSO digital long-period seismogram illustrating the P-wave signal arrival from the New Hebrides Islands on 26 November 1969	9/10
6	UBSO digital long-period seismogram illustrating the P-wave signal arrival from Sakhalin Island on 18 December 1969	11/12
7	Attenuation by the unphased sum and the phased sum relative to the average individual of a teleseismic P wave recorded at UBSO on 13 November from the southeast	14
8	Attenuation by the unphased sum and the phased sum relative to the average individual of a teleseismic P wave recorded at UBSO on 26 November 1969 from the southwest	15
9	Attenuation by the unphased sum and the phased sum relative to the average individual of a teleseismic P wave recorded at UBSO on 18 December 1969 from the northwest	16
10	Noise attenuation achieved by the unphased sum and the phased sum relative to an average individual for a noise sample recorded at UBSO on 13 November 1969 (phased sum beamed to a P wave from the southeast)	18
11	Noise attenuation achieved by the unphased sum and the phased sum relative to an average individual for a noise sample recorded at UBSO on 26 November 1969 (phased sum beamed to a P wave from the southwest)	19

## ILLUSTRATIONS, Continued

<u>Figure</u>		<u>Page</u>
12	Noise attenuation achieved by the unphased sum and the phased sum relative to an average individual for a noise sample recorded at UBSO on 18 December 1969 (phased sum beamed to a P wave from the northwest)	20
13	Improvement in signal-to-noise ratio exhibited by the unphased sum and the phased sum relative to an average individual for a teleseismic P wave recorded at UBSO on 13 November 1969 from the southeast	22
14	Improvement in signal-to-noise ratio exhibited by the unphased sum and the phased sum relative to an average individual for a teleseismic P wave recorded at UBSO on 26 November 1969 from the southwest	23
15	Improvement in signal-to-noise ratio exhibited by the unphased sum and the phased sum relative to an average individual for a teleseismic P wave recorded at UBSO on 18 December 1969 from the northwest	24
16	UBSO digital long-period seismogram illustrating the Rayleigh wave arrival from the northern coast of Chile on 13 November 1969	27/28
17	UBSO digital long-period seismogram illustrating the Rayleigh wave arrival from the New Hebrides Islands on 26 November 1969	29/30
18	UBSO digital long-period seismogram illustrating the Rayleigh wave arrival from Sakhalin Island on 18 December 1969	31/32
19	Attenuation by the sum and the phased sum relative to the average individual of a Rayleigh signal recorded at UBSO on 13 November 1969 from the southeast	33
20	Attenuation by the sum and the phased sum relative to the average individual of a Rayleigh signal recorded at UBSO on 26 November 1969 from the southwest	34
21	Attenuation by the sum and the phased sum relative to the average individual of a Rayleigh signal recorded at UBSO on 18 December 1969 from the northwest	35

## ILLUSTRATIONS, Continued

<u>Figure</u>		<u>Page</u>
22	Noise attenuation achieved by the unphased sum and the phased sum relative to an average individual for a noise sample recorded at UBSO on 13 November 1969 (phased sum beamed to a Rayleigh wave from the southeast)	37
23	Noise attenuation achieved by the unphased sum and the phased sum relative to an average individual for a noise sample recorded at UBSO on 26 November 1969 (phased sum beamed to a Rayleigh wave from the southwest)	38
24	Noise attenuation achieved by the unphased sum and the phased sum relative to an average individual for a noise sample recorded at UBSO on 18 December 1969 (phased sum beamed to a Rayleigh wave from the northwest)	39
25	Improvement in signal-to-noise ratio exhibited by the unphased sum and the phased sum relative to an average individual for a Rayleigh wave recorded at UBSO on 13 November 1969 from the southeast	40
26	Improvement in signal-to-noise ratio exhibited by the unphased sum and the phased sum relative to an average individual for a Rayleigh wave recorded at UBSO on 26 November 1969 from the southwest	41
27	Improvement in signal-to-noise ratio exhibited by the unphased sum and the phased sum relative to an average individual for a Rayleigh wave recorded at UBSO on 18 December 1969 from the northwest	43

\* \* \* \* \*

## TABLES

<u>Table</u>		<u>Page</u>
1	Epicentral data of events	13

### ABSTRACT

Three events from different directions were selected from which both a P and a Rayleigh waves energy was recorded by the seven vertical long-period seismographs of the UBSO array. Using the power density spectra of the signals and noise segments preceding the signals, signal-to-noise ratios were formed for the simple and phased summations. The simple summation indicated an improvement in signal-to-noise over a single detector of approximately 17 dB at the peak noise frequency of 0.0625 cps for the P-wave signal, but showed little or no improvement for the Rayleigh energy because of the large degree of Rayleigh signal loss. In all three cases the phased summations show improvement for both P and Rayleigh signals; however, the degree of improvement varied from event to event because of the directional properties of the noise sources.

# EVALUATION OF THE DETECTION CAPABILITIES OF THE UBSO LONG-PERIOD ARRAY

## 1. INTRODUCTION

### 1.1 GENERAL

The UBSO long-period array is a seven-element array of three-component long-period seismographs. The array has the shape of a hexagon with a spacing of 23.3 kilometers  $\pm 5$  percent between sites. Figure 1 shows the orientation of the array.

Collection of data and management of the array are accomplished with a digital system. The data samples are gain-ranged in 11 discreet steps of 6 dB each. The output from the gain-ranging amplifier is digitized at the site at the rate of one sample per second and after being gain-ranged and digitized the data samples are transmitted via commercial telephone circuits to the Central Recording Building (CRB). Data from all sites are received at the CRB and written on seven-track magnetic tape in an IBM-compatible format.

The data samples from the sites are also sent to a digital-to-analog converter. After the conversion to analog and additional filtering has been performed, the data are recorded on 16-millimeter film. The results of the additional filtering can be seen from the system frequency response in figure 2. It can also be seen from the same plot that the short-period noise (5-9 second) is allowed to pass through the digital tape system and is attenuated by filtering on the 16-millimeter film.

### 1.2 AUTHORITY

The research described in this report was supported by the Advanced Research Projects Agency, Nuclear Test Detection Office, and was monitored by the Air Force Technical Applications Center (AFTAC). Authorization for this study to be completed under Project VT/9703 was included in a letter of approval from the Project Officer on 25 August 1969.

### 1.3 METHOD OF STUDY

This report deals with the evaluation of the detection capability of the UBSO long-period array. The purpose is to show the effectiveness of simple summations and phased summations of the individual seismograph outputs in improving

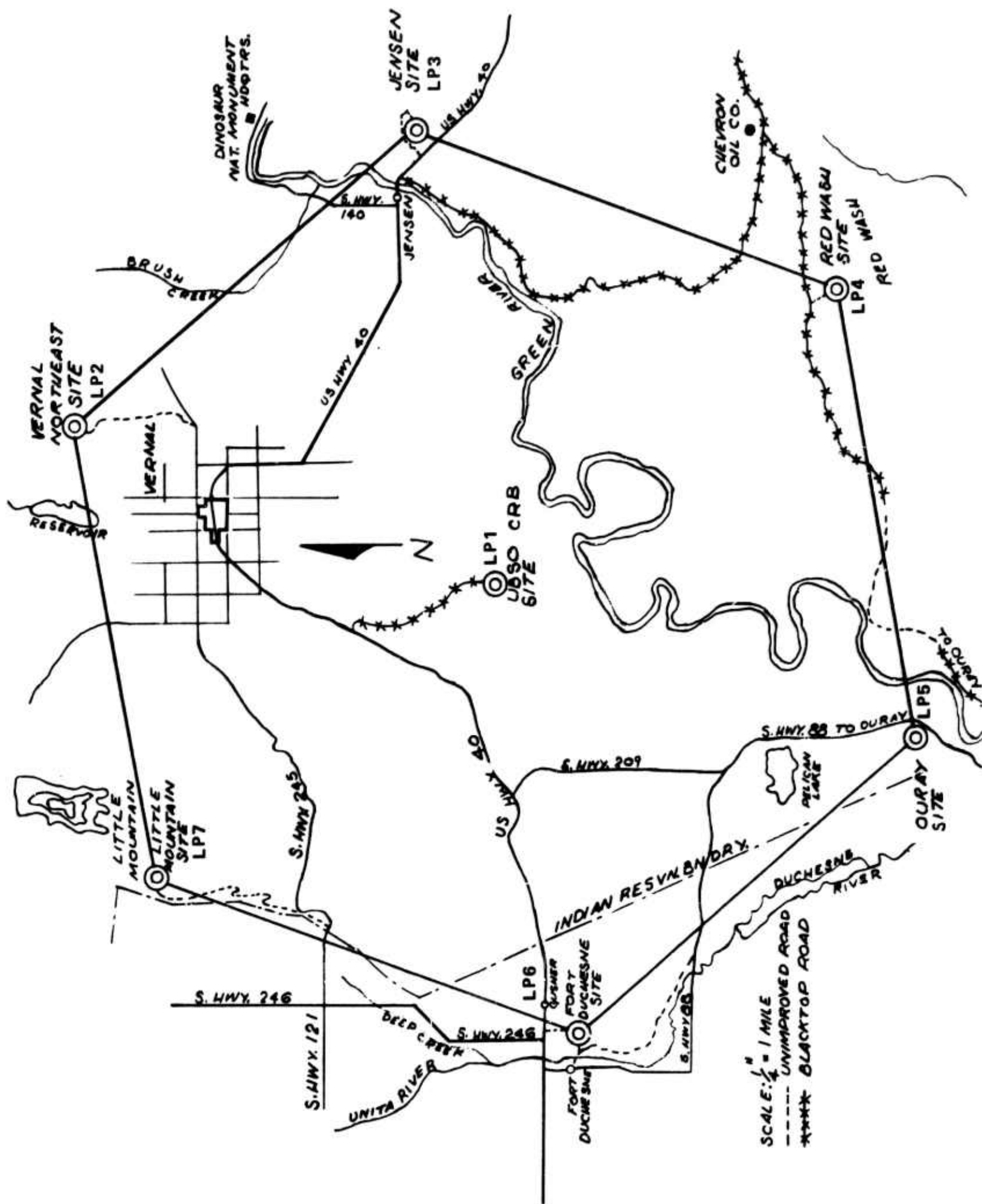


Figure 1. Uinta Basin Seismological Observatory LP Array

G 4989

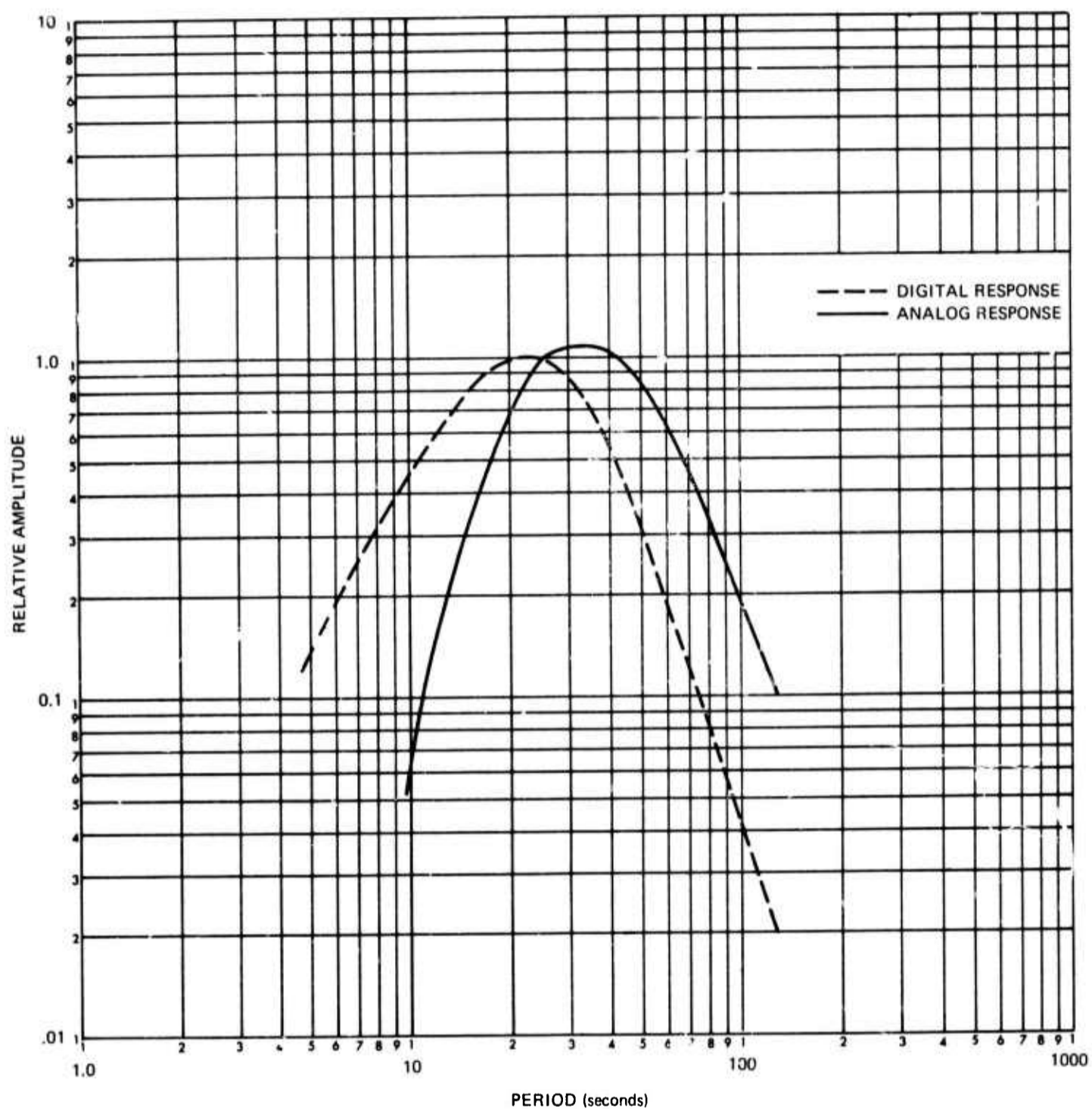


Figure 2. System responses of the long-period seismographs used in the UBSO long-period array

G 4743

signal-to-noise ratios of P-wave and Rayleigh-wave signals. The flow chart shown in figure 3 outlines the method of study.

Processing of data began with the selection of an appropriate signal and a 30-minute noise sample preceding the signal. The data samples were corrected for gain-ranging and demultiplexed into individual components before other processing was accomplished. An x-y digital plot was generated to visually evaluate the data and to obtain delay times. The delay times were measured from the digital plot using the peak trace amplitude within the first three cycles to determine the differences in the times of arrival at the array elements. Summations were formed by normalizing the individuals to the 25-second calibration and taking the mean of the individuals, with delay times being applied for the phased summations.

The signal-to-noise ratios were formed by using the power density spectra of the signal and the noise. The power density spectra were computed using 10-percent lags and the Parzen smoothing method over a 30-minute noise sample, a 6-minute P-wave signal, and a 10-minute Rayleigh wave signal. The mean of the power density spectra of the outputs of the seven individual vertical instruments was used as the spectrum of the average individual instrument. This average individual spectrum was used to determine the signal and noise attenuations and signal-to-noise improvement of the spectra of the summations by forming ratios.

All data samples used in this report were taken from the UBSO digital tape seismograms. However, since the 5- to 9-second microseisms dominate the digital tapes, it was necessary to make all preliminary analysis from the 16-millimeter analog film which has been filtered to exclude the 5- to 9-second noise. Assuming that this noise could be filtered by post filtering since it is outside the long-period signal frequency band, this report concentrates mainly on the frequencies within the signal band. All spectral plots will include the frequencies from 0.01 cps to 0.2 cps, but the plots concerning the signal spectra will be of little importance between 0.1 cps and 0.2 cps.

## 2. P-WAVE SIGNAL

Three events were selected for the P-wave study with each event arriving from a different direction. The time segment from which the signal power density spectra were obtained included all three body phases, P, PP, PPP. Since the apparent velocities of the three body phases are almost the same, the beam steered to provide maximum enhancement of the P wave is essentially steered to all three phases.

Figure 4 shows a 13 November 1969 recording of several body phases on the UBSO seven individual vertical long-period seismographs and the summation

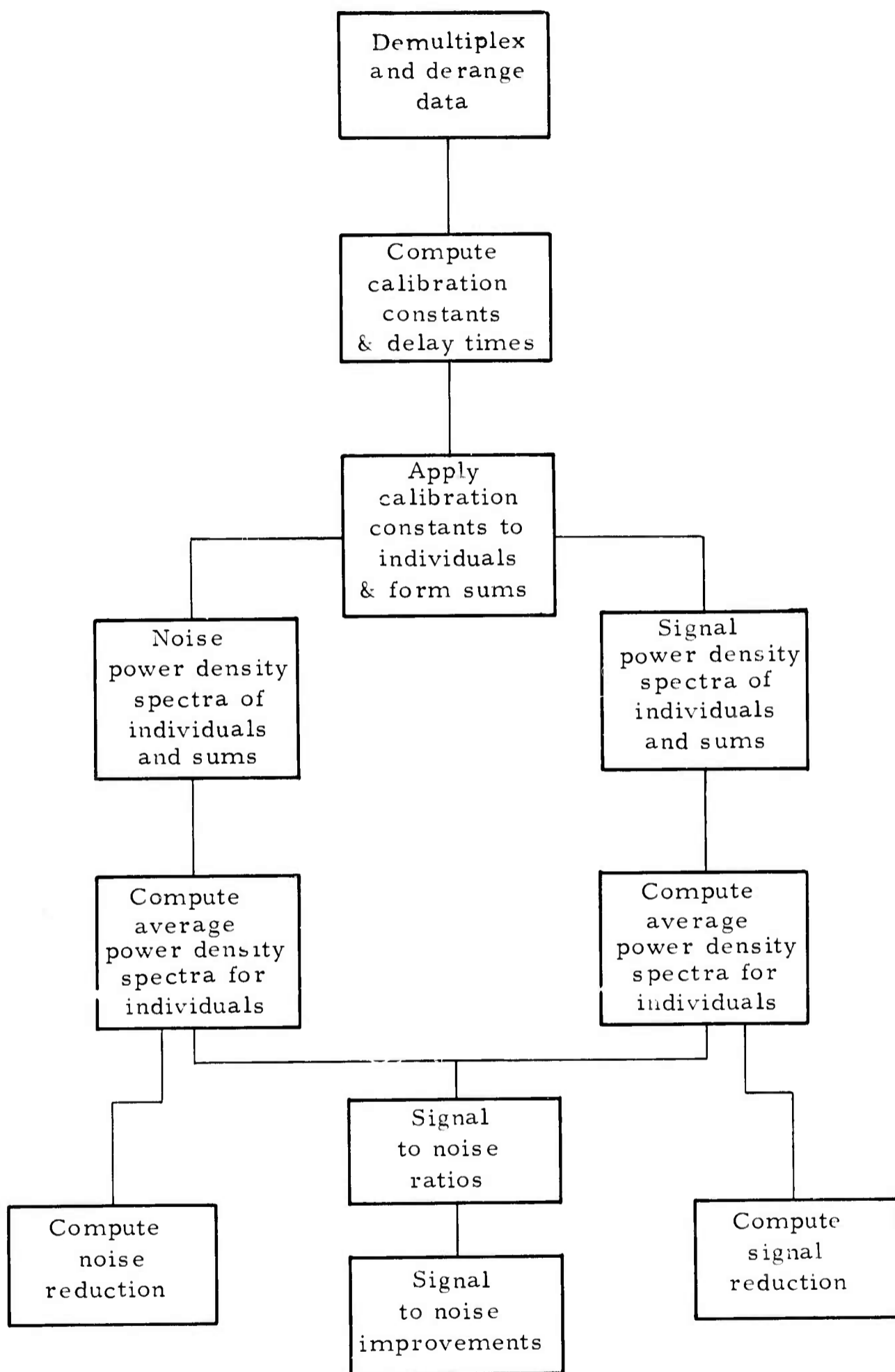


Figure 3. Flow diagram of method of study

and phased summations that were generated from them. From the digital plot the P, PP, and PPP phases can be identified. The event, arriving from the southeast, had its epicenter just off the coast of northern Chile, a great circle distance of approximately 75 degrees from UBSO.

On 26 November the UBSO long-period array recorded an event from the New Hebrides Islands area, southwest of the observatory, at a great circle distance of approximately 95 degrees. The body phases (P, PP, PPP) can be seen on the digital plot (figure 5).

Figure 6 is the digital plot of a signal from the northwest recorded on 18 December 1969. The event from Sakhalin Island occurred approximately 70 degrees from UBSO. This event has a much deeper focus than the other two events and depth phases can be seen on the digital plot. Table 1 may be used to supplement the information on the events selected for the study.

## 2.1 P-WAVE SIGNAL LOSS

Power density spectra for the average individual and the summations were computed for the three P-wave signals. The plots of these spectra are in appendix 1. From the signal spectra it was found that the peak power frequencies were 0.055 cps, 0.039 cps, and 0.047 cps for the 13 November, 26 November, and 18 December 1969 events, respectively. Even though this report will treat the signal power spectra as being pure signal, the samples consist of signal plus noise. This is evident in the 18 December signal spectrum (appendix 1, figure 3) which shows a high frequency noise component peaking at 0.125 cps.

The signal loss in dB relative to the average individual spectrum resulting from sum ratios and phased sum ratios for the three events from different directions are shown in figures 7, 8, and 9. The plots show that for each event less than 1 dB of signal loss occurred in the P-wave signal frequency band. The loss at the higher frequencies is attributed primarily to the attenuation of noise in the signal time segments rather than actual signal. The following table was prepared to facilitate direct comparison of the signal loss at the peak power frequencies of the summations relative to the average individual seismograms.

<u>Signal loss at peak power frequency</u>				
<u>Direction from UBSO</u>	<u>Distance (degrees)</u>	<u>Peak power frequency</u>	<u>Summation loss dB</u>	<u>Phase summation loss dB</u>
SE	75	0.055 cps	0.6	0.1
SW	95	0.039	0.5	0.2
NW	67	0.047	0.5	0.2

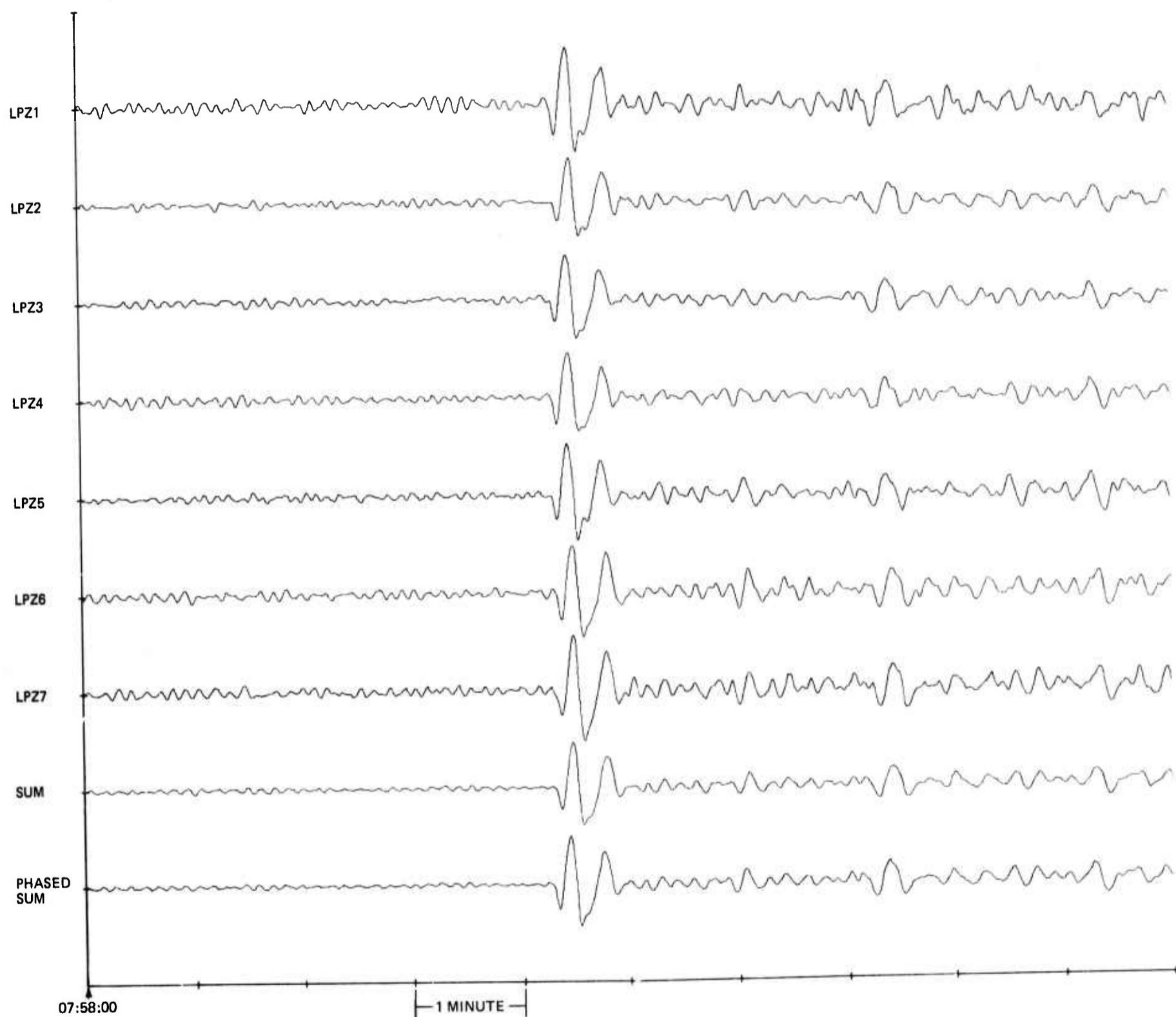
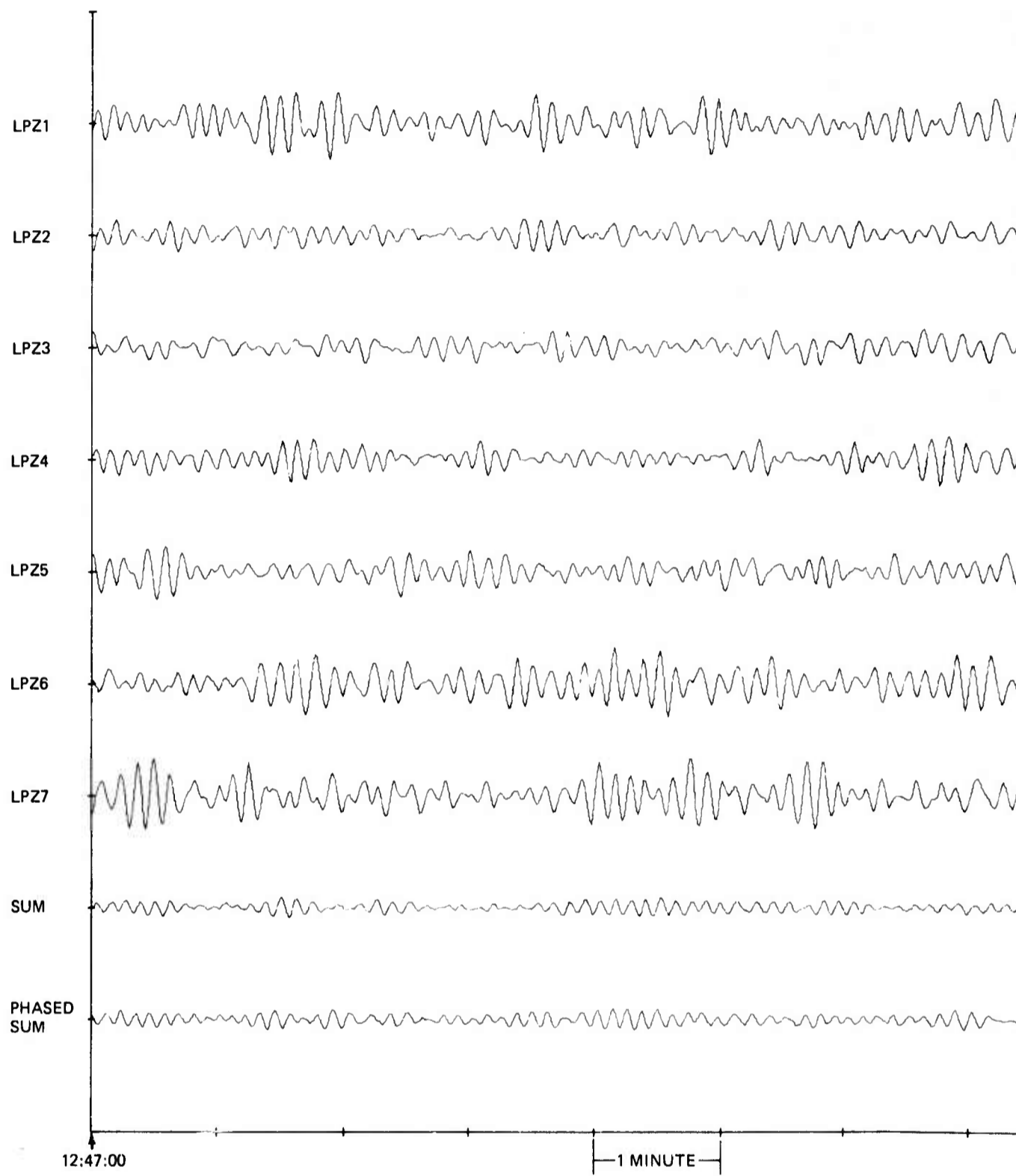


Figure 4. UBSO digital long-period seismogram illustrating the P-wave signal arrival from the northern coast of Chile on 13 November 1969. Epicentral data:  $\Delta \approx 75^\circ$ ,  $h = \text{normal}$ , magnitude  $\approx 5.8$ . (Vertical scale is 1 millimeter = 99.2 millimicrons)



A

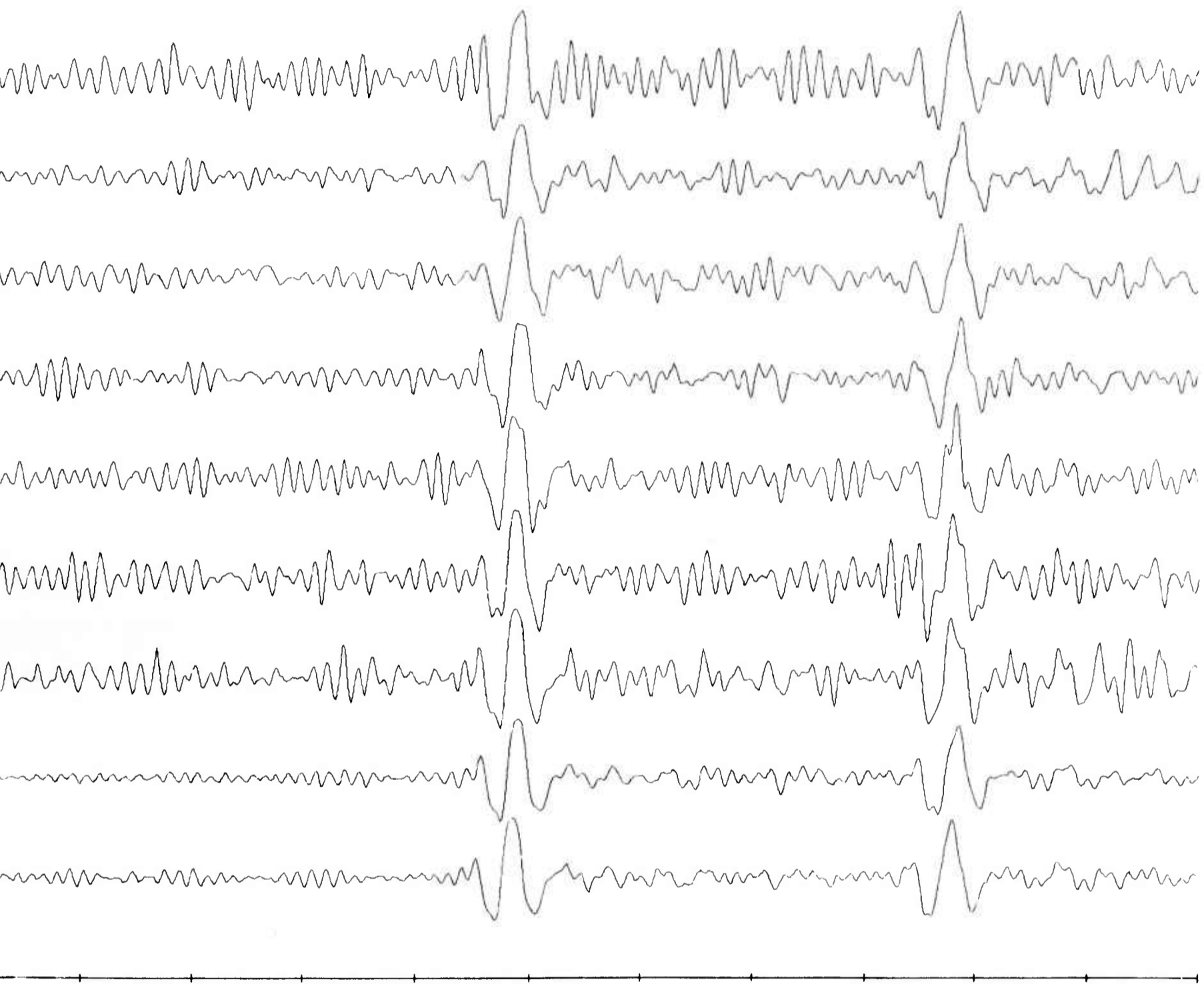
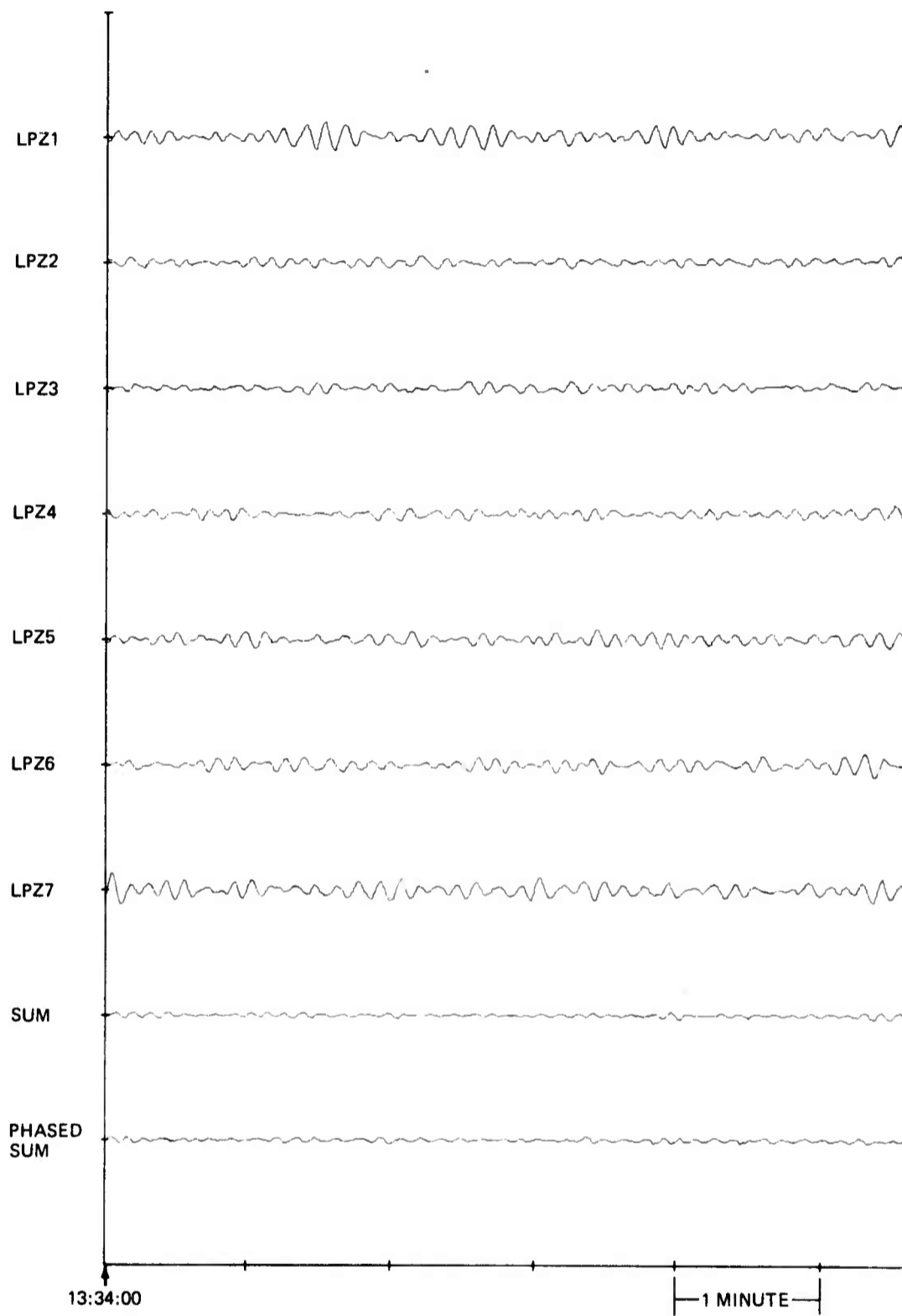


Figure 5. UBSO digital long-period seismogram illustrating the P-wave signal arrival from the New Hebrides Islands on 26 November 1969. Epicentral data:  $\Delta \simeq 95^\circ$ ,  $h = \text{normal}$ , magnitude  $\simeq 4.6$ . (Vertical scale is 1 millimeter = 55.1 millimicrons)

B

-9/10-

TR 69-53



A

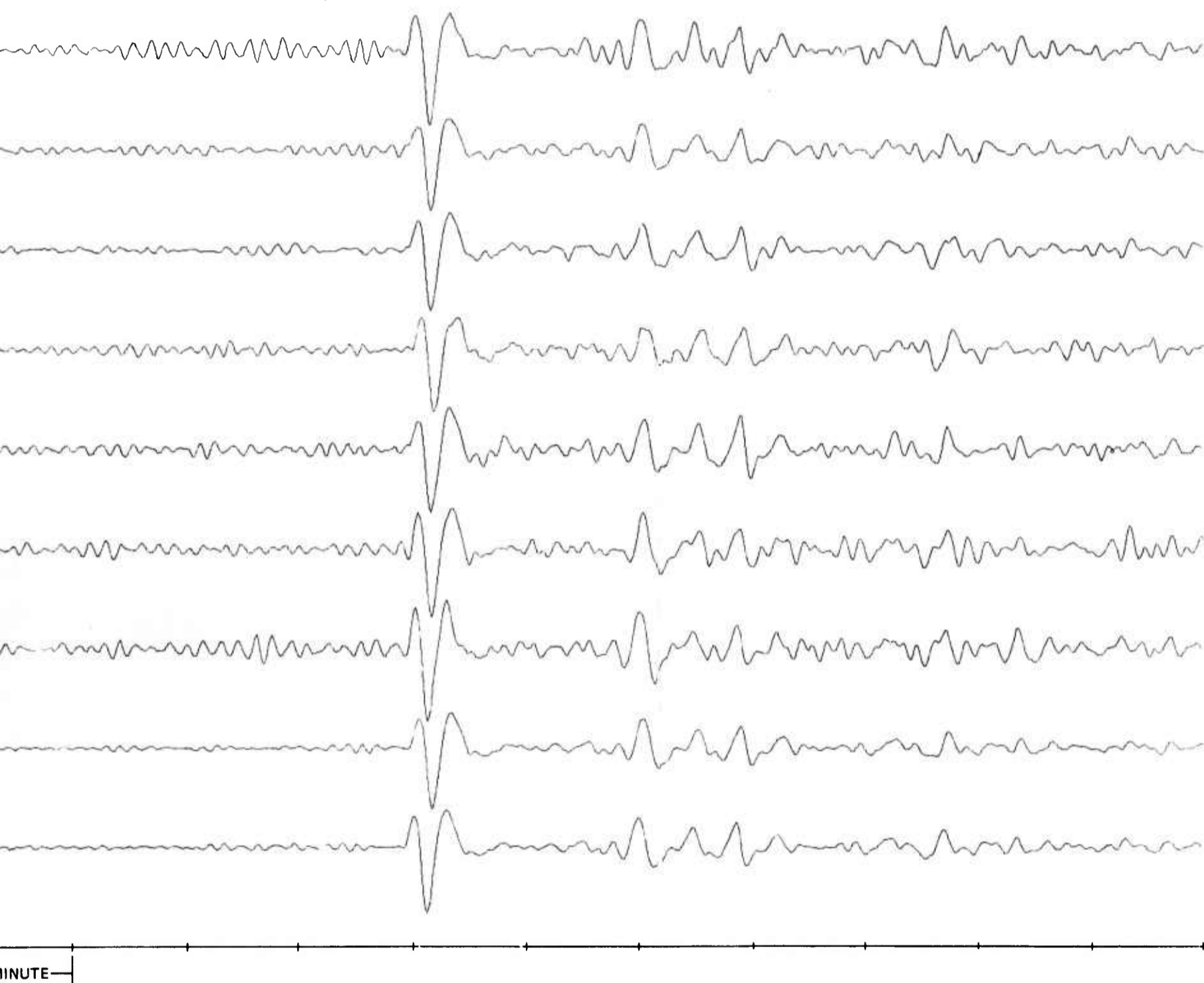


Figure 6. UBSO digital long-period seismogram illustrating the P-wave signal arrival from Sakhalin Island on 18 December 1969. Epicentral data:  $\Delta \approx 70^\circ$ ,  $h \approx 344$  km, magnitude  $\approx 5.9$ . (Vertical scale is 1 millimeter = 218.2 millimicrons)

B

-11/12-

TR 69-53

Table 1. Epicentral data of events<sup>a</sup>

<u>Day</u>	<u>Origin time</u>	<u>Distance from UBSO (degrees)</u>	<u>Direction from UBSO</u>	<u>Latitude (degrees)</u>	<u>Longitude (degrees)</u>	<u>Epicentral region</u>	<u>Depth</u>	<u>CGS mtg MB</u>
13 Nov 69	075129.5	75	SE	27.8 S	71.6 W	Near coast of No. Chile	Normal	5.8
26 Nov 69	133813.6	95	SW	16.8 S	167.7 E	New Hebrides Islands	Normal	4.6
18 Dec 69	133205.2	70	NW	46.3 N	142.5 E	Sakhalin Is.	344 km	5.9

<sup>a</sup> Epicentral data received from C&GS "Preliminary Determination of Epicenter" cards.

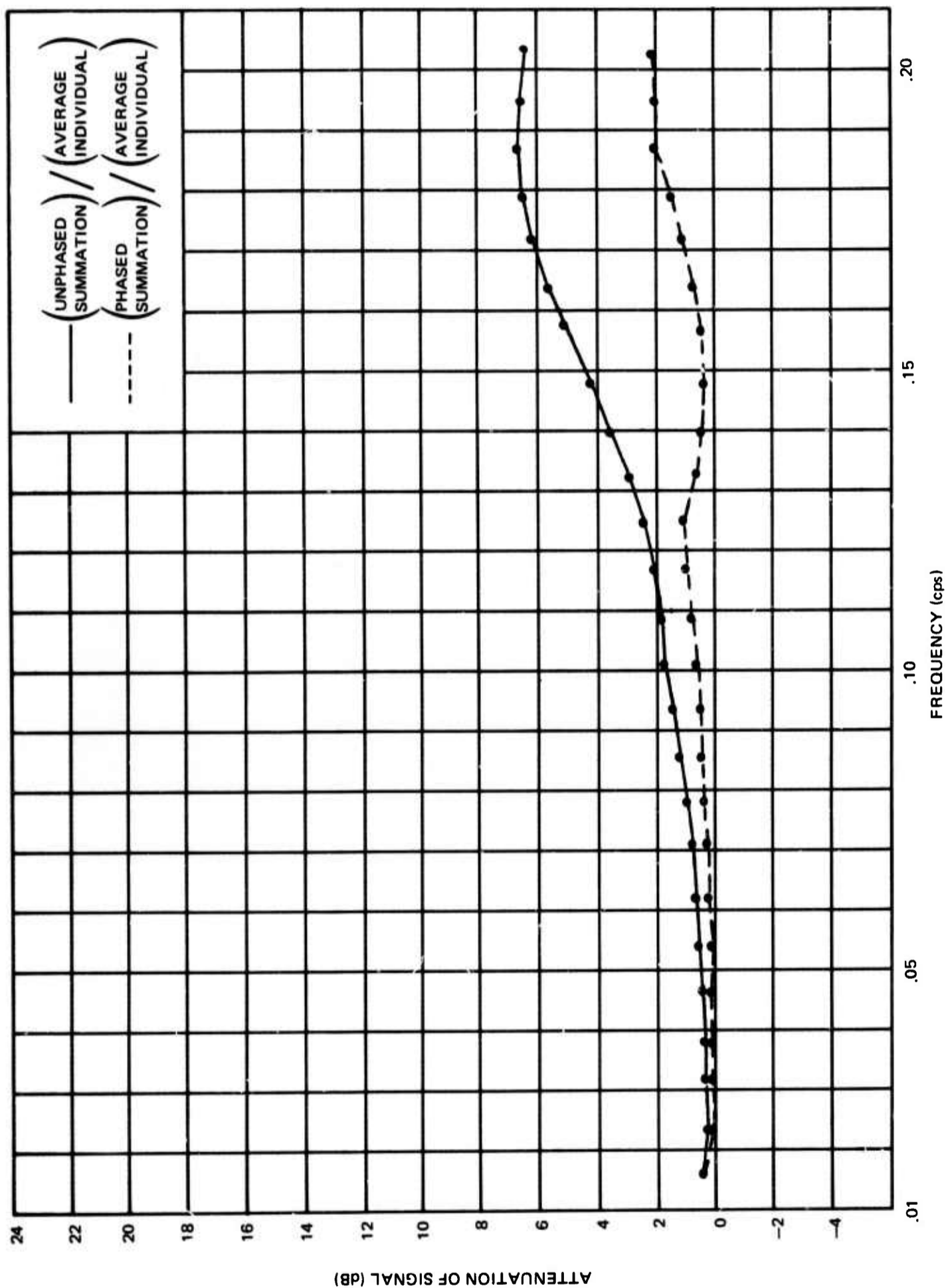


Figure 7. Attenuation by the unphased sum and the phased sum relative to the average individual of a teleseismic P wave recorded at UBSO on 13 November 1969 from the southeast

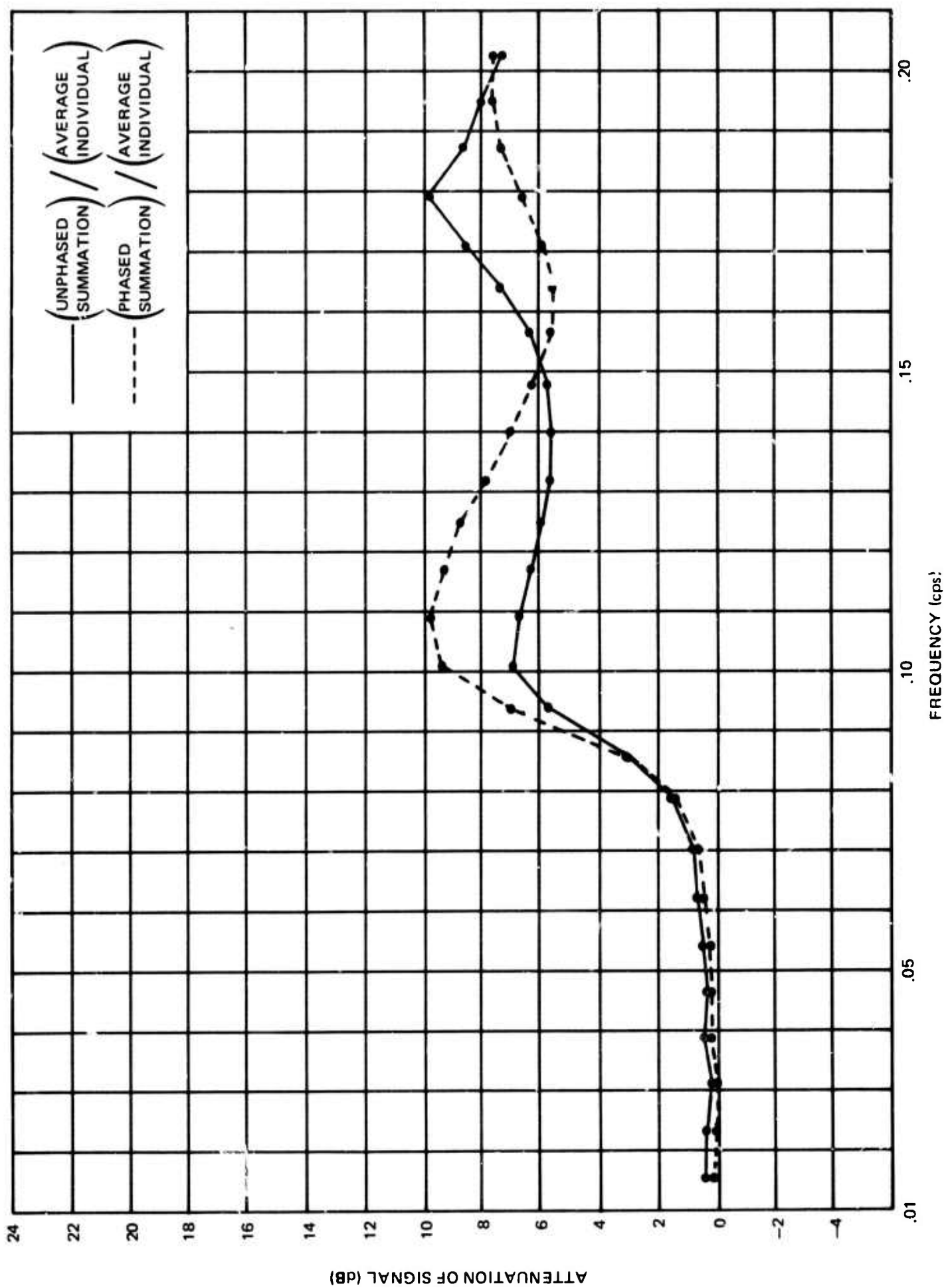


Figure 8. Attenuation by the unphased sum and the phased sum relative to the average individual of a teleseismic P wave recorded at UBSO on 26 November 1969 from the southwest

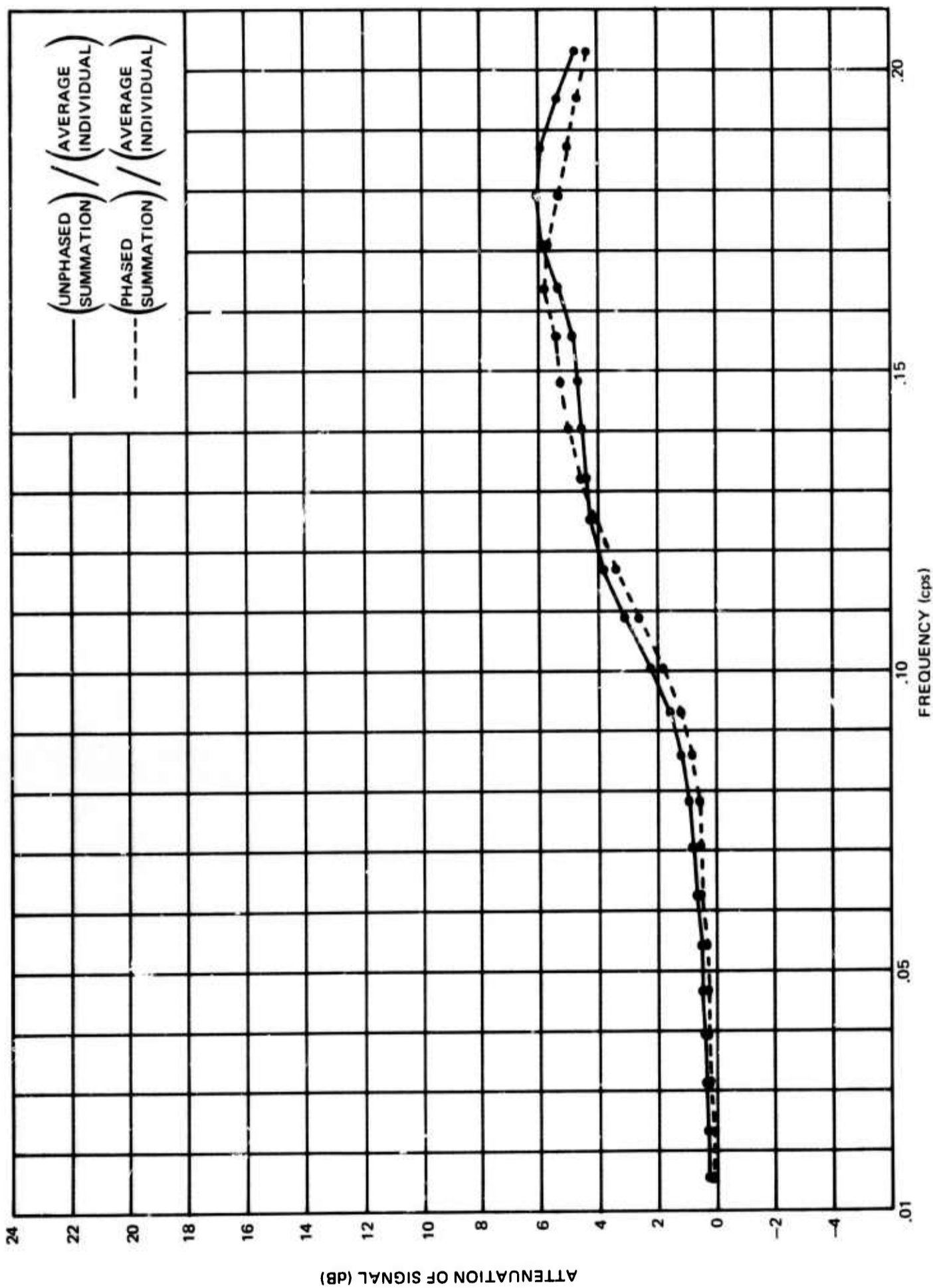


Figure 9. Attenuation by the unphased sum and the phased sum relative to the average individual of a teleseismic P wave recorded at UBSO on 18 December 1969 from the northwest

From the table it is apparent that the improvement of the sum over the phase sum is 0.5 dB for the event from the SE, while the improvement for the other events is 0.3 dB. The relatively small amount of improvement of the phase sum over the straight sum is expected for events at these distances, because the apparent velocities of the body phases across the UBSO array are so great that the maximum delay time over the 23.3 kilometer spacing would be only 3 to 4 seconds. Events occurring at a closer distance than those used in this report would probably give slightly more loss in signal of the straight summation.

## 2.2 NOISE LOSS

The power density spectra plots of the 30-minute noise segments preceding the three P-wave signals are shown in appendix 2. The expected noise peaks in the two frequency bands of 0.05 cps to 0.083 cps and the 0.11 cps to 0.2 cps can be seen in the average individual power density spectra. The large increase in the power density of the higher frequency band (0.11 cps to 0.2 cps) from sample to sample can be seen from the plots. This increase is attributed to the seasonal change in microseismic noise level associated with the winter season. The degree of attenuation of noise spectra of the summations relative to the average individual power density spectra for the three noise samples can be seen in figures 10, 11, and 12. The data indicate that the unphased summation attenuated the noise from approximately 12 dB to over 18 dB between 0.05 cps to 0.083 cps. The phased summation for the event from the SE (13 November) shows approximately the same amount of attenuation as the unphased summations, while phased summations of the events from the SW (26 November) and the NW (18 December) show greater variance in their attenuation of the noise. In the noise frequency band of interest, the phased sum of the SW event varied from 10 dB to 20 dB of noise attenuation, relative to the average individual, while the phased sum of NW event varied from 9 dB to 14 dB. This variance of noise attenuation in relatively small frequency bands is probably due to the presence of a single noise source which is much stronger than the noise sources in the other directions. As the phased sum is beamed in a direction approaching the direction of the strong noise source, the phased sum attenuates the noise less than the straight sum. (This effect will become more apparent in our discussion of Rayleigh waves as the velocity of the noise is much closer to the velocity of the Rayleigh wave than the apparent velocity of the P wave.)

## 2.3 SIGNAL-TO-NOISE IMPROVEMENT FOR P WAVES

The signal-to-noise ratios were calculated using the power density spectra of the signals and noise. The plots of the signal-to-noise ratio for the three P-wave signals are shown in appendix 3.

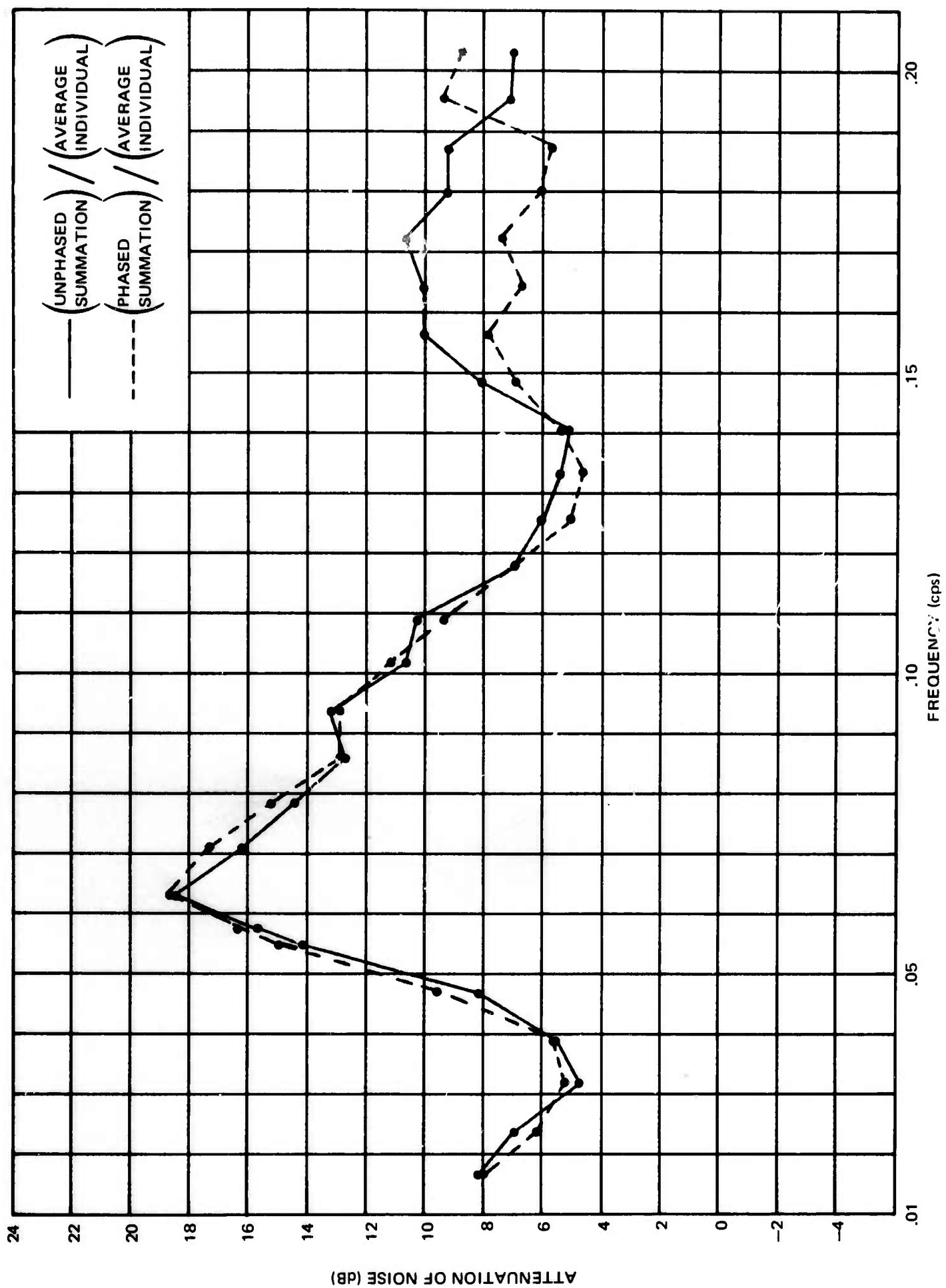


Figure 10. Noise attenuation achieved by the unphased sum and the phased sum relative to an average individual for a noise sample recorded at UBSO on 13 November 1969 (phased sum beamed to a P wave from the southeast)

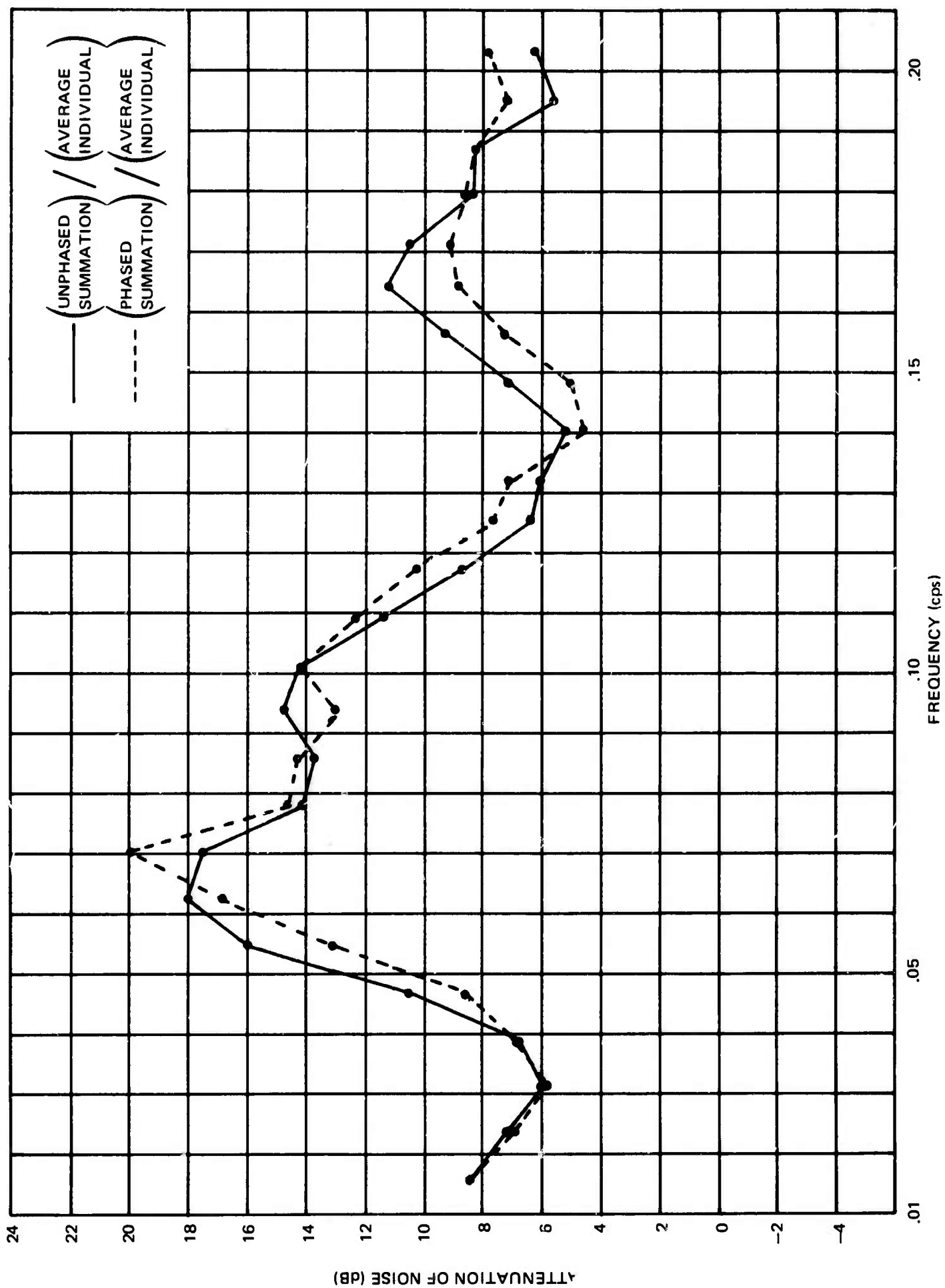


Figure 11. Noise attenuation achieved by the unphased sum and the phased sum relative to an average individual for a noise sample recorded at UBISO on 26 November 1969 (phased sum beamed to a P wave from the southwest)

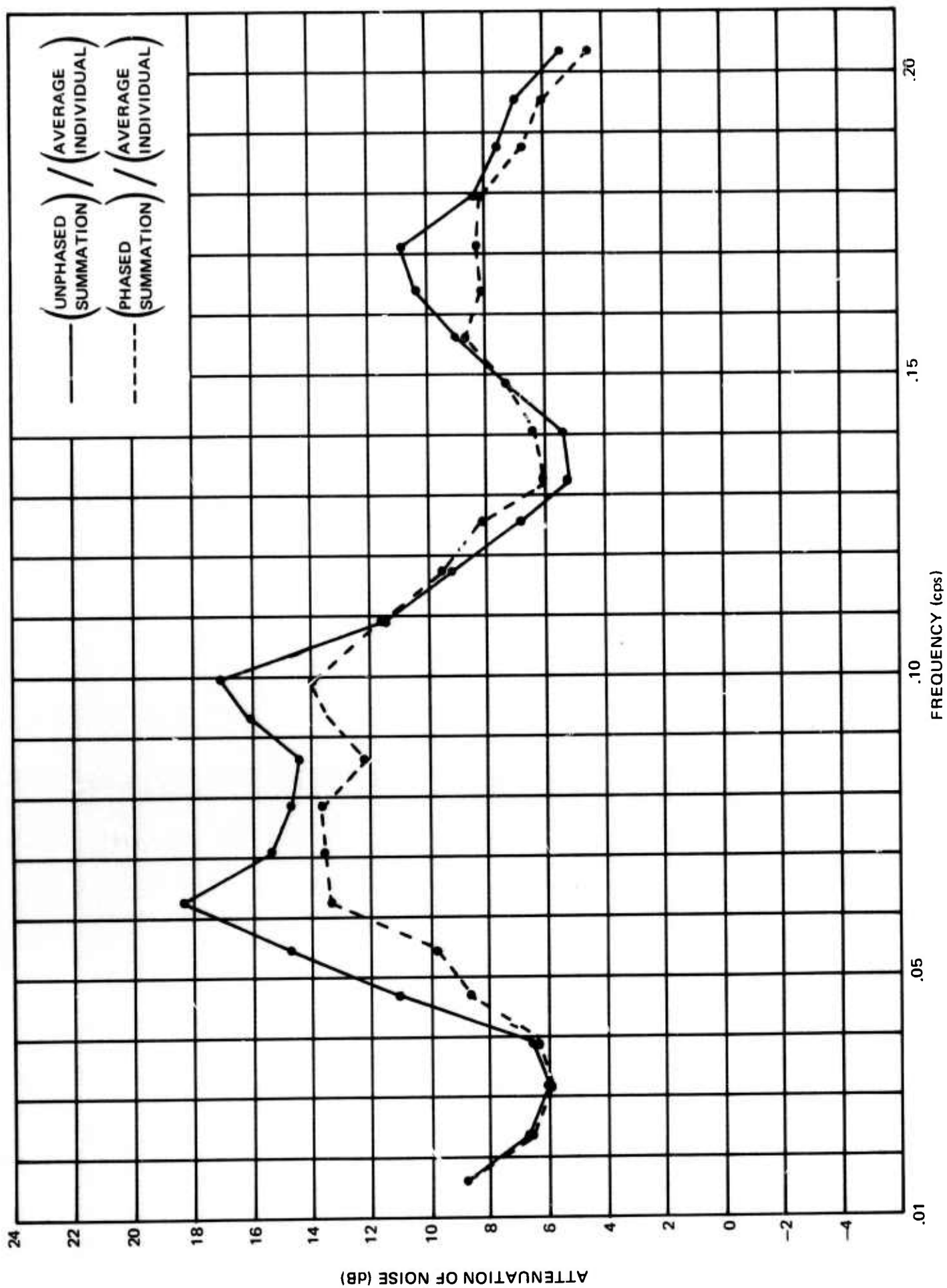


Figure 12. Noise attenuation achieved by the unphased sum and the phased sum relative to an average individual for a noise sample recorded at UBISO on 18 December 1969 (phased sum beamed to a P wave from the northwest)

The signal-to-noise improvement (figures 13, 14, and 15) of the unphased sum and phased sum as compared to the averaged individual seismogram indicates that the unphased sum of the three signals had maximum improvement of over 17 dB for the three samples chosen at approximately 0.0625 cps (the frequency of the peak noise power). However, the frequency of maximum improvement achieved by the phased sum varied from sample to sample because of the directional characteristics of the noise sources. The improvement at a given frequency is primarily determined by the direction to which the beam is tuned and the directional characteristics of the noise source at that particular wave number. The signal-to-noise improvement of the unphased sum versus the phased sum is primarily determined by the noise attenuation since there is a very small amount of signal loss due to summations of P-wave signals.

The event recorded from the SE and SW on 13 and 26 November showed that over most of the band, the unphased sum and phased sum offered about the same degree of signal-to-noise improvement. However, the phased sum of the NW event (18 December) shows about 4 dB less improvement than the unphased sum but attenuated the noise more than 11 dB, relative to the individual seismogram, over the entire signal band.

The following table shows the signal-to-noise ratio improvement of the two summations at the frequency of peak signal power.

S/N Improvement at peak signal power frequency

<u>Direction of event</u>	<u>Peak power frequency</u>	<u>Sum improvement</u>	<u>Phase sum improvement</u>
SE	.055 cps	13.5 dB	14.8 dB
SW	.039 cps	6.2 dB	6.6 dB
NW	.047 cps	10.5 dB	8.4 dB

As expected, the event that occurred on 13 November with a frequency closer to the peak noise power (.0625 cps) showed the greatest improvement on both summations, while the event of 26 November (SW), with a frequency farther away from the peak noise frequency, was improved least.

The following table shows the improvement due to the noise attenuation at the average peak noise power frequency.

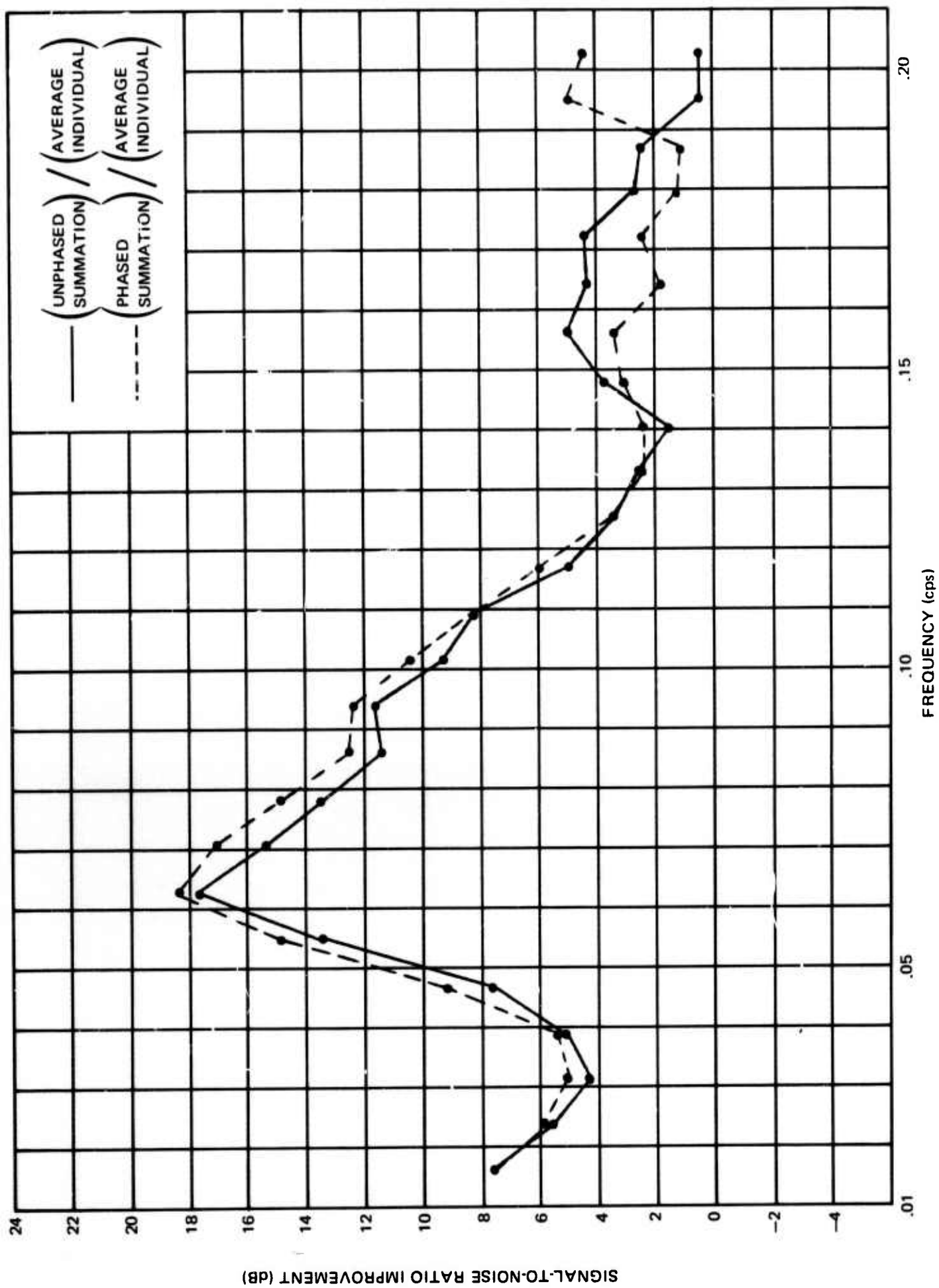


Figure 13. Improvement in signal-to-noise ratio exhibited by the unphased sum and the phased sum relative to an average individual for a teleseismic P wave recorded at UBEO on 13 November 1969 from the southeast

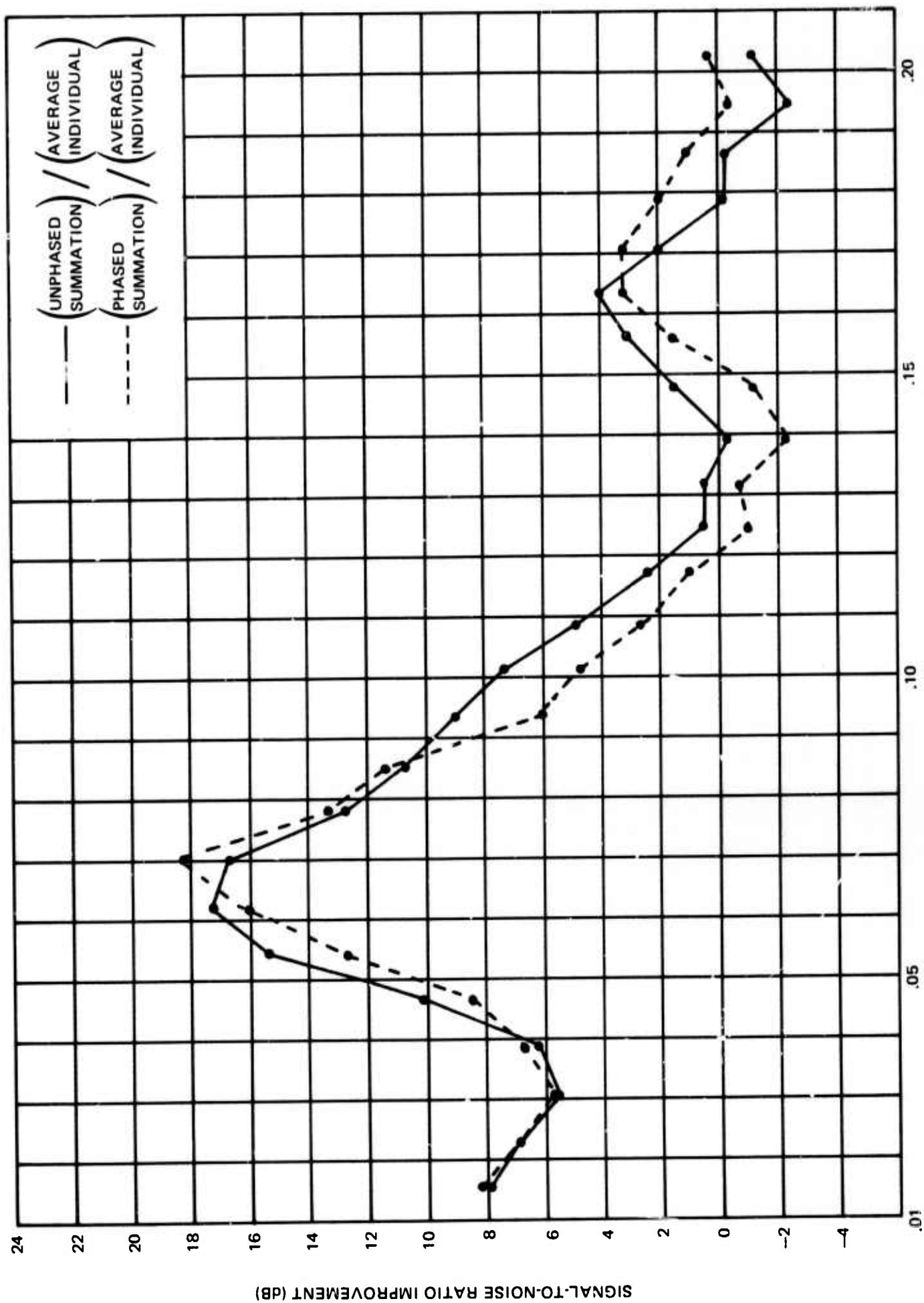


Figure 14. Improvement in signal-to-noise ratio exhibited by the unphased sum and the phased sum relative to an average individual for a teleseismic P wave recorded at UBSO on 26 November 1969 from the southwest

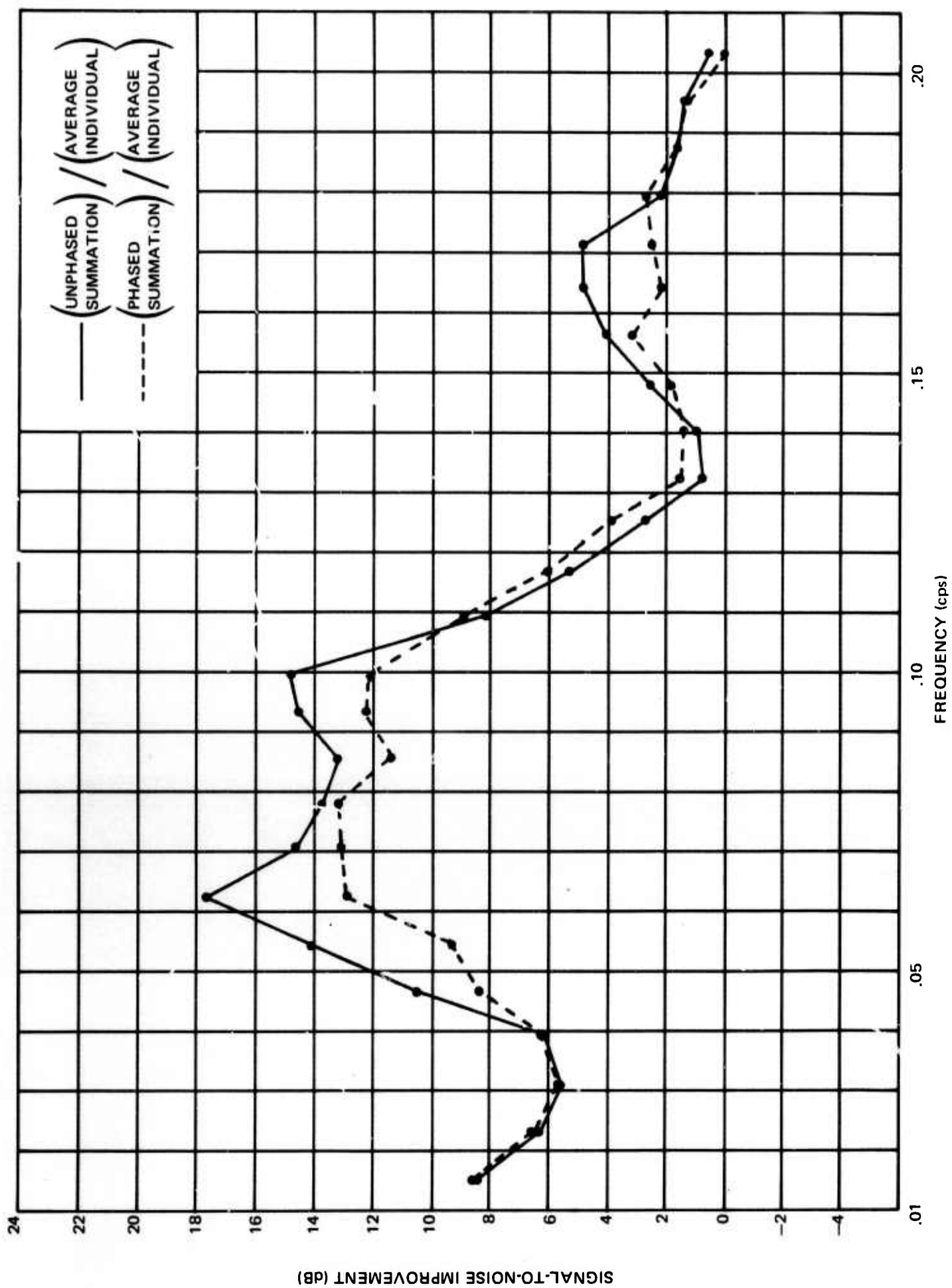


Figure 15. Improvement in signal-to-noise ratio exhibited by the unphased sum and the phased sum relative to an average individual for a teleseismic P wave recorded at UBSO on 18 December 1969 from the northwest.

S/N Improvement at average peak noise power (.0625 cps)

<u>Direction of event</u>	<u>Sum improvement</u>	<u>Phase sum improvement</u>
SE	17.8 dB	18.5 dB
SW	17.3 dB	16.5 dB
NW	17.8 dB	13.0 dB

3. RAYLEIGH WAVES

The Rayleigh waves used to determine the detection capability of the UBSO long-period array were from the same events as those used for the P-wave study. The epicentral location, date, magnitude, and additional information are shown in table 1. The digital plots showing the recordings of the seven individual vertical long-period instruments recorded on UBSO digital tape are shown in figures 16, 17, and 18. Also included on each plot are the unphased sum and phased sum generated from the digital samples of the seven instruments.

3.1 ATTENUATION OF RAYLEIGH WAVE SIGNALS

The complexity of Rayleigh waves complicates the determination of the amount of signal loss on the summations. Note the element-to-element variation in characteristics shown on the digital plots of the 13 November event (figure 16). The coda of the Rayleigh signal from the 26 November event shows more element-to-element consistency than did the 13 November event. The Rayleigh waves of the 18 December event is to a large extent overridden by the background noise; but the spectral data indicate a minimum amount of variation from seismograph to seismograph.

This lack of consistency after the first few cycles makes accurate determination of the most representative value of the power on the individual traces difficult because of the great variance in power at the shorter periods of the Rayleigh wave signal from instrument to instrument. The mean of the power density spectra of the seven vertical traces was selected to represent the individual density spectra over the 10-minute signal segment.

The dispersive characteristic of Rayleigh waves further degrades the effectiveness of the unphased summation because signal loss due to instrument separation is greatest at the shorter periods. With the peak power of the average individual being concentrated in the higher frequencies, the amount of signal loss on the straight sum should be considered at not only the peak power of the individual, but at the frequency of the first few cycles. The following table

presents the frequency of the first few cycles (obtained from digital plot) and the peak power frequency of the power density spectra (shown in appendix 1).

#### Frequencies in the Rayleigh wave

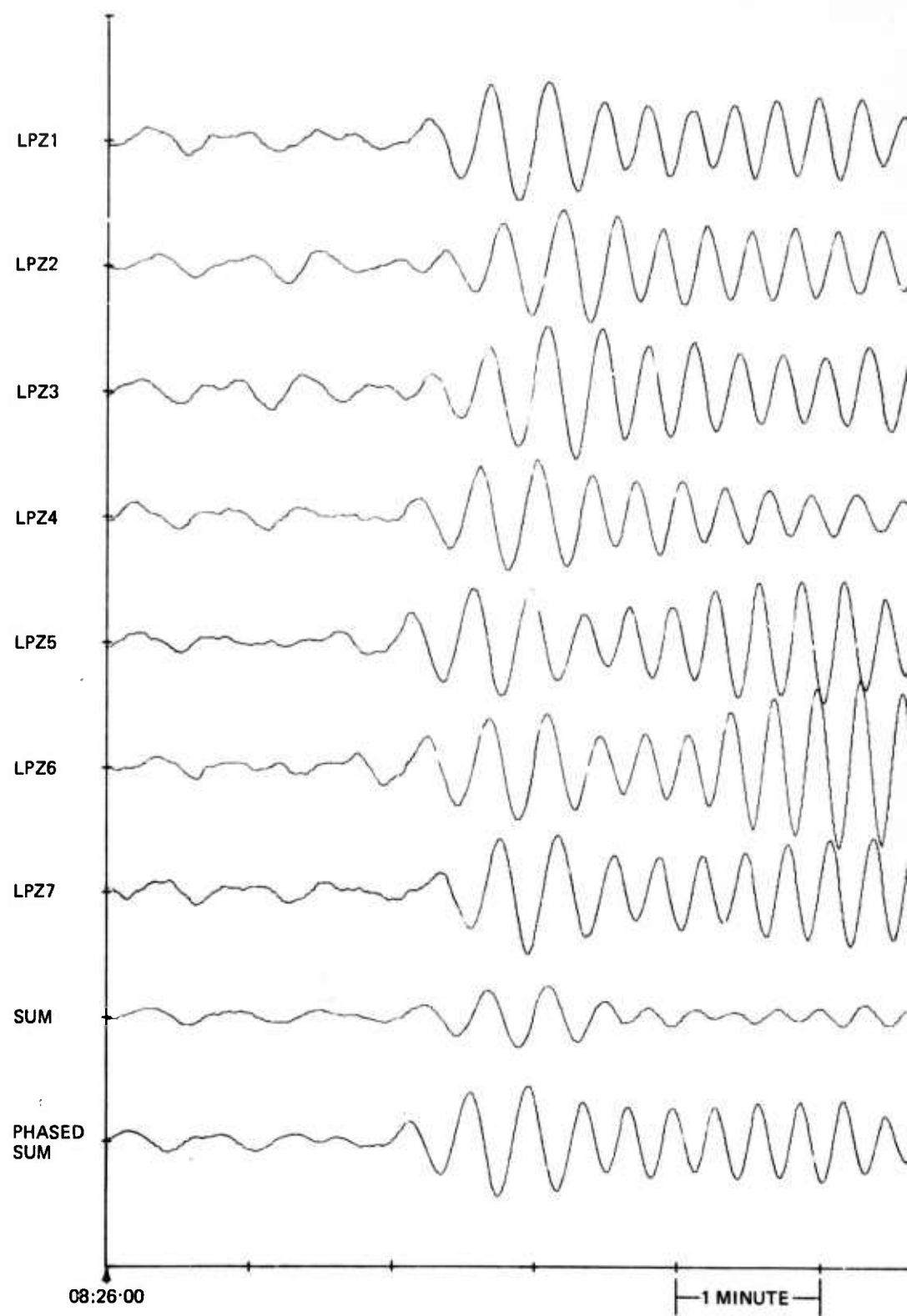
<u>Date</u>	<u>Frequency of first few cycles (cps)</u>	<u>Individual peak power (cps)</u>	<u>Unphased peak power (cps)</u>	<u>Phased peak power (cps)</u>
13 Nov 69	0.041	0.056	0.039	0.054
26 Nov 69	0.031	0.047	0.039	0.047
18 Dec 69	0.034	0.031	0.031	0.031

The degree of signal loss at selected frequencies of the power density can be seen in figures 19, 20, and 21. As to be expected from the instrument separation of the LP array, the unphased sum shows greater signal loss at all frequencies in the Rayleigh wave frequency-band than the phased sum. The maximum attenuation of the unphased sum occurred at the higher frequencies of the coda of the Rayleigh waves of the three events. Note that the 18 December event shows little effects of dispersion and had less than 10 dB of signal loss at the higher frequencies while the two events showing this maximum dispersive effect lose over 18 dB of power. At the frequencies of the first few cycles of each event the degree of signal loss was only 7 dB, 7.9 dB, and 3.2 dB, respectively.

The phased sum also suffered greater signal loss in the higher Rayleigh frequencies but the maximum attenuation was only 4.4 dB on the 13 November event. An interesting observation is the signal loss of the phased sum on the 26 November event. This event showed the dispersive effects, but had less than 1 dB of signal loss in the Rayleigh wave frequency band. The good predictability of this Rayleigh wave compared to the other two events indicates the possibility that the signal loss at the higher frequencies on the 13 November and the 18 December events is due more to the inability to determine the signal power of the average individual than to the array design.

### 3.2 NOISE ATTENUATION

The two noise fields that usually peak between 0.05 cps to 0.083 cps and between 0.11 cps to 0.2 cps were discussed in section 2.2. As was the case in the P-wave discussion, the signal frequency band for Rayleigh waves is outside the higher frequency noise band. Therefore, the Rayleigh wave study also concentrated primarily on the lower frequency band; however, all spectral plots include both frequency bands.



A

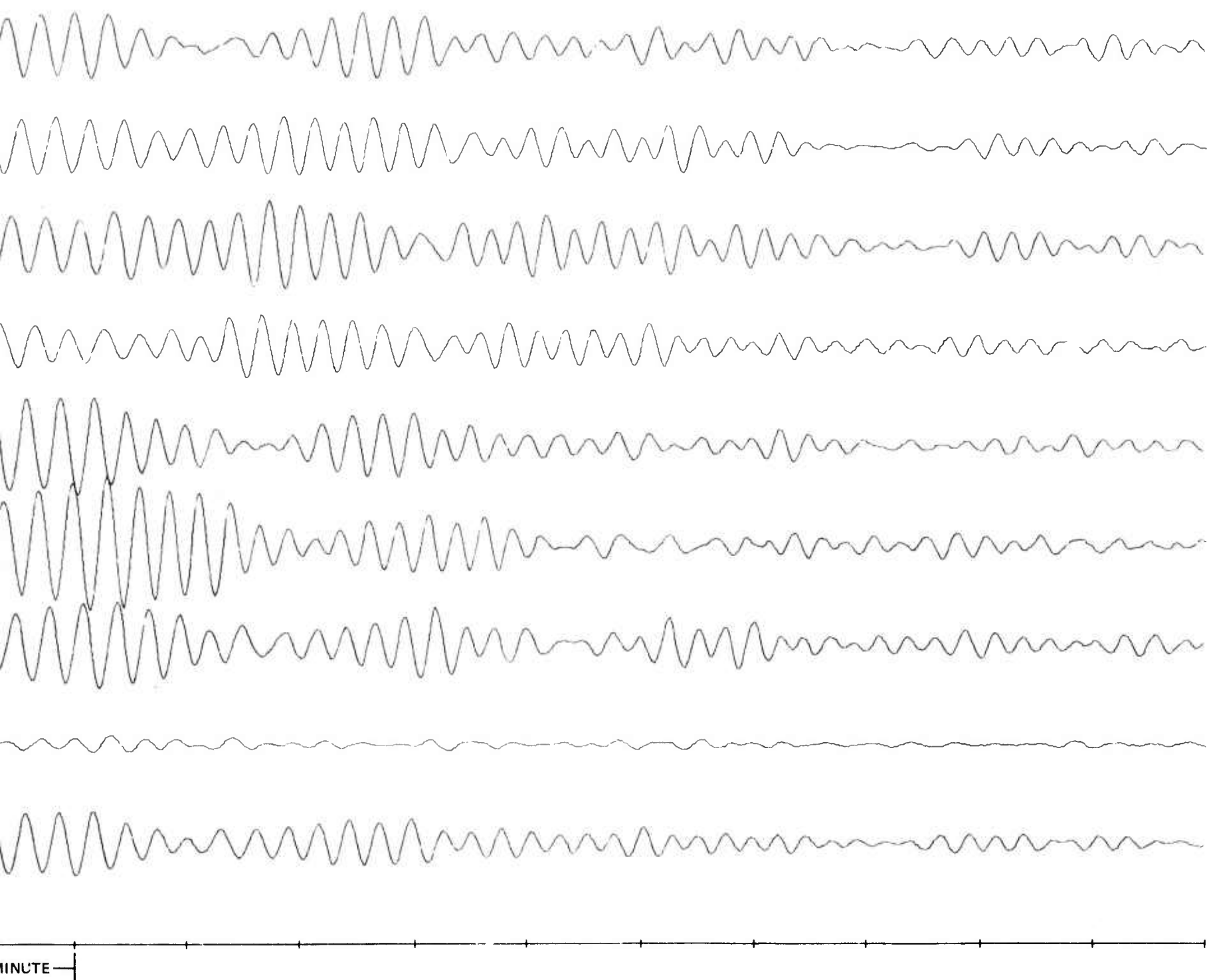
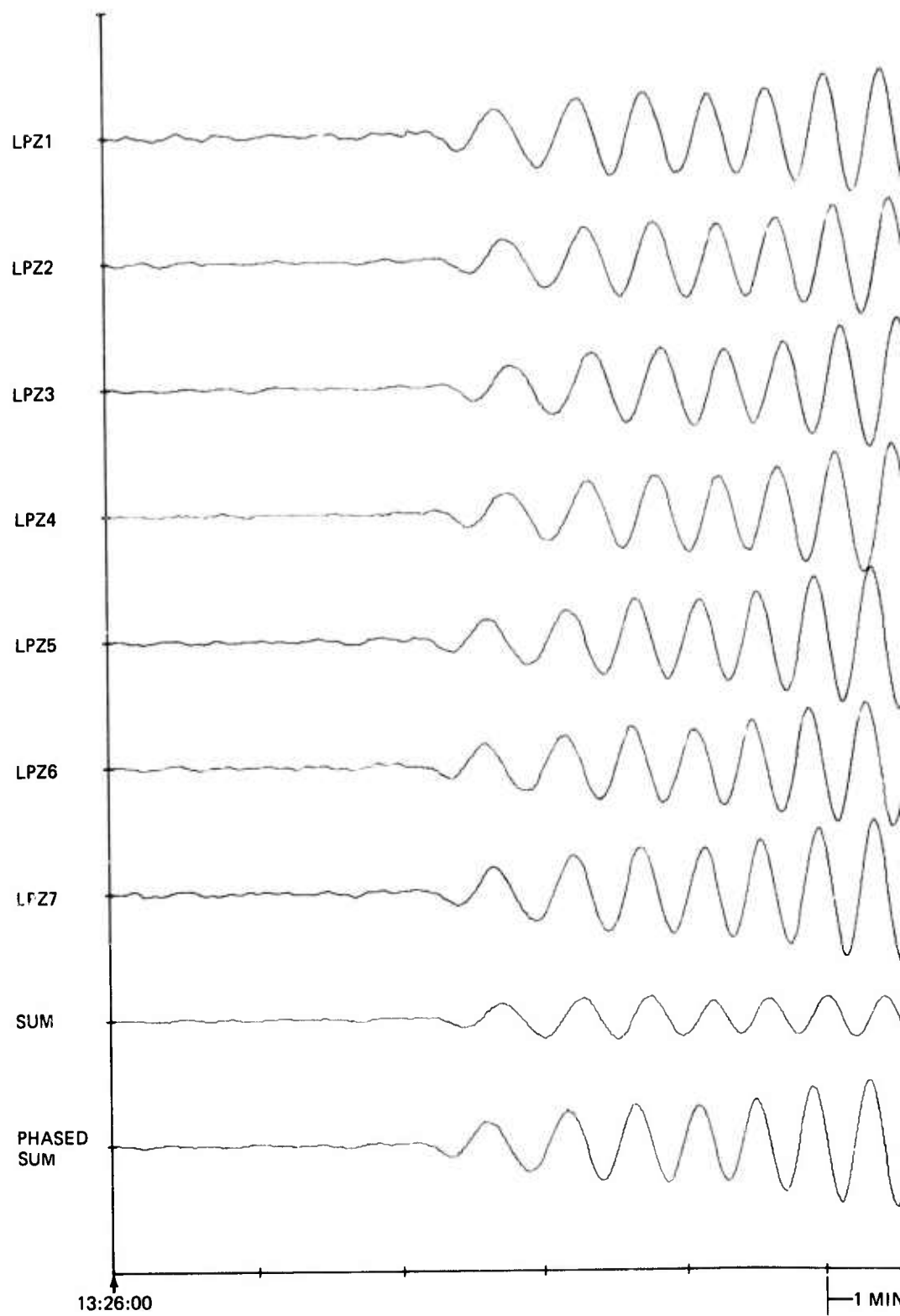


Figure 16. UBSO digital long-period seismogram illustrating the Rayleigh wave arrival from the northern coast of Chile on 13 November 1969. Epicentral data:  $\Delta \approx 75^\circ$ ,  $h = \text{normal}$ , magnitude  $\approx 5.8$ . (Vertical scale is 1 millimeter = 496.2 millimicrons)

B

-27/28-

TR 69-53



A

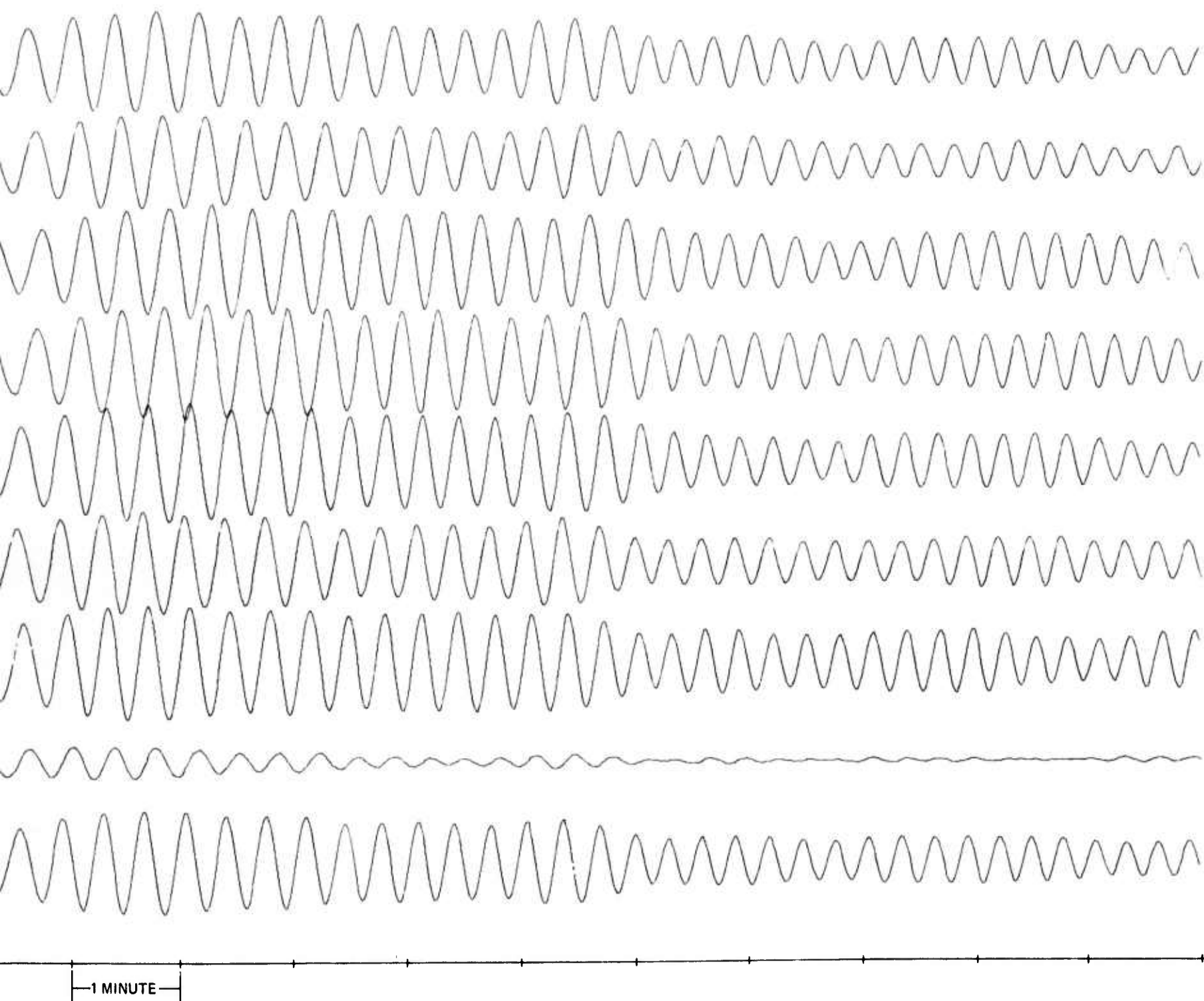
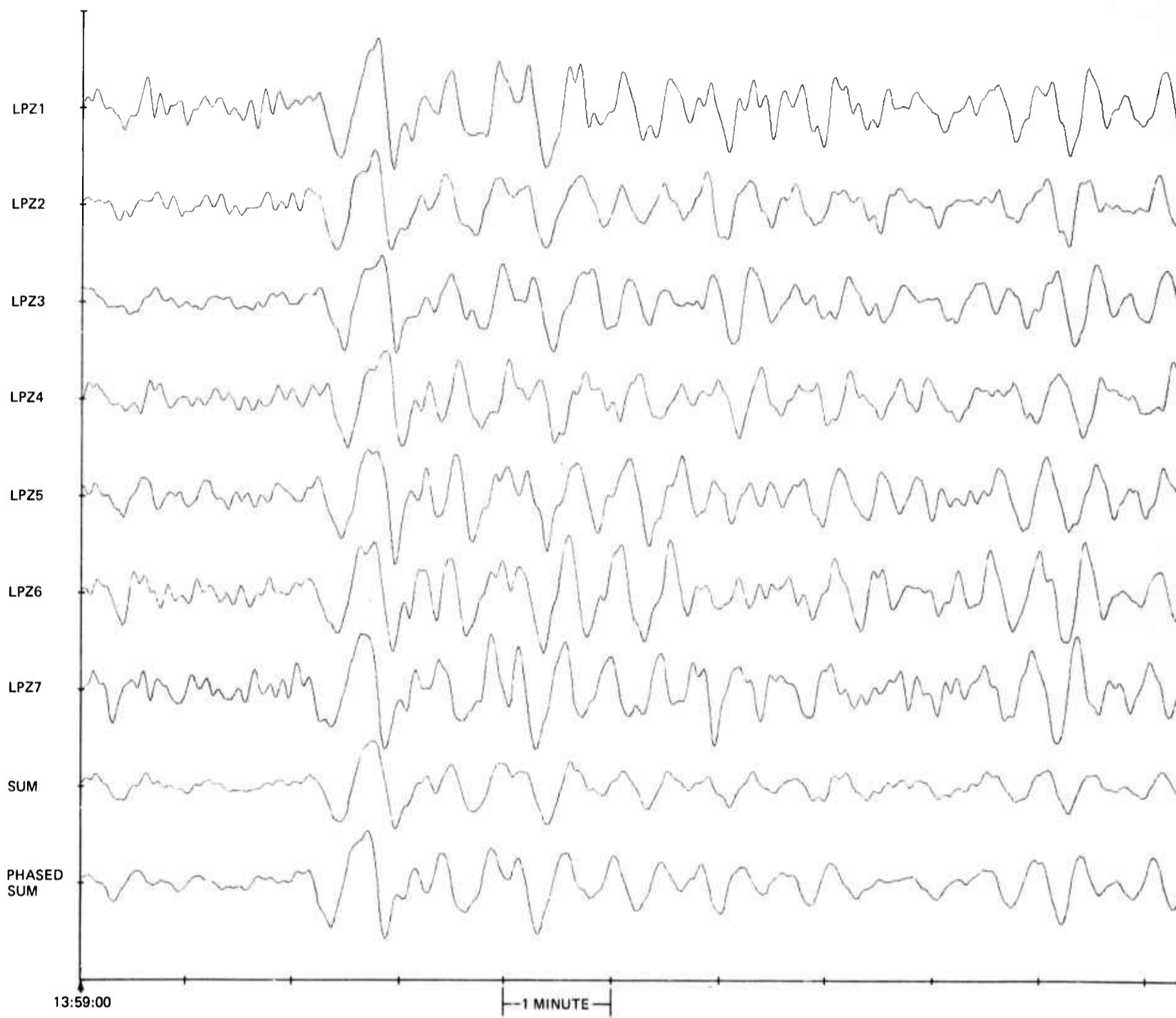


Figure 17. UBSO digital long-period seismogram illustrating the Rayleigh wave arrival from the New Hebrides Islands on 26 November 1969. Epicentral data:  $\Delta \approx 95^\circ$ ,  $h = \text{normal}$ , magnitude  $\approx 4.6$ . (Vertical scale is 1 millimeter = 1101.5 millimicrons)



A

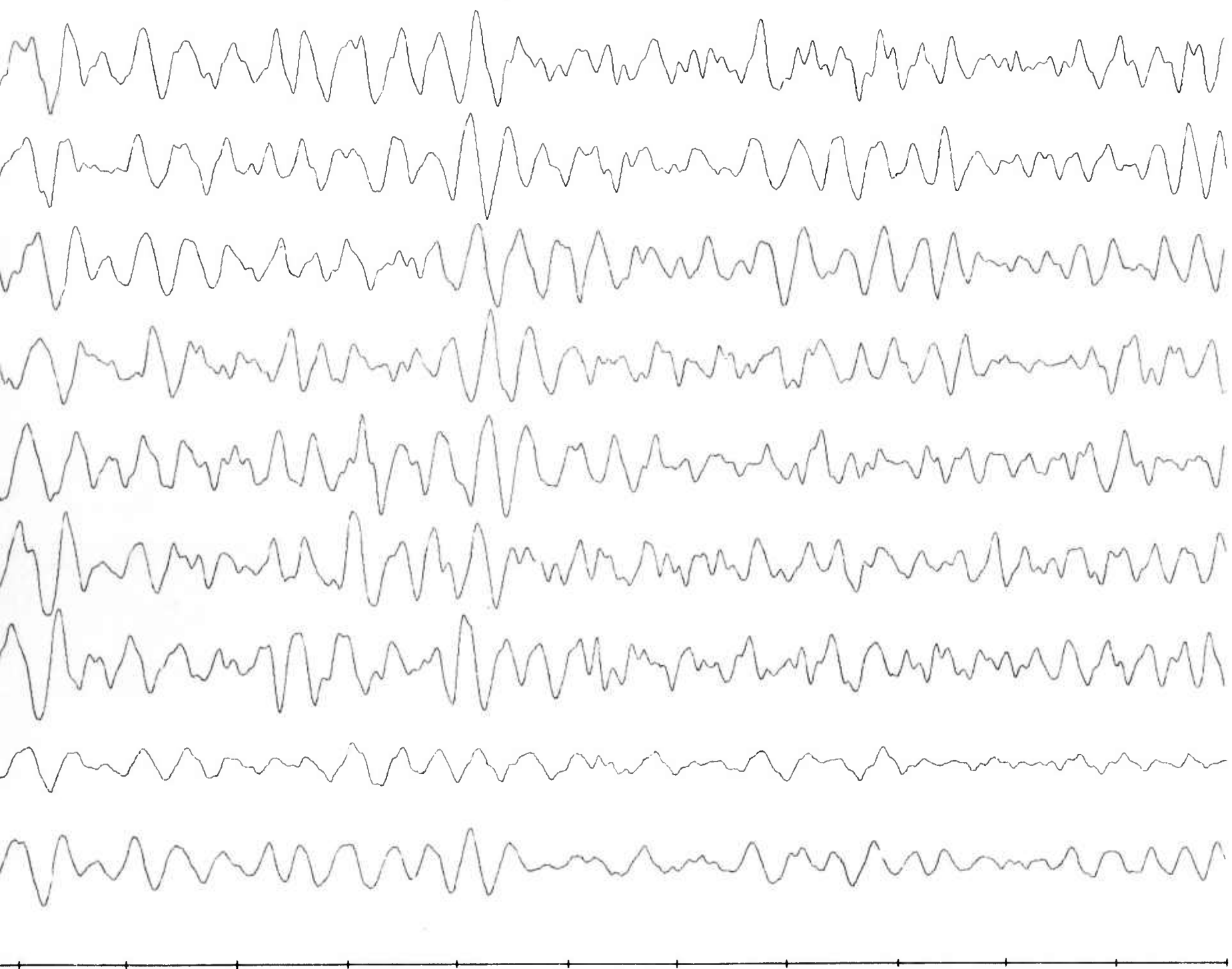


Figure 18. UBSO digital long-period seismogram illustrating the Rayleigh wave arrival from Sakhalin Island on 18 December 1969. Epicentral data:  $\Delta \approx 70^{\circ}$ ,  $h \approx 344$  km, magnitude  $\approx 5.9$ . (Vertical scale is 1 millimeter = 171.8 millimicrons)

B

-31/32-

TR 69-53

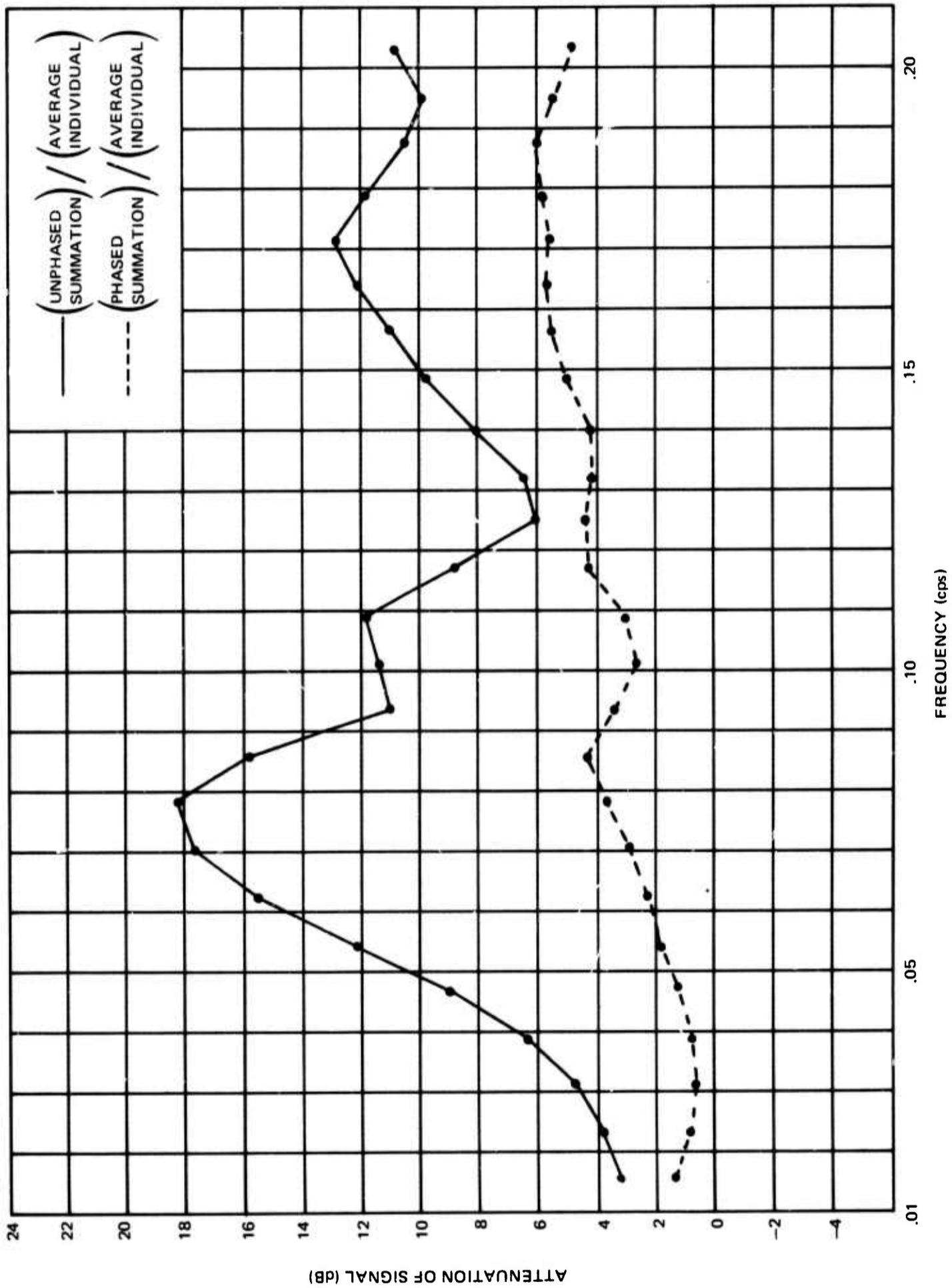


Figure 19. Attenuation by the sum and the phased sum relative to the average individual of a Rayleigh signal recorded at UBSO on 13 November 1969 from the southeast

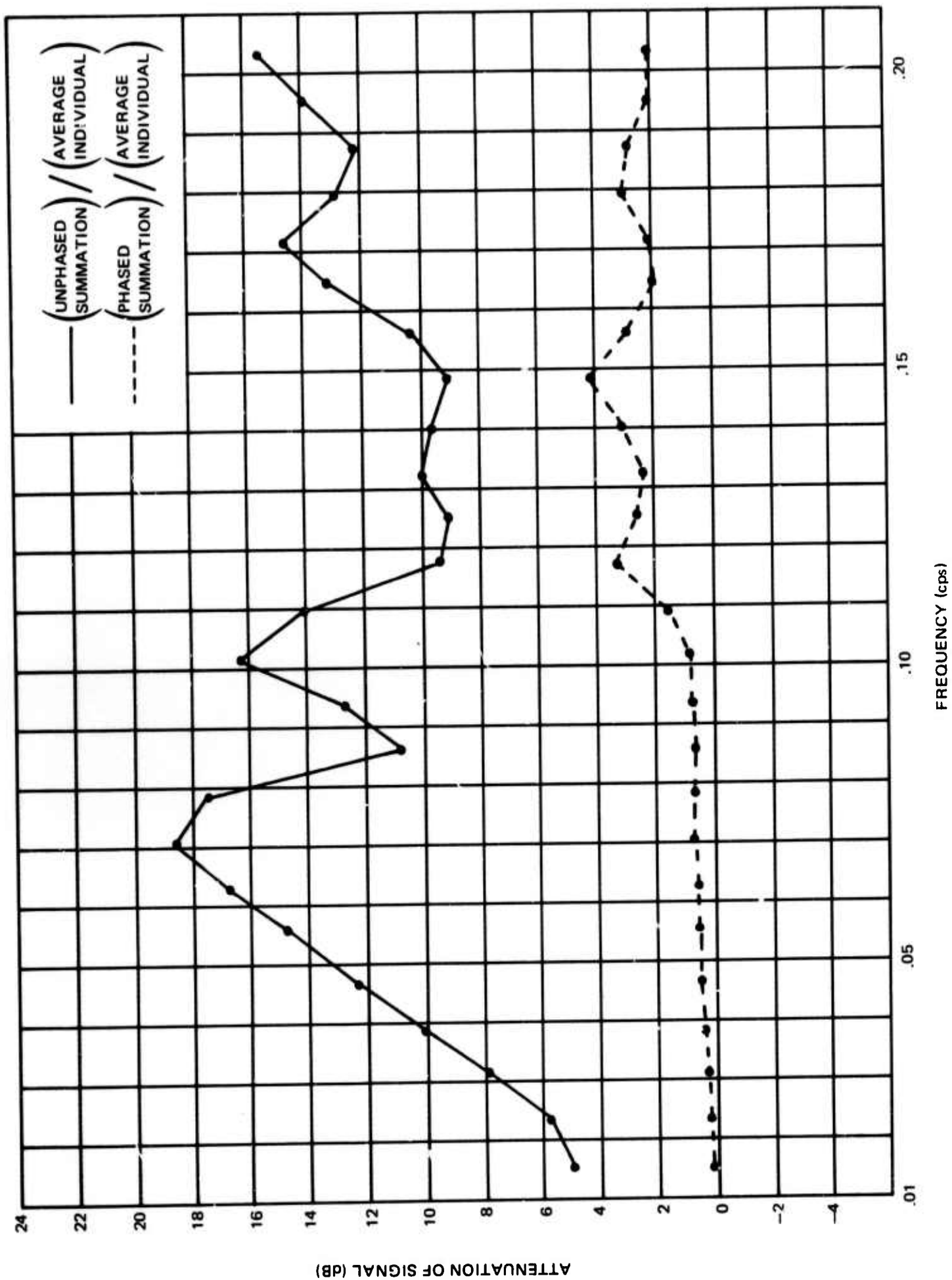


Figure 20. Attenuation by the sum and the phased sum relative to the average individual of a Rayleigh signal recorded at UBSO on 26 November 1969 from the southwest

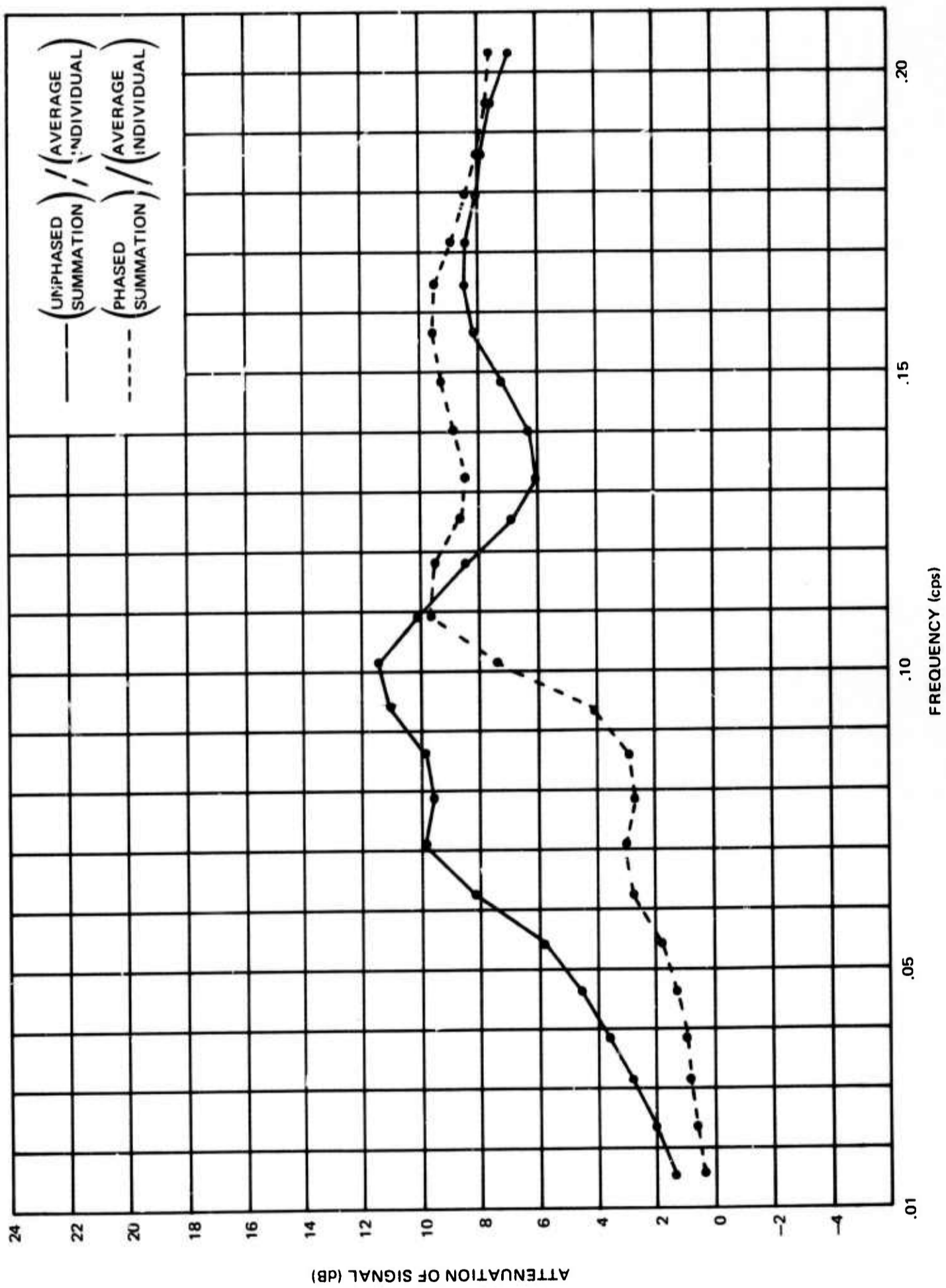


Figure 21. Attenuation by the sum and the phased sum relative to the average individual of a Rayleigh signal recorded at UBSO on 18 December 1969 from the northwest

The noise power density spectra (shown in appendix 2) of the noise segment recorded preceding the events on 13 November, 26 November, and 18 December indicate that the frequencies of the peak noise power in the lower frequency band were 0.066, 0.064, and 0.055 cps, respectively.

The spectral density of individuals of 18 December noise segment indicated a large increase in power at approximately 0.055 cps and secondarily at approximately 0.07 cps, a peak occurring in all three samples. Review of the UBSO 16-millimeter film, from which the higher frequency noise has been filtered, there was an apparent increase in the average trace amplitude of the background noise on the 18 December sample relative to the earlier events. Further investigations indicated that the noise band peaking at 0.055 cps was from the WNW traveling at a velocity across the array of approximately 3.4 km per second.

The attenuation of the noise by both the phased and unphased summations relative to the average individual can be seen in figures 22, 23, and 24. On all three noise samples the unphased sum shows maximum improvement of over 17 dB at 0.0625 cps, which is approximately the peak noise frequency on 13 and 26 November. The unique peak noise frequency at 0.055 cps on the 18 December sample was attenuated by the same amount as the other samples but the phased sum showed approximately 8 dB less improvement than the unphased sum. This lack of improvement on the phased sum between 0.04 cps and 0.07 cps is assumed to result from the fact that the event and the noise source are from close to the same general direction from UBSO.

On the phased sum of all three noise samples it is apparent that it is difficult to predict the amount of attenuation in the Rayleigh wave frequency band. With the predominant noise traveling at approximately the same velocity and frequency as the Rayleigh waves from an event, the amount of attenuation is primarily determined by the strength of the noise source in the direction of the beam.

### 3.3 SIGNAL-TO-NOISE IMPROVEMENT FOR RAYLEIGH WAVES

The signal-to-noise improvement of the phased and unphased summations relative to the average individual were calculated from the signal-to-noise using the power density spectra. A plot of the signal-to-noise ratios of the average individual, phased sum, and unphased sum can be seen in appendix 3. The events of 13 November and 26 November show greater improvement in signal-to-noise (figures 25 and 26) on the phased sum than the unphased sum. The phased sum indicated improvement of over 6 dB in the Rayleigh wave signal on the two events, while the unphased sum had a maximum improvement of only 2.9 dB. This maximum occurred on the two events at the frequency of the unphased summation's maximum noise attenuation.

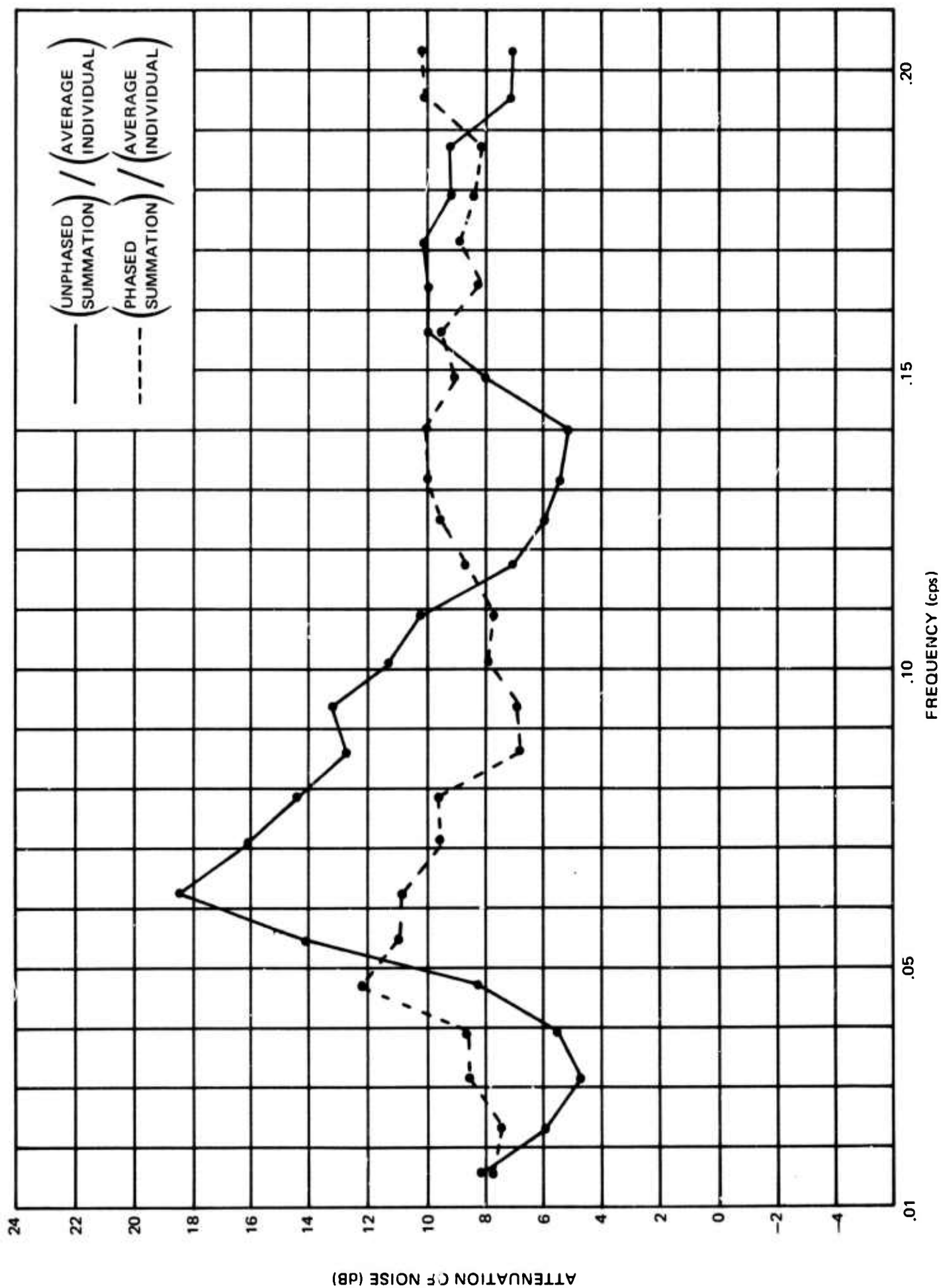


Figure 22. Noise attenuation achieved by the unphased sum and the phased sum relative to an average individual for a noise sample recorded at UBSO on 13 November 1969 (phased sum beamed to a Rayleigh wave from the southeast)

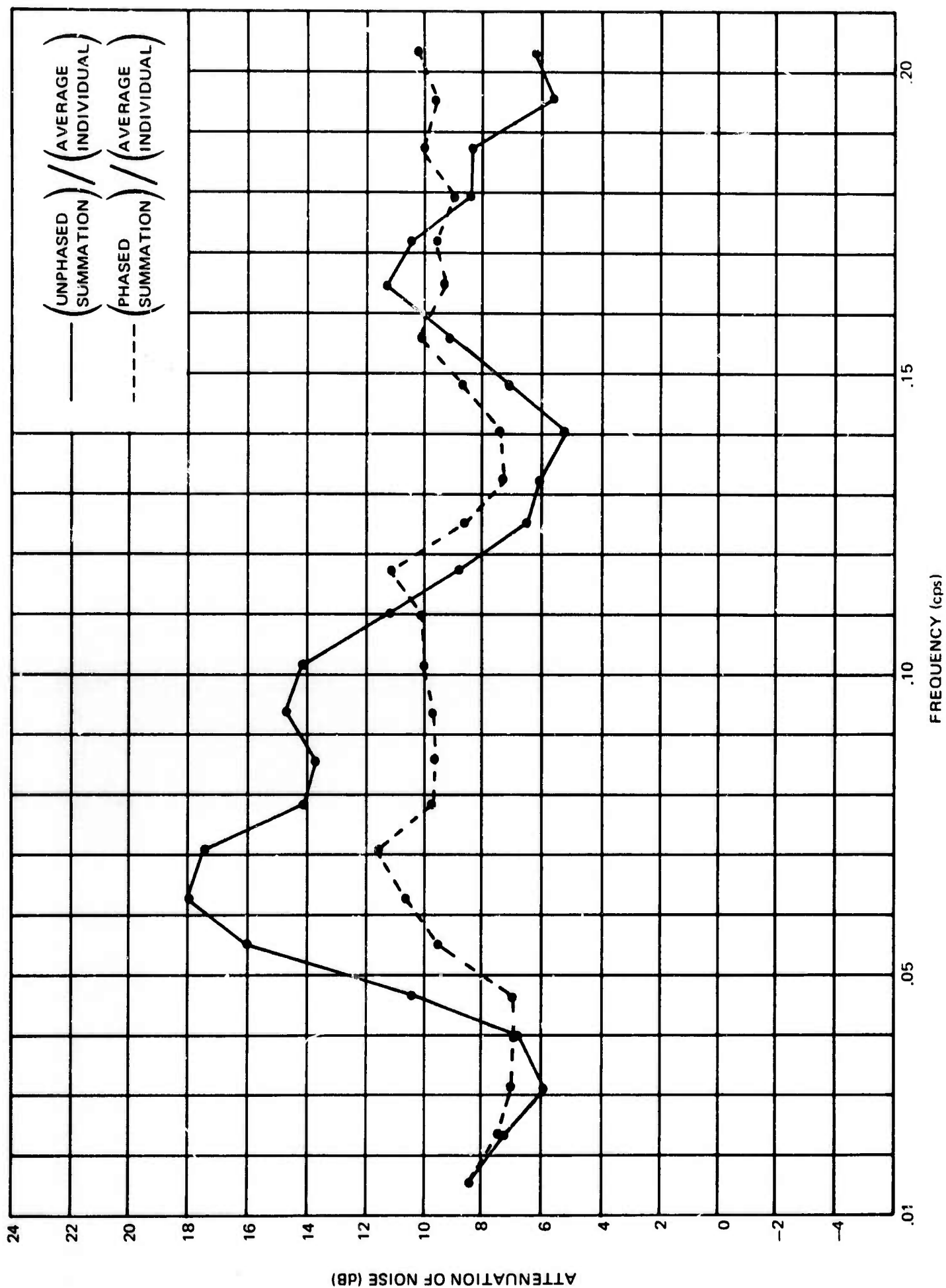


Figure 23. Noise attenuation achieved by the unphased sum and the phased sum relative to an average individual for a noise sample recorded at UBSO on 26 November 1969 (phased sum beamed to a Rayleigh wave from the southwest)

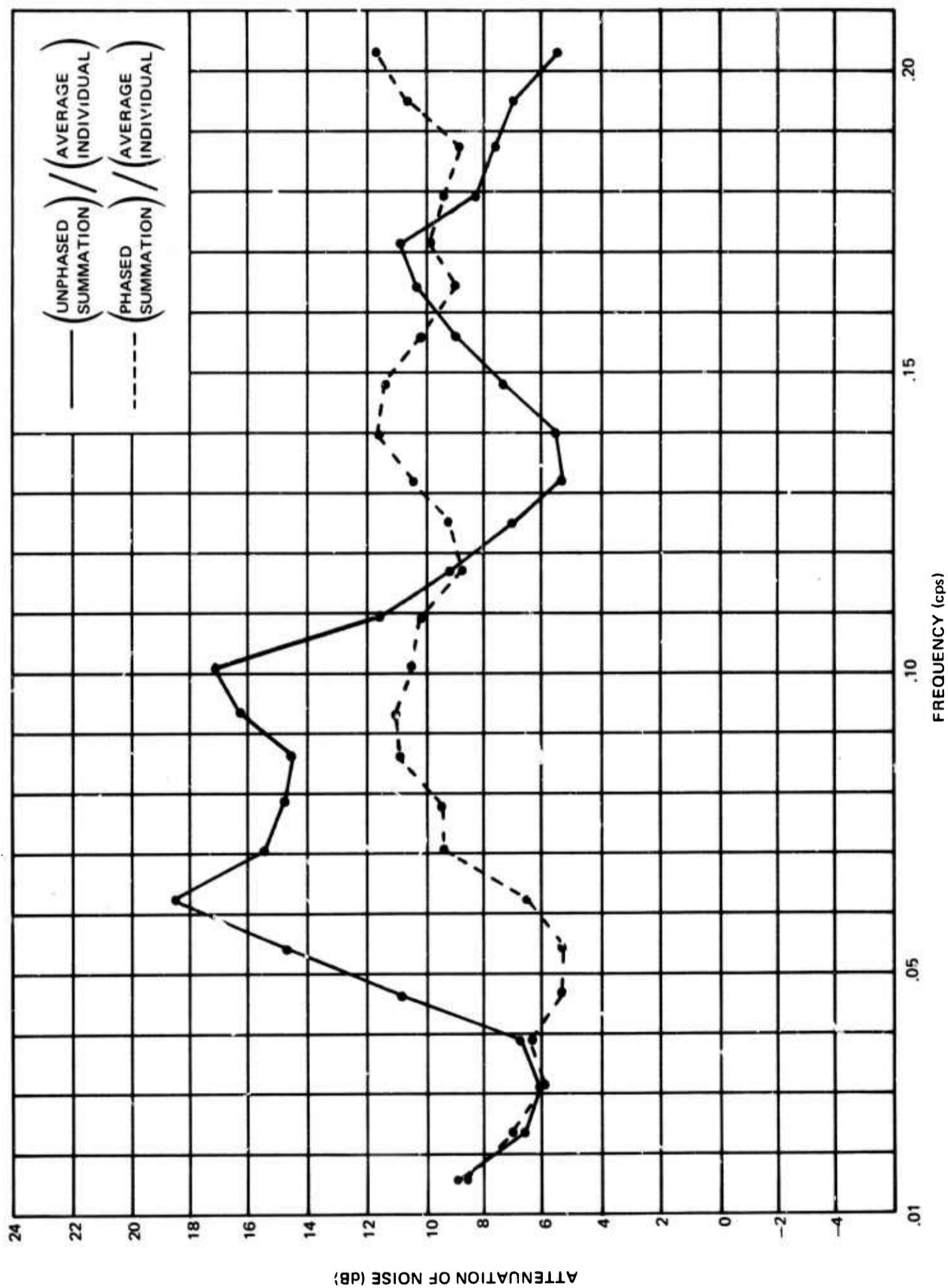


Figure 24. Noise attenuation achieved by the unphased sum and the phased sum relative to an average individual for a noise sample recorded at UBSO on 18 December 1969 (phased sum beamed to a Rayleigh wave from the northwest)

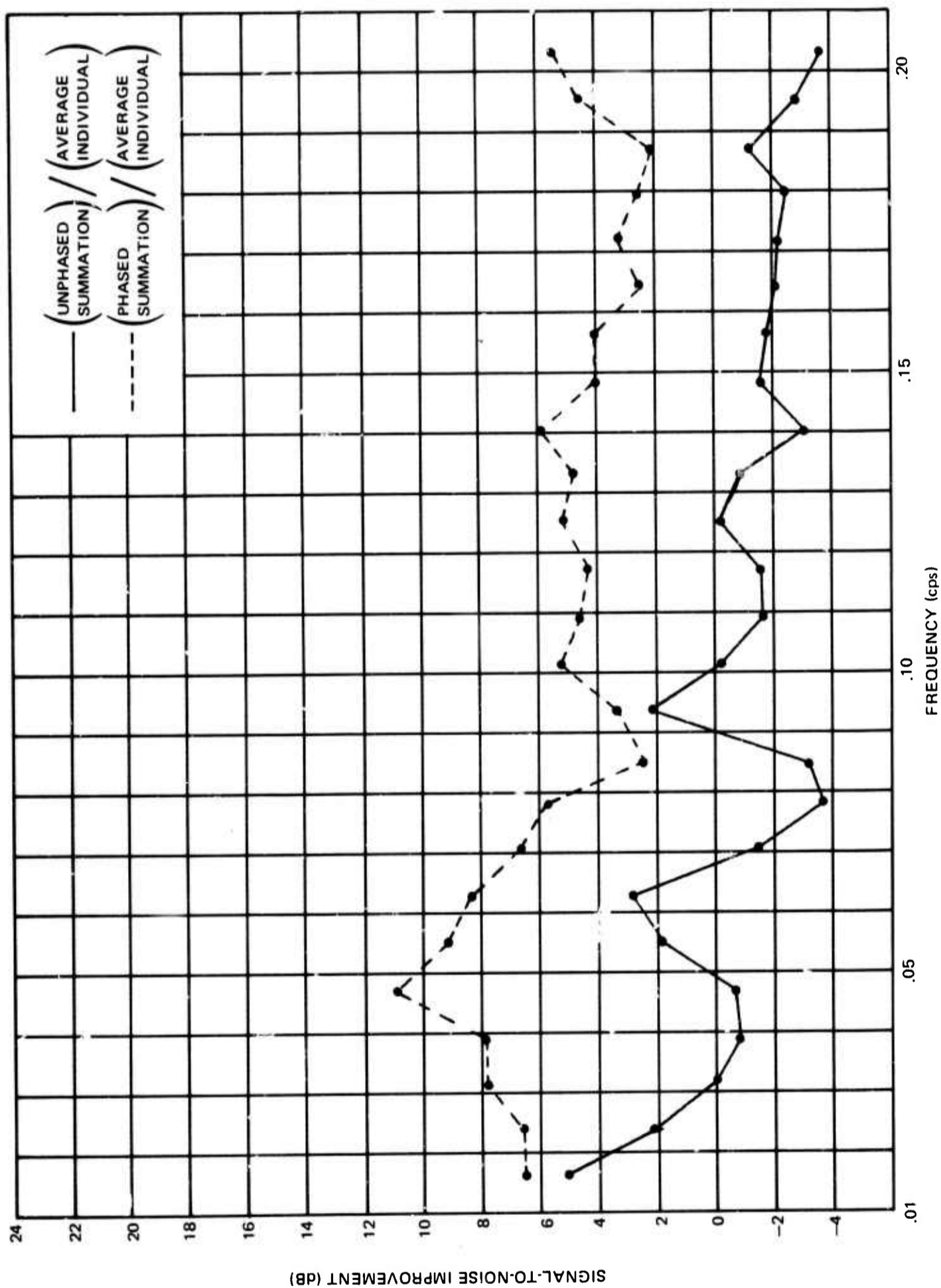


Figure 25. Improvement in signal-to-noise ratio exhibited by the unphased sum and the phased sum relative to an average individual for a Rayleigh wave recorded at UBSO on 13 November 1969 from the southeast

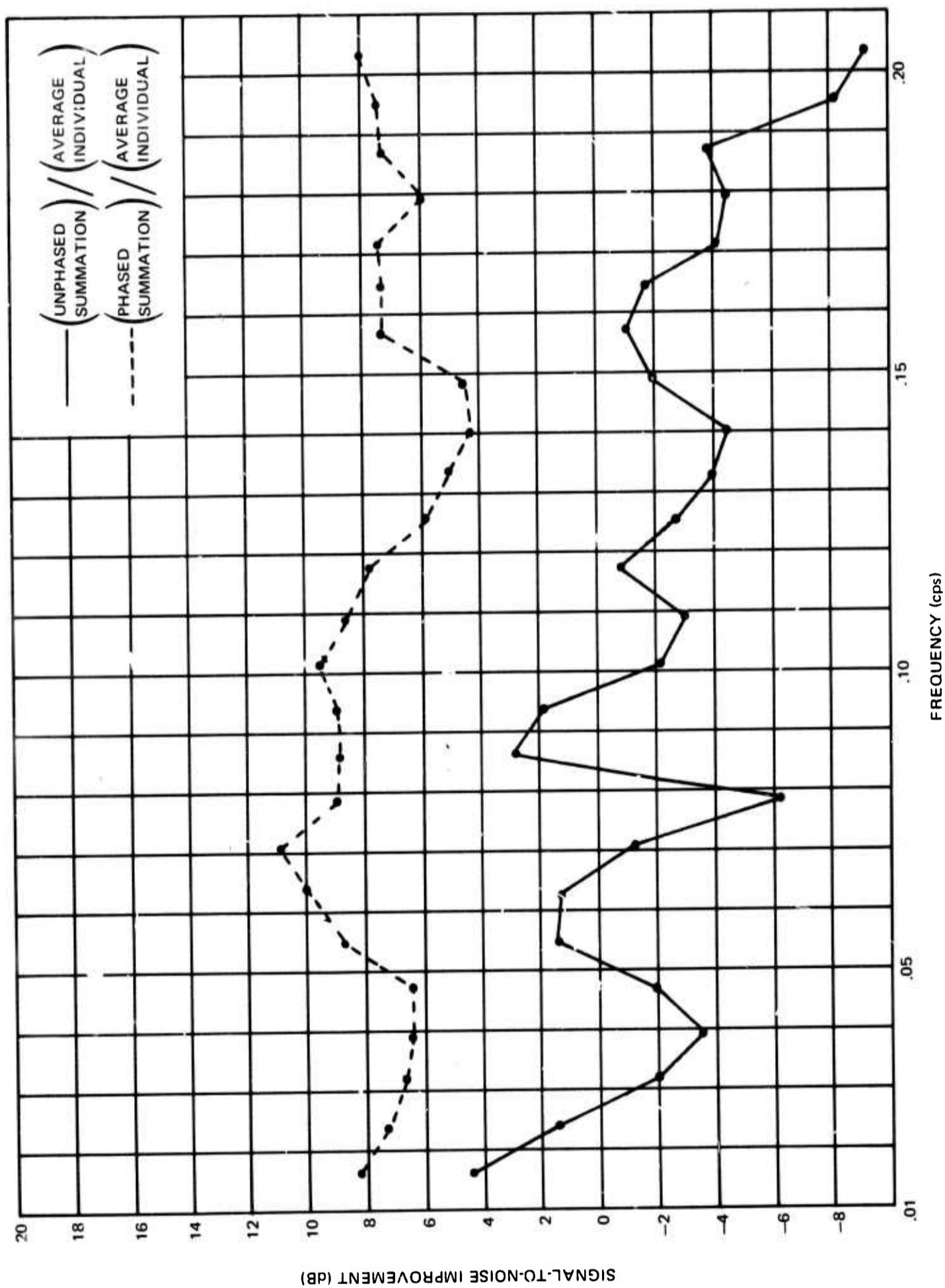


Figure 26. Improvement in signal-to-noise ratio exhibited by the unphased sum and the phased sum relative to an average individual for a Rayleigh wave recorded at UBSO on 26 November 1969 from the southwest

The phased summation on 18 December (figure 27) event shows the effect of noise on a beam steered to the direction of a strong noise source. The phased sum shows 3.4 dB to slightly over 6 dB in the Rayleigh wave frequency band. The unphased sum of this event shows a large improvement over the unphased summations of the other two events because the signal is attenuated to a lesser degree.

With only three events, the degree of improvement in signal-to-noise by summation is difficult to determine accurately because of the complexity of the Rayleigh waves and the variation in the noise level and frequency content.

In general, the unphased summations of the UBSO array show little improvement due to the large degree of signal loss. The phased summation improves the signal-to-noise more, but the degree of improvement varies because of the directional properties of the noise.

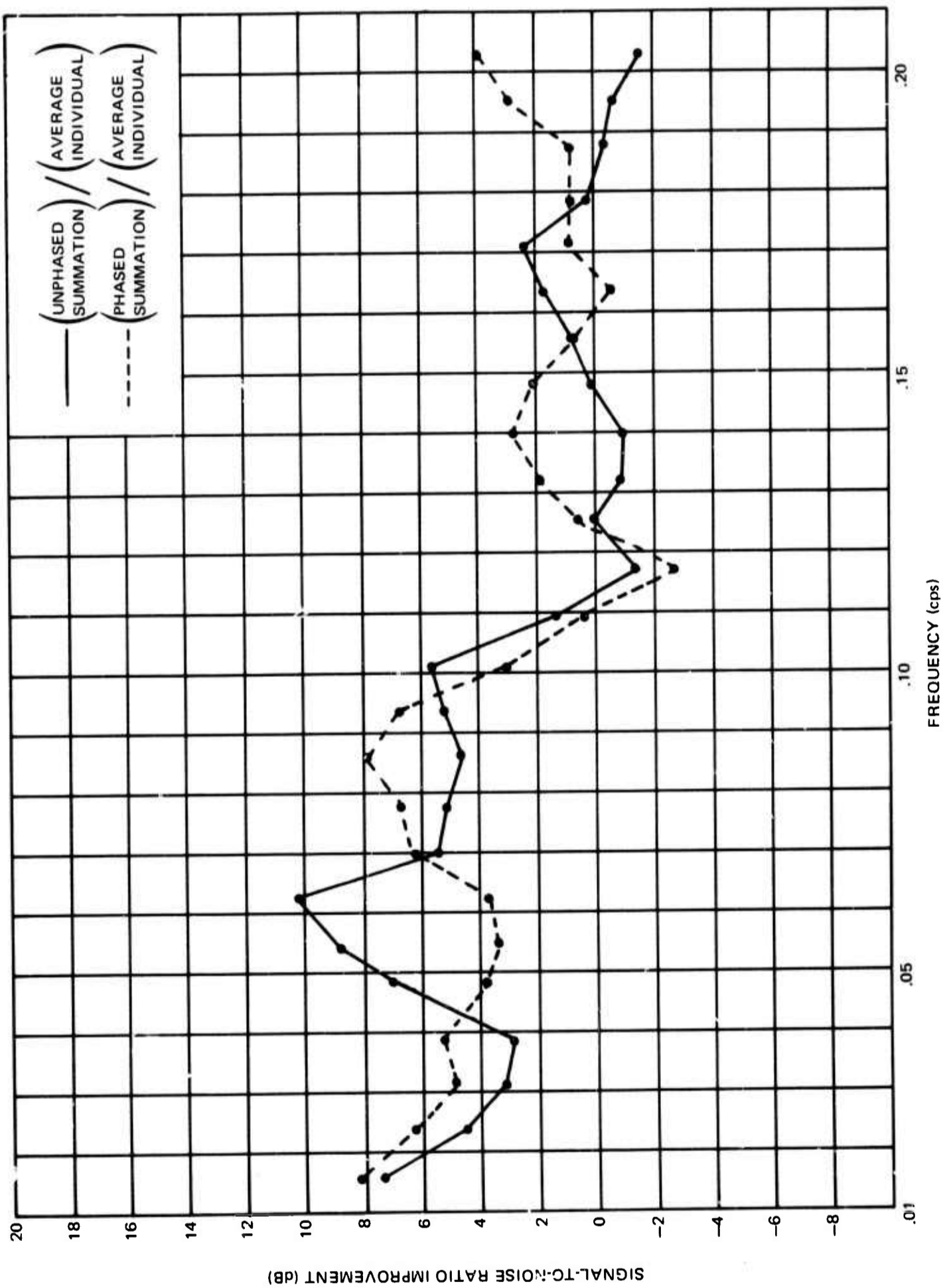


Figure 27. Improvement in signal-to-noise ratio exhibited by the unphased sum and the phased sum relative to an average individual for a Rayleigh wave recorded at UBSO on 18 December 1969 from the northwest

APPENDIX 1 to TECHNICAL REPORT NO. 69-53

POWER DENSITY SPECTRA OF SIGNAL SEGMENTS FOR  
EACH DATA SAMPLE

---

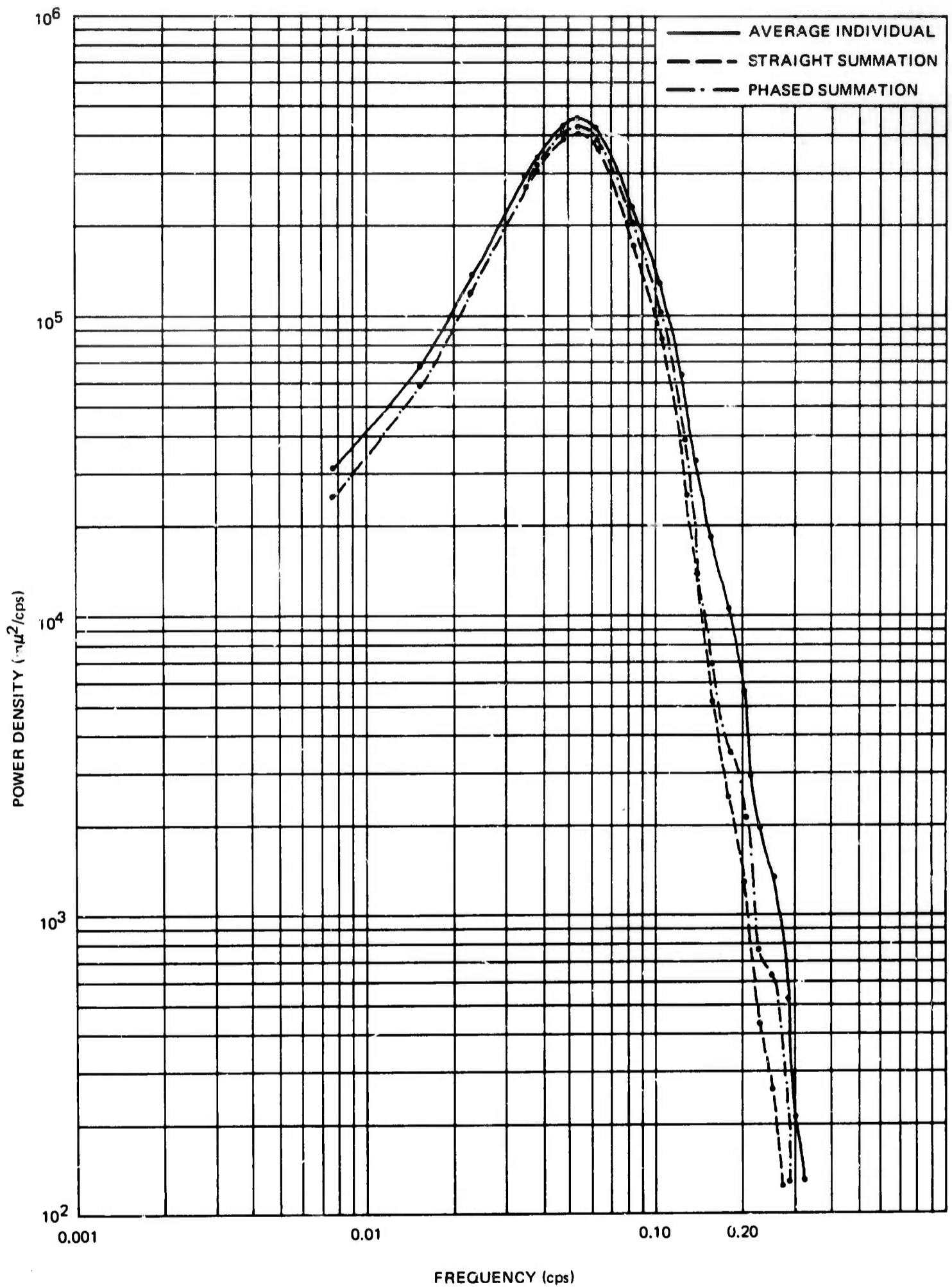


Figure 1. Power density spectra for a time segment containing P, PP, and PPP recorded at UBSO on 13 November 1969 from the southeast

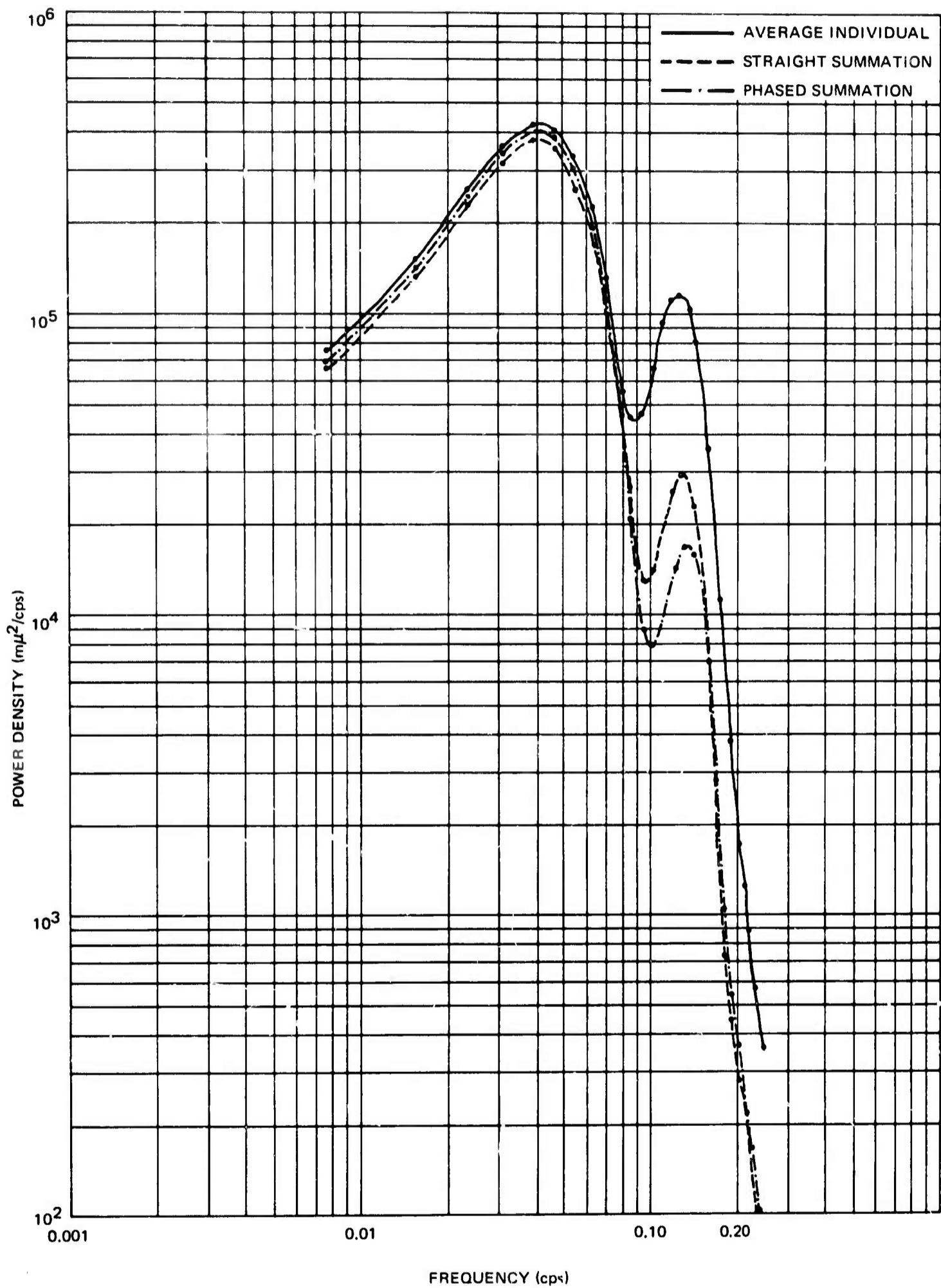


Figure 2. Power density spectra for a time segment containing P, PP, and PPP recorded at UBSO on 26 November 1969 from the southwest

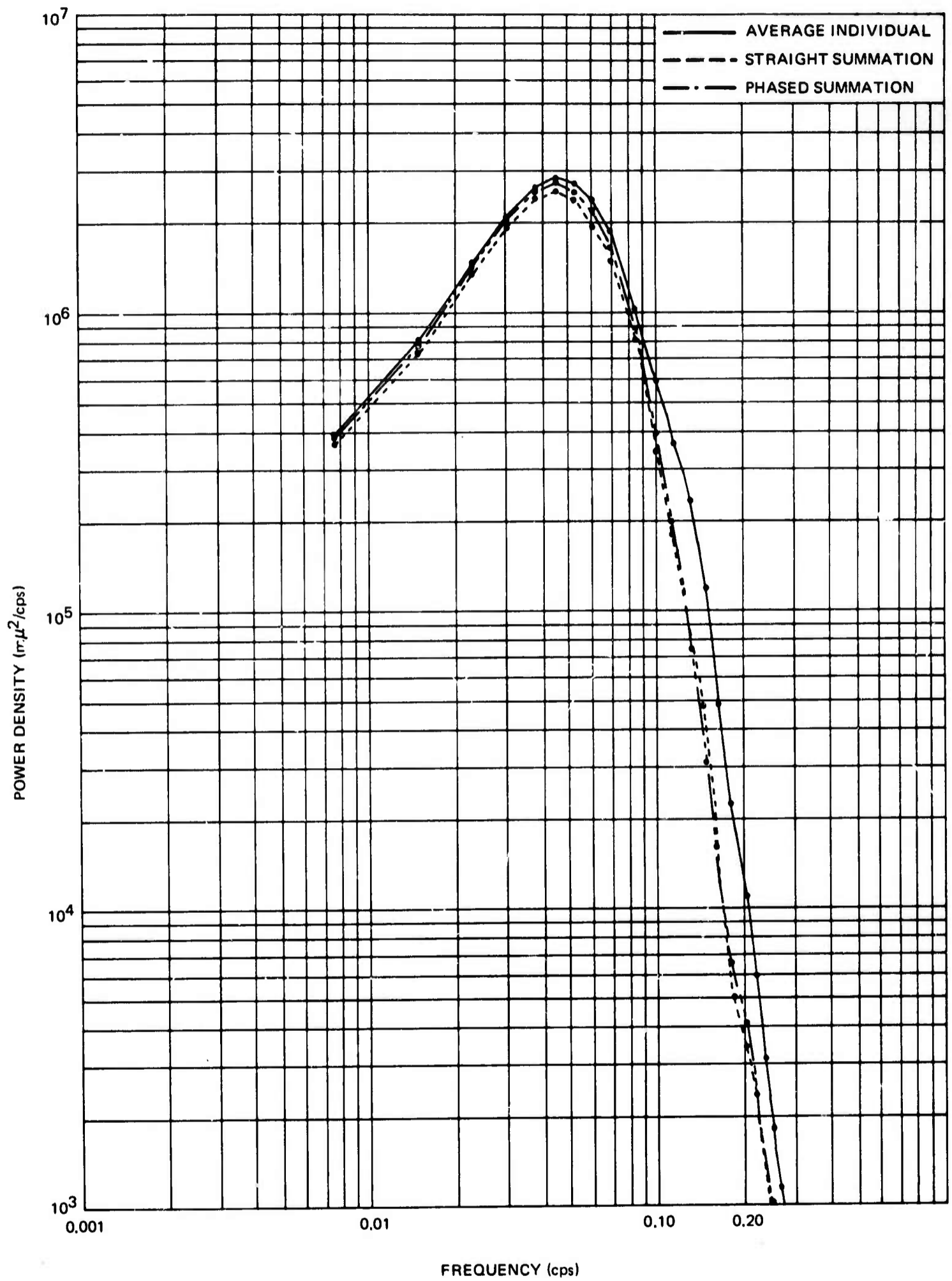


Figure 3. Power density spectra for a time segment containing P, PP, and PPP recorded at UBSO on 18 December 1969 from the northwest

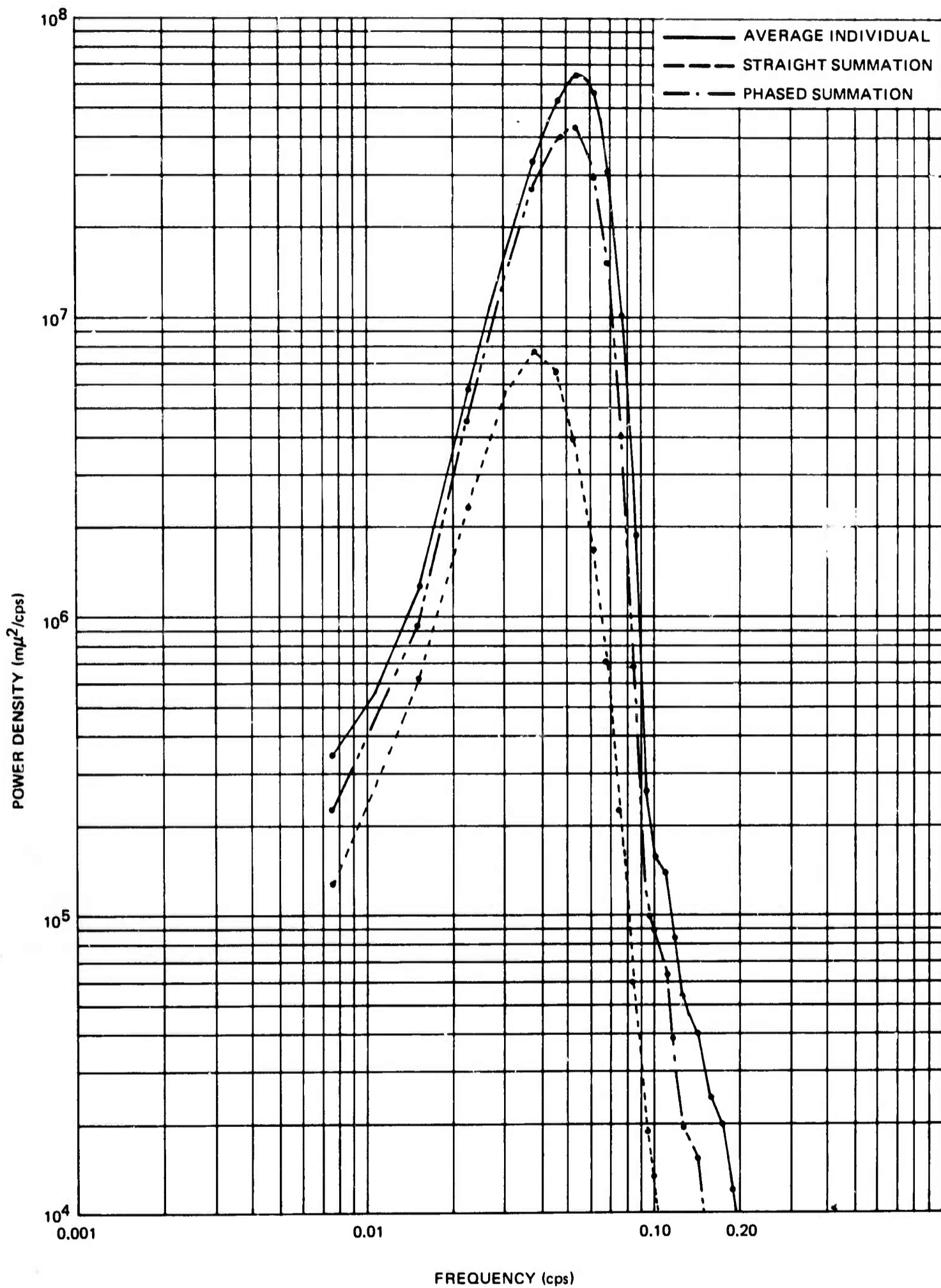


Figure 4. Power density spectra for a Rayleigh wave recorded at UBSO on 13 November 1969 from the southeast

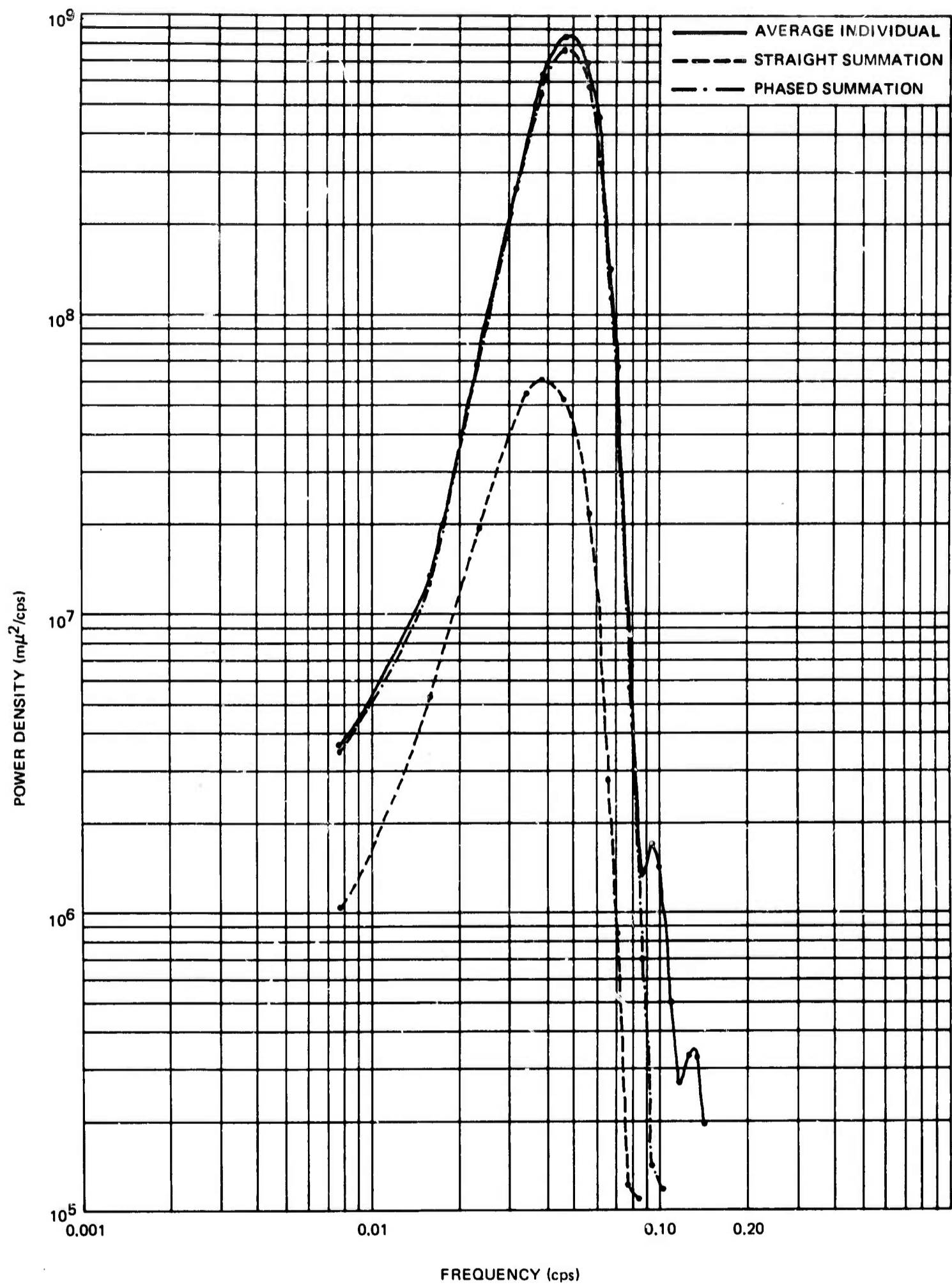


Figure 5. Power density spectra for a Rayleigh wave recorded at UBSO on 26 November 1969 from the southwest

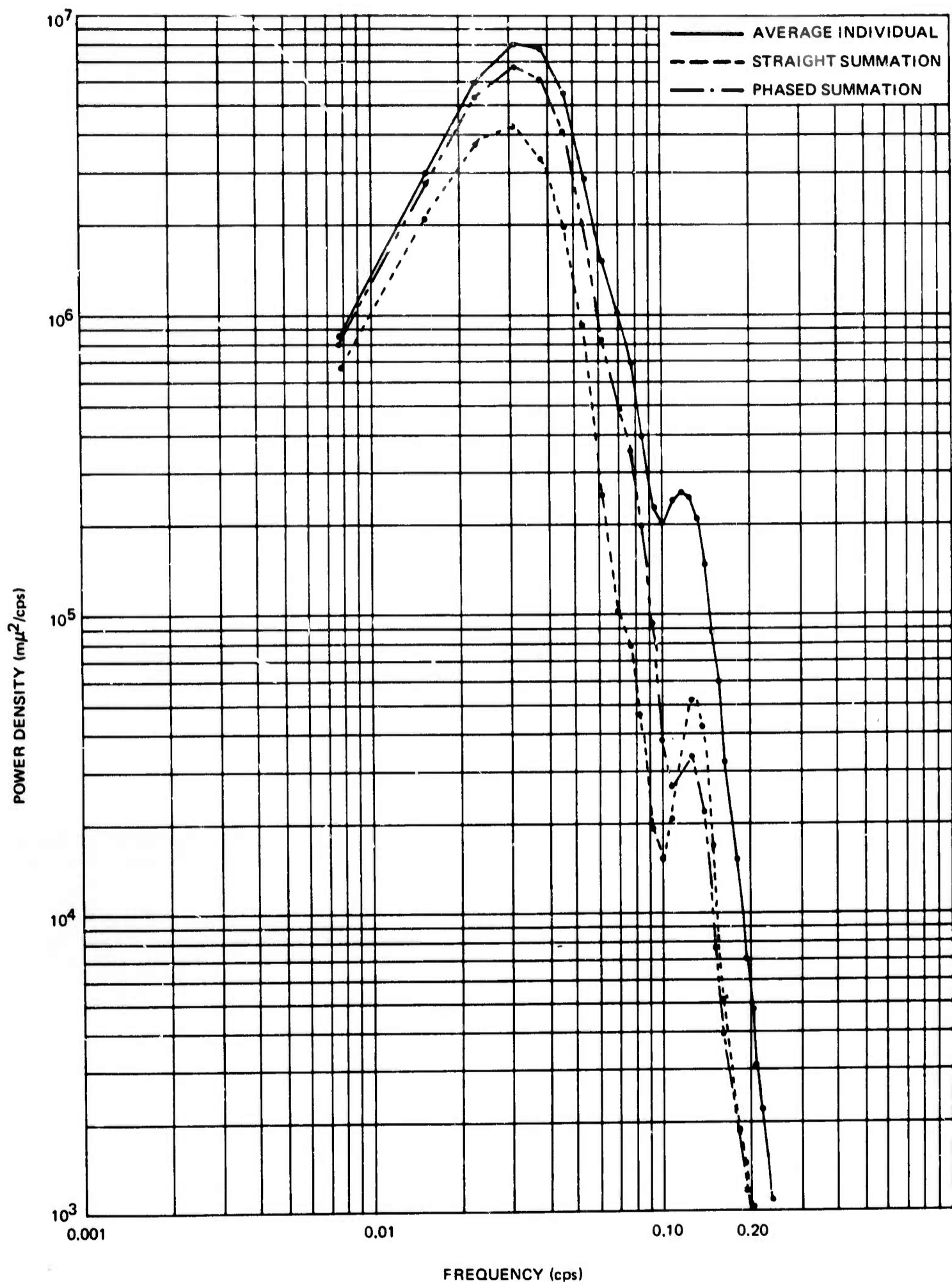


Figure 6. Power density spectra for a Rayleigh wave recorded at UBSO on 18 December 1969 from the northwest

APPENDIX 2 to TECHNICAL REPORT NO. 69-53

POWER DENSITY SPECTRA OF NOISE SEGMENTS FOR  
EACH DATA SAMPLE

---

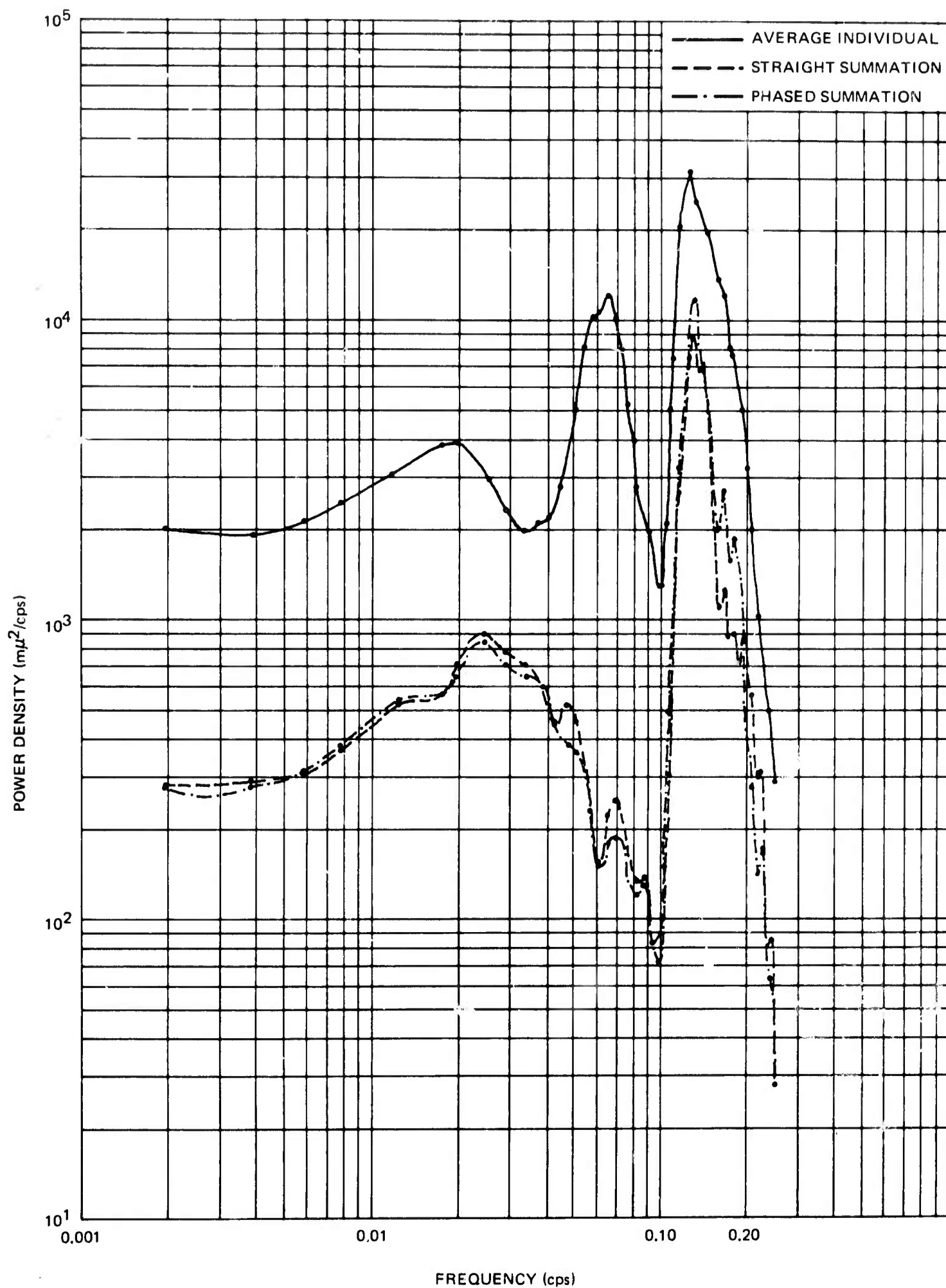


Figure 1. Power density spectra for the noise preceding a teleseismic P wave recorded at UBSO on 13 November 1969 from the southeast

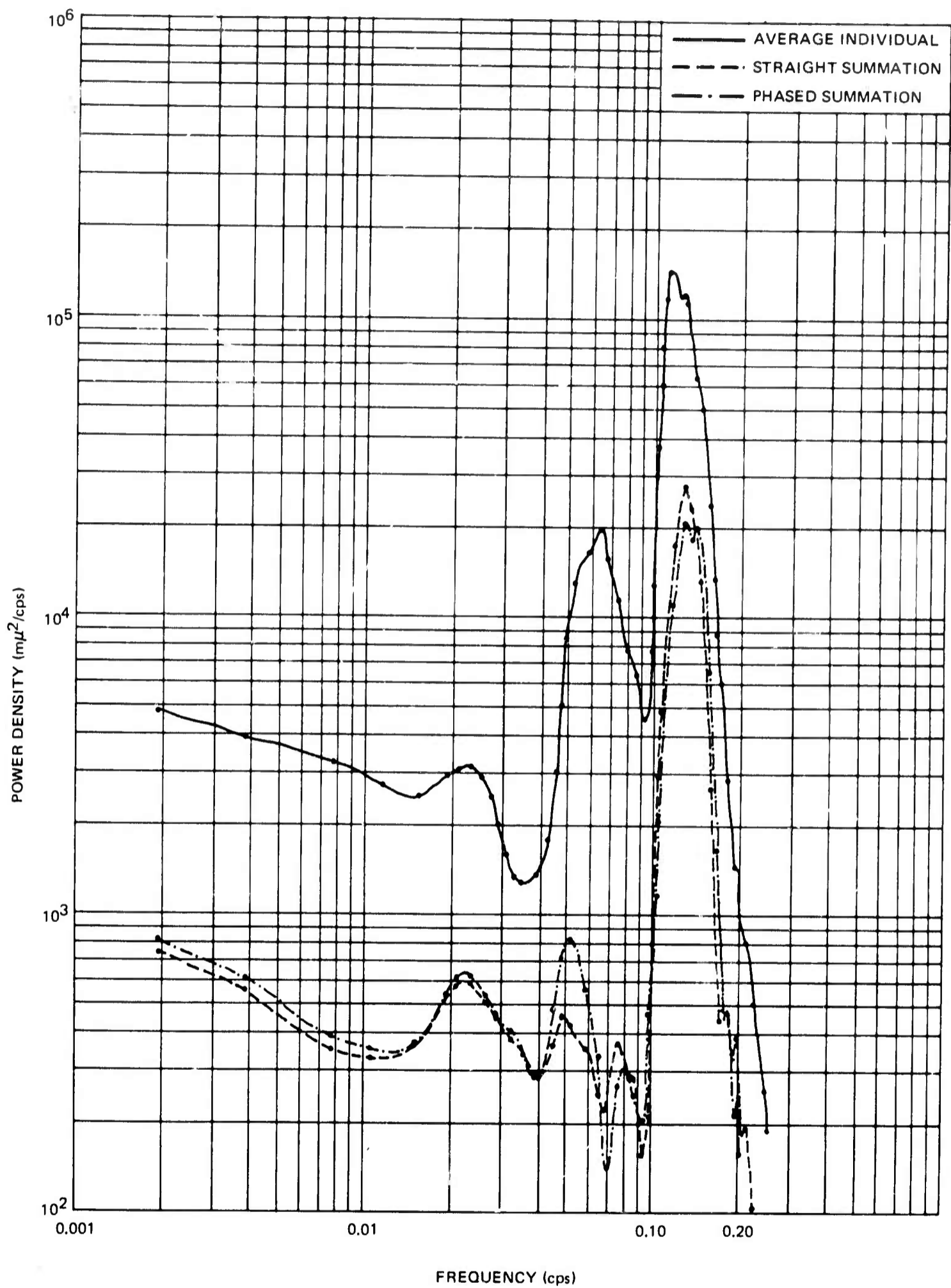


Figure 2. Power density spectra for the noise preceding a teleseismic P wave recorded at UBSO on 26 November 1969 from the southwest

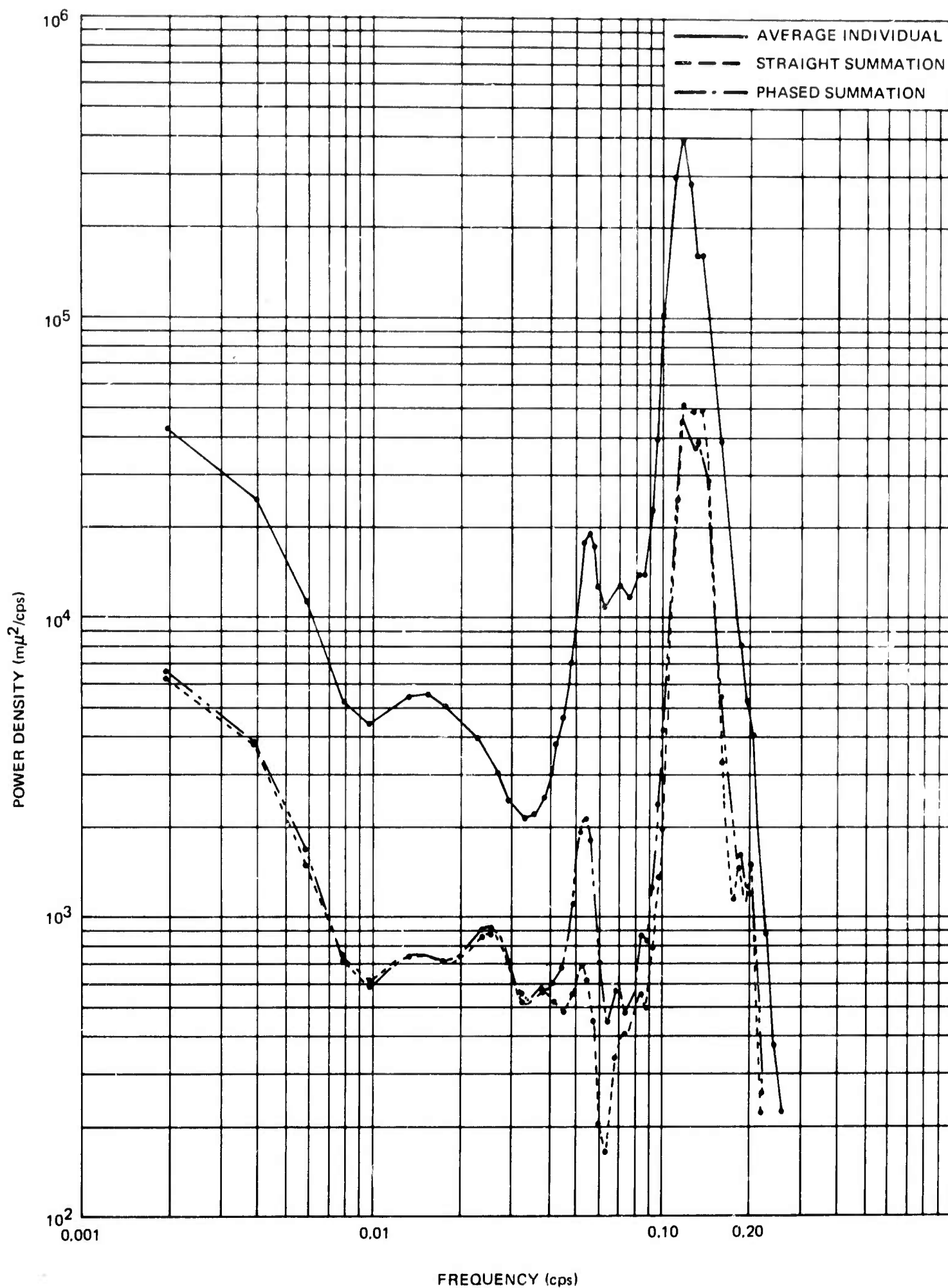


Figure 3. Power density spectra for the noise preceding a teleseismic P wave recorded at UBSO on 18 December 1969 from the northwest

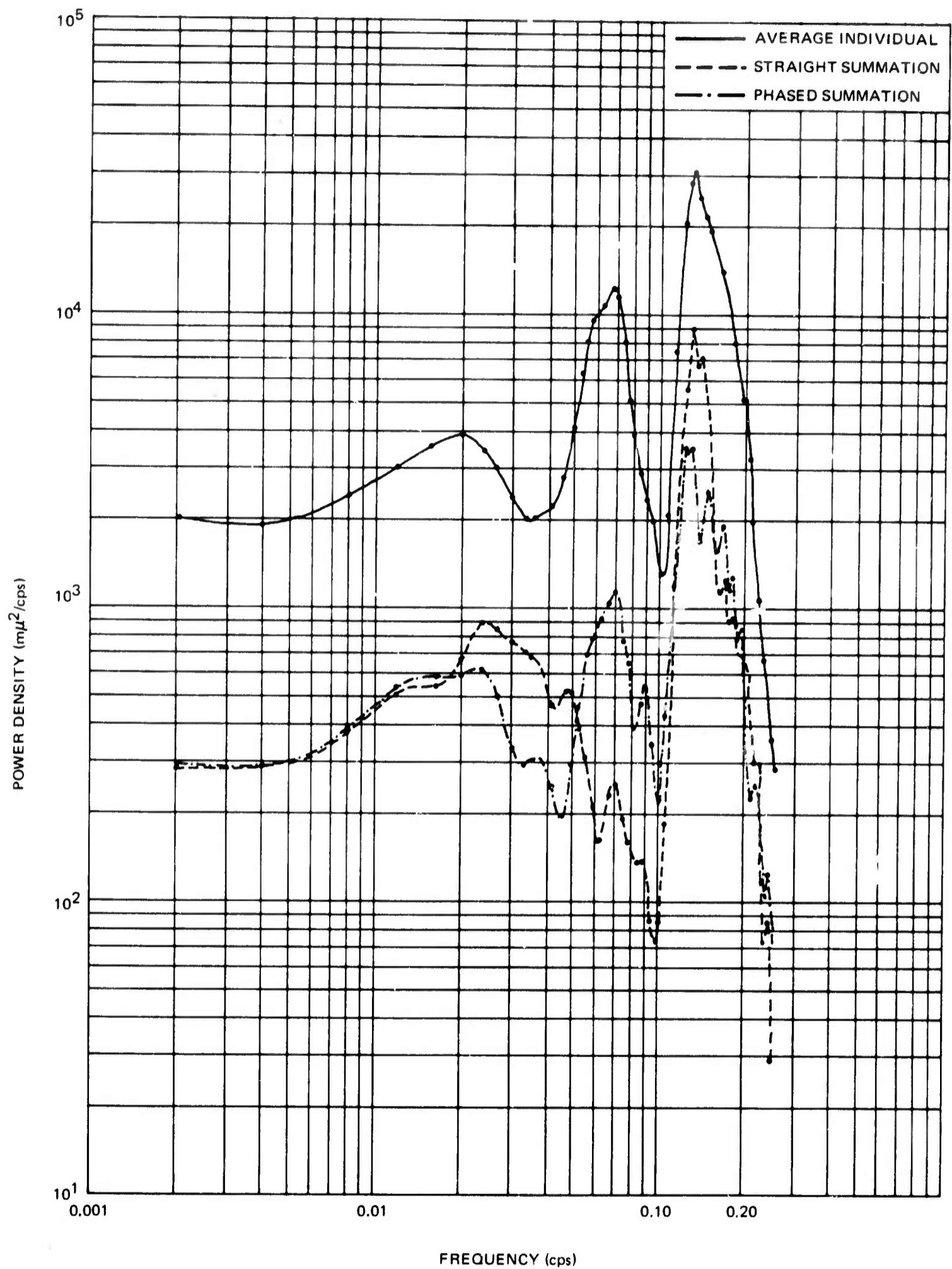


Figure 4. Power density spectra for the noise preceding a teleseismic Rayleigh wave signal recorded at UBSO on 13 November 1969 from the southeast

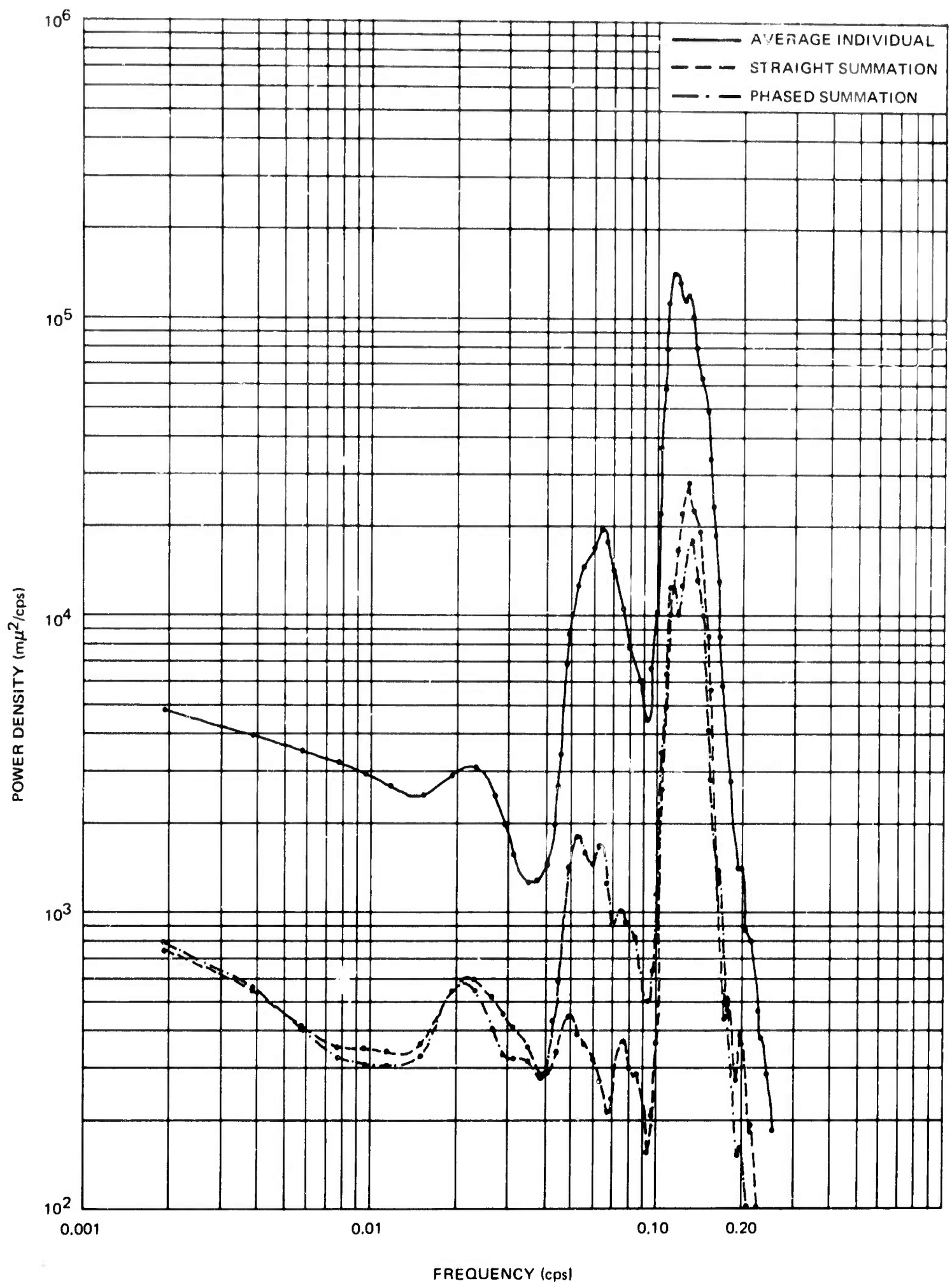


Figure 5. Power density spectra for the noise preceding a teleseismic Rayleigh wave signal recorded at UBSO on 26 November 1969 from the southwest

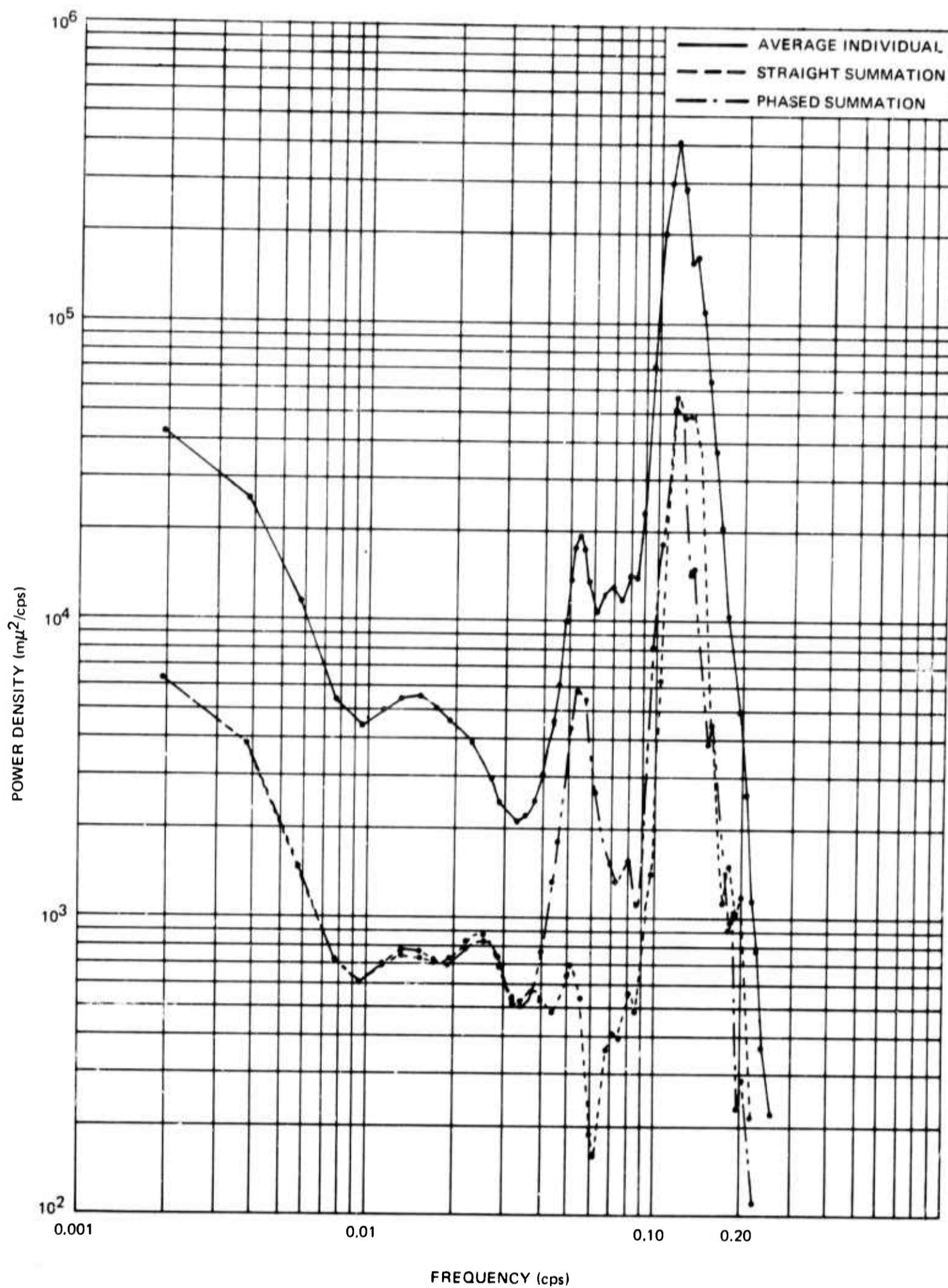


Figure 6. Power density spectra for the noise preceding a teleseismic Rayleigh wave signal recorded at UBSO on 18 December 1969 from the northwest

APPENDIX 3 to TECHNICAL REPORT NO. 69-53

SIGNAL-TO-NOISE RATIOS FOR EACH DATA SAMPLE

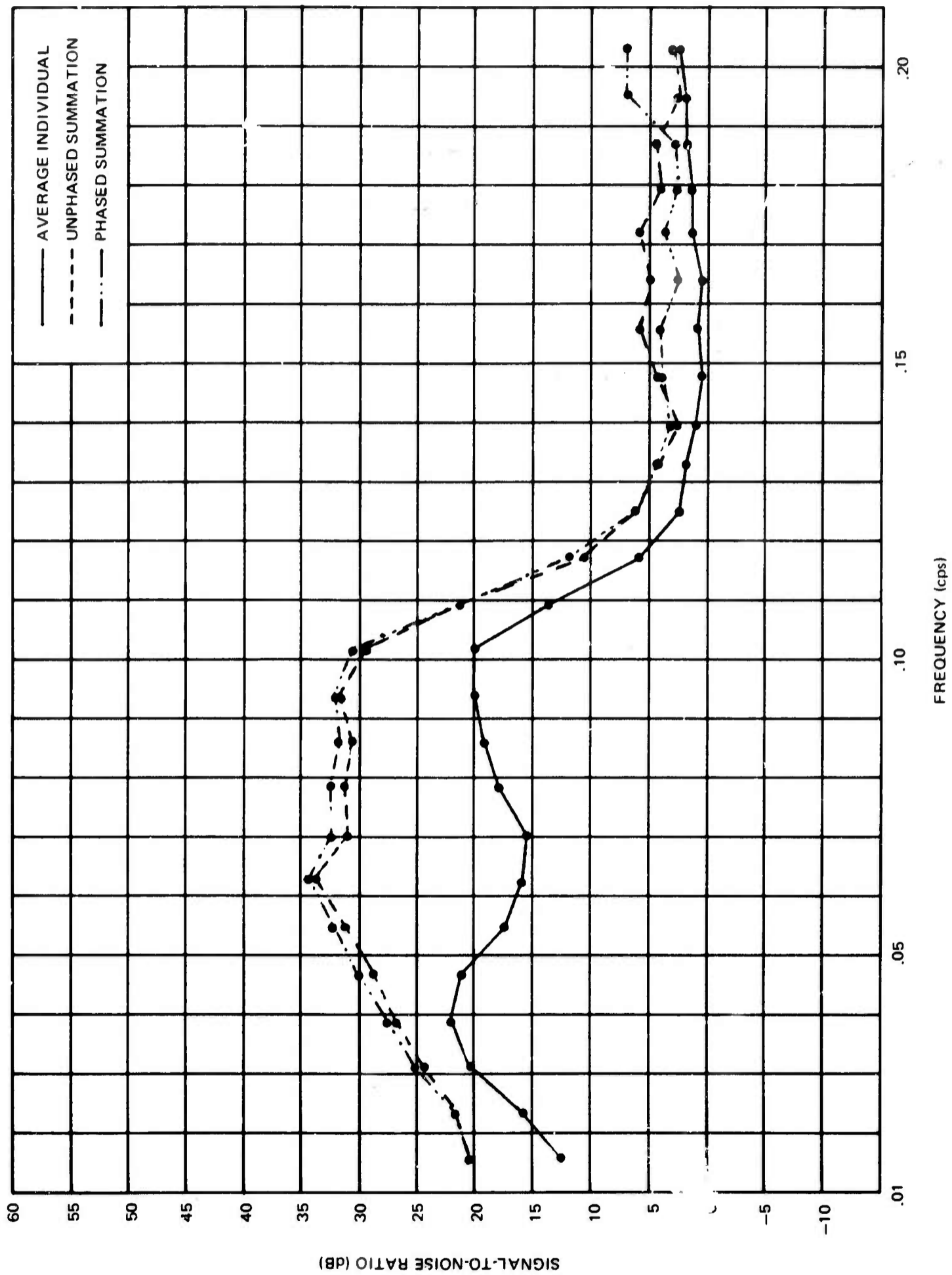


Figure 1. Signal-to-noise ratios calculated for a teleseismic P wave recorded at UBSO on 13 November 1969 from the southeast

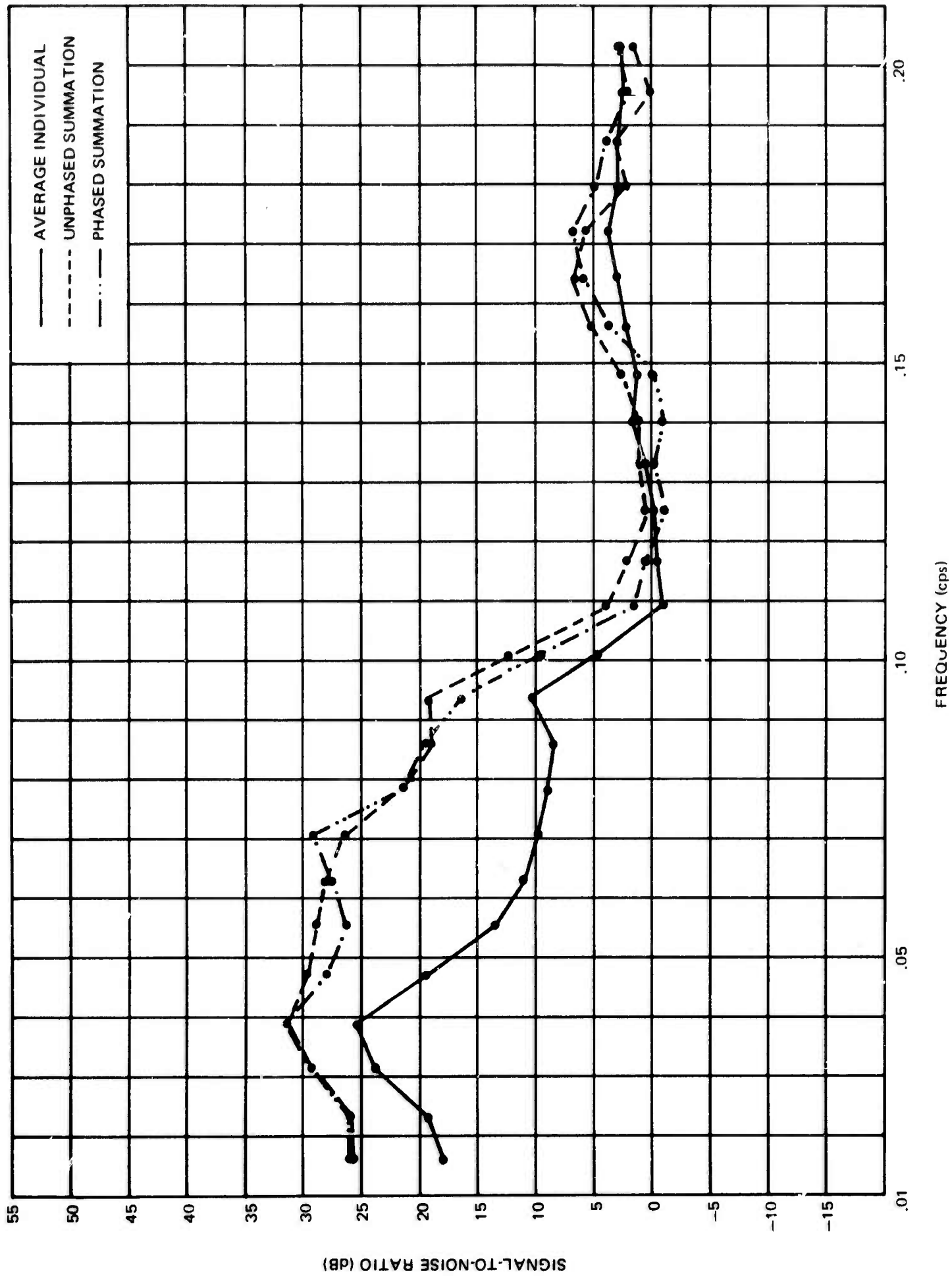


Figure 2. Signal-to-noise ratios calculated for a teleseismic P wave recorded at UBSO on 26 November 1969 from the southwest

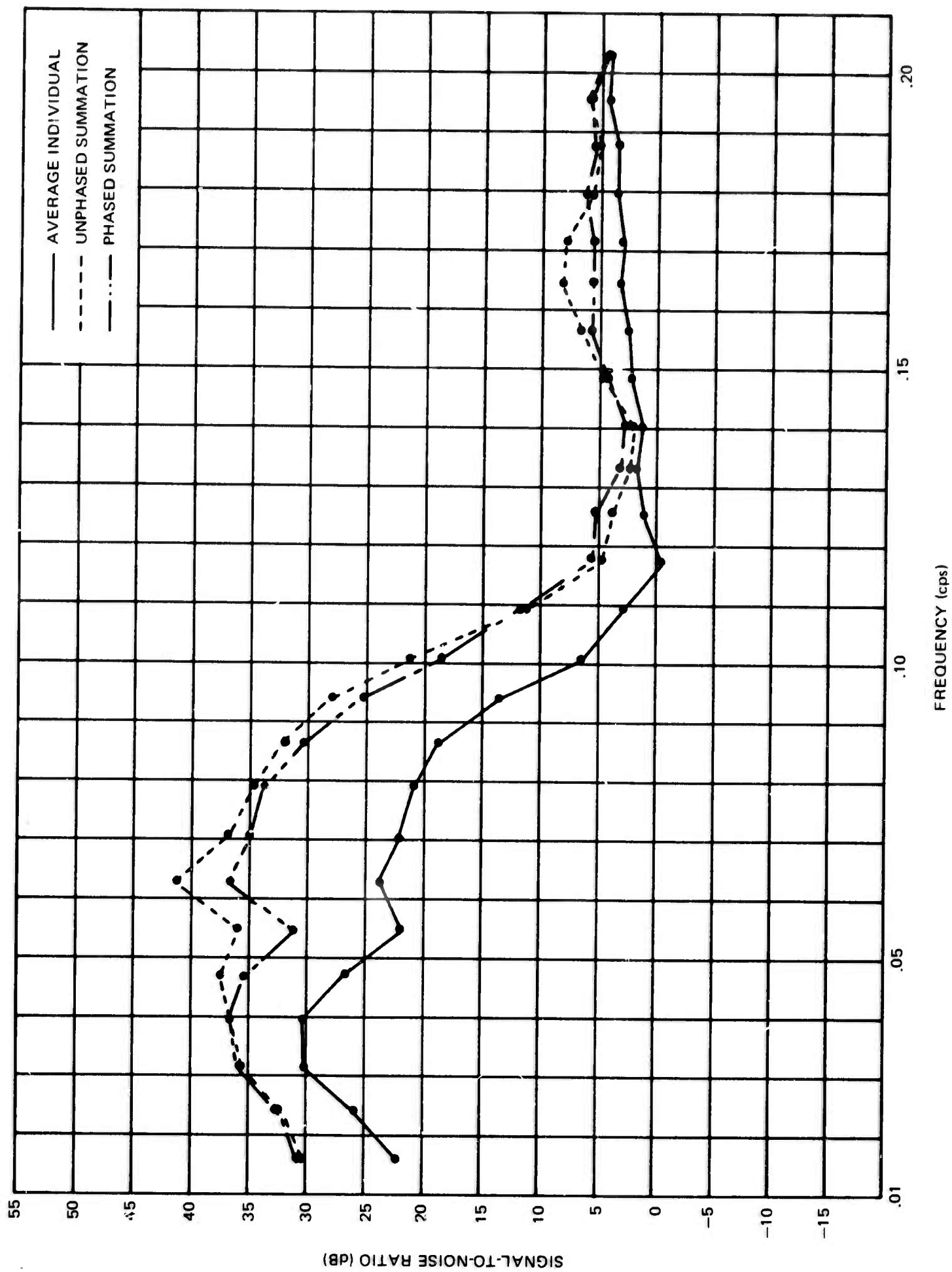


Figure 3. Signal-to-noise ratios calculated for a teleseismic P wave recorded at UBSO on 18 December 1969 from the northwest

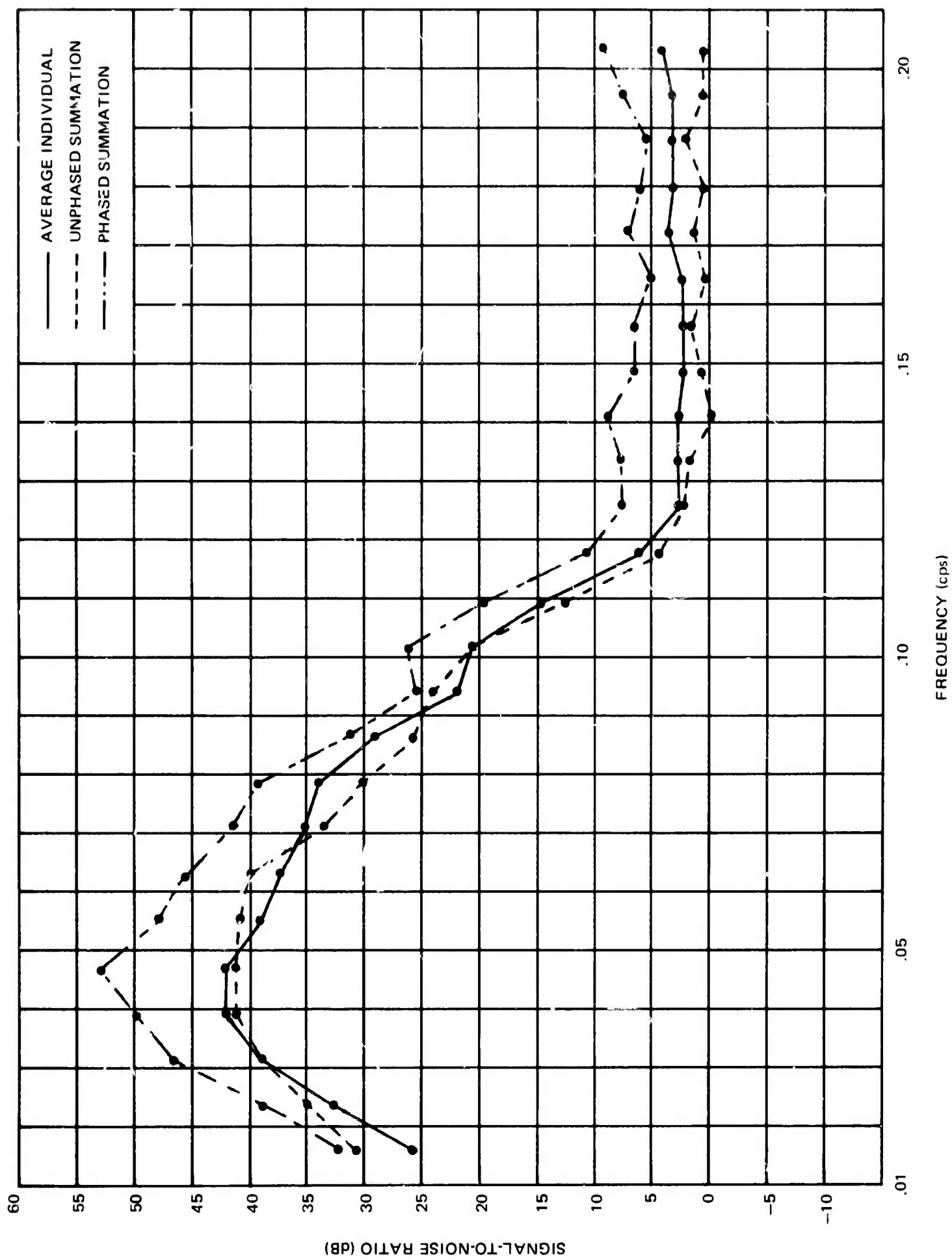


Figure 4. Signal-to-noise ratios calculated for a Rayleigh wave recorded at UBSO on 13 November 1969 from the southeast

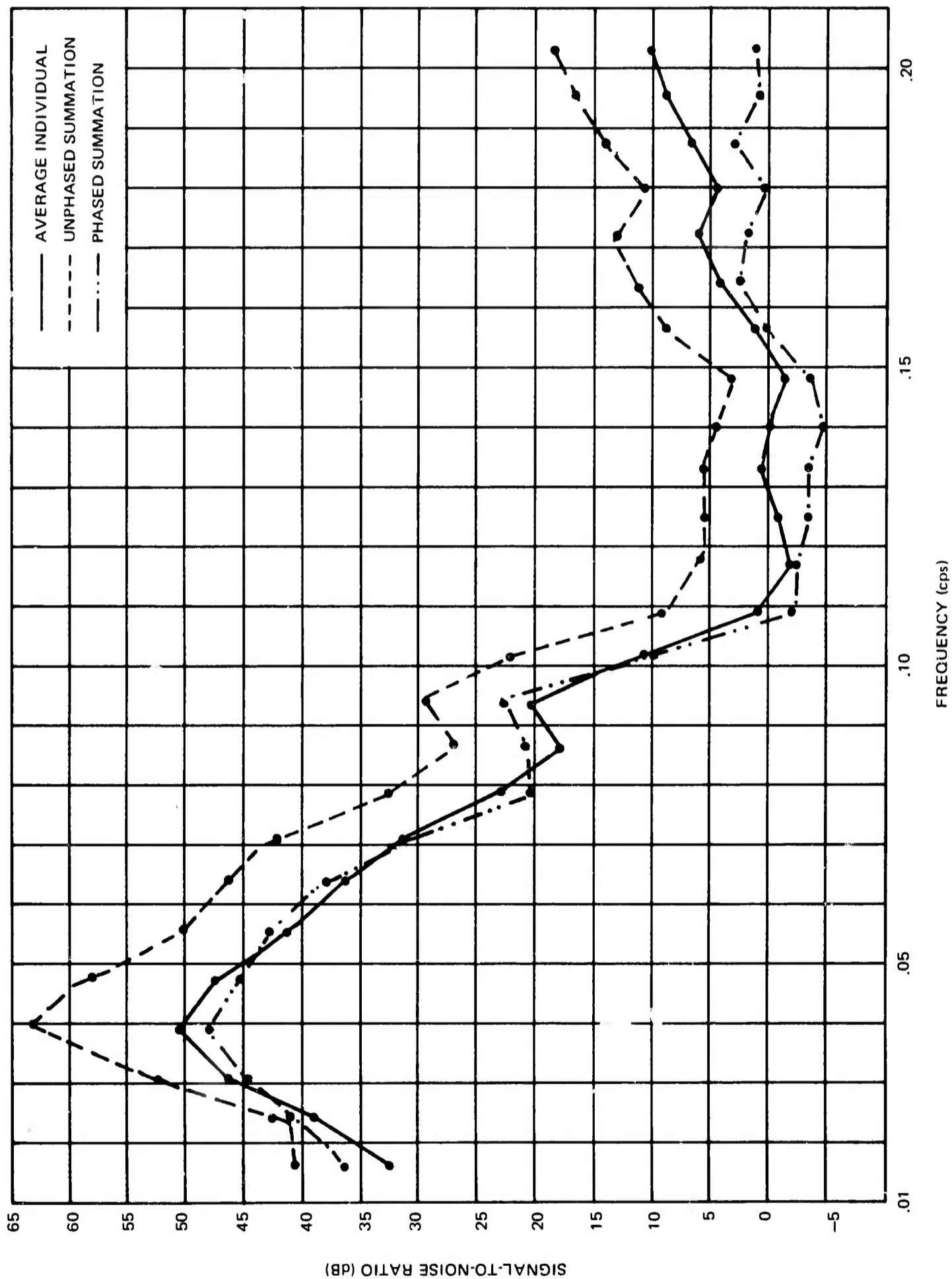


Figure 5. Signal-to-noise ratios calculated for a Rayleigh wave recorded at UBSO on 26 November 1969 from the southwest

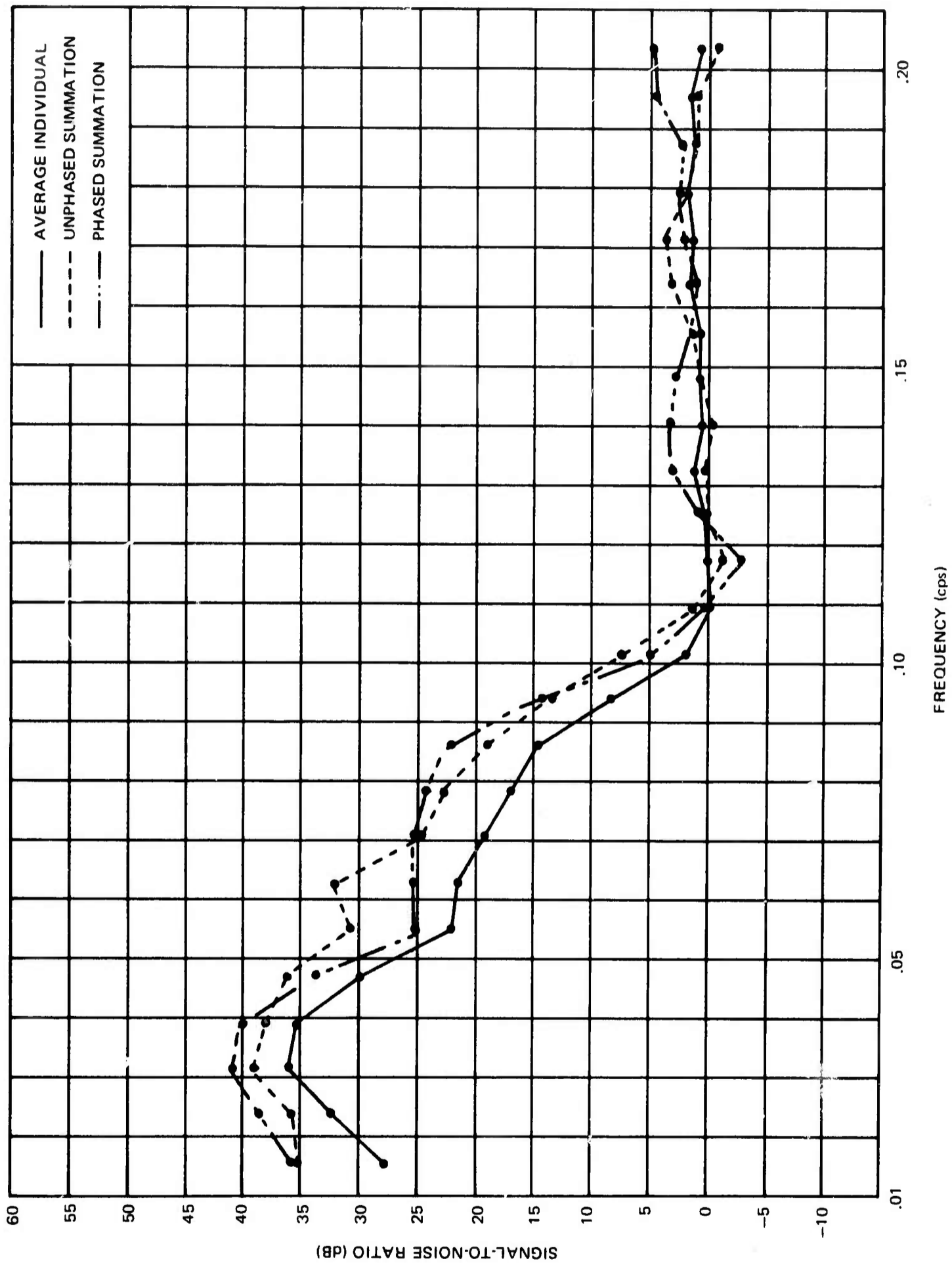


Figure 6. Signal-to-noise ratios calculated for a Rayleigh wave recorded at UBSO on 18 December 1969 from the northwest

Unclassified

Security Classification

## DOCUMENT CONTROL DATA - R &amp; D

(Security classification of title, body of abstract and indexing annotation must be entered when the overall report is classified)

1. ORIGINATING ACTIVITY (Corporate author) Geotech, A Teledyne Company 3401 Shiloh Road Garland, Texas 75040		2a. REPORT SECURITY CLASSIFICATION Unclassified	
		2b. GROUP	
3. REPORT TITLE Evaluation of the Detection Capabilities of the UBSO Long-Period Array			
4. DESCRIPTIVE NOTES (Type of report and inclusive dates)			
5. AUTHOR(S) (First name, middle initial, last name) Don R. Phillips John M. Ward			
6. REPORT DATE 10 February 1970		7a. TOTAL NO. OF PAGES 67	7b. NO. OF REFS
8a. CONTRACT OR GRANT NO. F33657-69-C-0759		9a. ORIGINATOR'S REPORT NUMBER(S) 69-53	
b. PROJECT NO. VELA T/9703			
c. ARPA Order No. 624		9b. OTHER REPORT NO(S) (Any other numbers that may be assigned this report)	
d. ARPA Program Code No. 8F10			
10. DISTRIBUTION STATEMENT This document is subject to special export controls and each transmittal to foreign governments or foreign nationals may be made only with prior approval of Chief, AFTAC.			
11. SUPPLEMENTARY NOTES		12. SPONSORING MILITARY ACTIVITY Advanced Research Projects Agency Nuclear Test Detection Office Washington, D. C.	
13. ABSTRACT Three events from different directions were selected from which both a P and a Rayleigh waves energy was recorded by the seven vertical long-period seismographs of the UBSO array. Using the power density spectra of the signals and noise segments preceding the signals, signal-to-noise ratios were formed for the simple and phased summations. The simple summation indicated an improvement in signal-to-noise over a single detector of approximately 17 dB at the peak noise frequency of 0.0625 cps for the P-wave signal, but showed little or no improvement for the Rayleigh energy because of the large degree of Rayleigh signal loss. In all three cases the phased summations show improvement for both P and Rayleigh signals; however, the degree of improvement varied from event to event because of the directional properties of the noise sources.			

14.	KEY WORDS	LINK A		LINK B		LINK C	
		ROLE	WT	ROLE	WT	ROLE	WT
	Long-period array						
	P-wave						
	Rayleigh wave						
	Phased summation						
	Unphased summation						